

**INVESTIGATION OF A LANDSLIDE PRONE AREA, BUKIT
TINGGI, MALAYSIA USING INTEGRATED GEOPHYSICAL
ENGINEERING AND ENVIRONMENTAL ISOTOPE
TECHNIQUES**

TARIQ (MOH'D KHIER) ALKHAMAISEH

**FACULTY OF SCIENCE
UNIVERSITY OF MALAYA
KUALA LUMPUR**

2019

**INVESTIGATION OF A LANDSLIDE PRONE AREA,
BUKIT TINGGI, MALAYSIA USING INTEGRATED
GEOPHYSICAL ENGINEERING AND
ENVIRONMENTAL ISOTOPE TECHNIQUES**

TARIQ (MOH'D KHIER) ALKHAMAISEH

**THESIS SUBMITTED IN FULFILMENT OF THE
REQUIREMENTS FOR THE DEGREE OF DOCTOR OF
PHILOSOPHY**

**DEPARTMENT OF GEOLOGY
FACULTY OF SCIENCE
UNIVERSITY OF MALAYA
KUALA LUMPUR**

2019

UNIVERSITY OF MALAYA
ORIGINAL LITERARY WORK DECLARATION

Name of Candidate: **TARIQ (MOH'D KHIER) ALKHAMAISEH**

Matric No: **SHC140012**

Name of Degree: **DOCTOR OF PHILOSOPHY**

Title of Thesis: **INVESTIGATION OF A LANDSLIDE PRONE AREA, BUKIT
TINGGI, MALAYSIA USING INTEGRATED GEOPHYSICAL
ENGINEERING AND ENVIRONMENTAL ISOTOPE TECHNIQUES**

Field of Study: **GEOLOGY**

I do solemnly and sincerely declare that:

- (1) I am the sole author/writer of this Work;
- (2) This Work is original;
- (3) Any use of any work in which copyright exists was done by way of fair dealing and for permitted purposes and any excerpt or extract from, or reference to or reproduction of any copyrighted work has been disclosed expressly and sufficiently and the title of the Work and its authorship have been acknowledged in this Work;
- (4) I do not have any actual knowledge nor do I ought reasonably to know that the making of this work constitutes an infringement of any copyrighted work;
- (5) I hereby assign all and every right in the copyright to this Work to the University of Malaya ("UM"), who henceforth shall be owner of the copyright in this Work and that any reproduction or use in any form or by any means whatsoever is prohibited without the written consent of UM having been first had and obtained;
- (6) I am fully aware that if in the course of making this Work I have infringed any copyright whether intentionally or otherwise, I may be subject to legal action or any other action as may be determined by UM.

Candidate's Signature

Date:

Subscribed and solemnly declared before,

Witness's Signature

Date:

Name:

Designation:

**INVESTIGATION OF A LANDSLIDE PRONE AREA, BUKIT TINGGI,
MALAYSIA USING INTEGRATED GEOPHYSICAL ENGINEERING AND
ENVIRONMENTAL ISOTOPE TECHNIQUES**

ABSTRACT

Population growth and extension of settlements over risky areas have resulted in an increased impact of a natural disaster. Slope failures, landslides and subsidence of foundation have been identified as the most commonly occurring natural disasters after floods. On the other hand, a detailed analysis of the triggering factors is often hindered by the lack of information gathered from the field measurements. The vicinity of Sekolah Menengah Kebangsaan Bukit Tinggi in Pahang province is considered as one of the natural terrain areas (weathered granite) which are prone to landslide hazards and should be effectively monitored prior to any forewarning of slope movements. This study is conducted to improve understanding between the triggering factors of a landslide in the study area and the suitable preventive measures by using integrated geophysical, geotechnical, and environmental isotope techniques. The 2D inversion results of resistivity technique suggest the presence of a two-layer structure. Moreover, an apparent break in the unit is indicative of the presence of weak fractured zone. As also demonstrated clearly by the seismic refraction data, the depth to bedrock (a sharp boundary interface approximately at a depth of 15 m) varies, which is mainly attributed to variation in thickness of the overlying backfill material. Furthermore, the obtained results from Hydrogen and Oxygen isotopes present a regression line that represents the local meteoric water line as follows: $\delta D = 7.416 \delta^{18}O + 7.428$ ($R^2 = 0.88$). This line is similar to the global meteoric water line and also to the recent global relationship of $\delta D = (8.17 \pm 0.07) \delta^{18}O + (11.27 \pm 0.65)$. The isotope data of surface and groundwater used for this study are all distributed along the local meteoric water line, indicating that the stable isotopes of both surface and groundwater do not have effects of evaporation and can thus be regarded as conservative. From this study, a good relationship between

the electrical (resistivity) and geotechnical (soil strength) properties with the empirical equation $RS = 31.733 (N60) - 165.88$ and regression coefficient $R^2 = 0.77$ is observed. Meanwhile, based on the correlation between the elastic property and weathering profile, the subsurface materials were divided into three zones as follows: Residual soil, highly weathered granite, and moderately weathered granite with p-wave velocity 300 – 900 ms^{-1} , 900 – 1800 ms^{-1} , 1800 – 3000 ms^{-1} respectively. Moreover, according to integrated results obtained from different techniques, the slip surface zone is located at a depth of 15 - 23 m from the ground surface where the materials show some large differences of properties based on the primary velocity obtained. The weak zone may occur due to water infiltration downward through surface cracks, which intensively weakened the subsurface materials mainly by chemical weathering. This study thus helped us to investigate and predict various physical properties of the subsurface material (soils and rocks) with reduced cost and to apply them in understanding the underground structural characteristics of the landslide prone study area.

Keywords: Landslide, Borehole, Seismic refraction, Electrical resistivity tomography, Wenner – Schlumberger, Standard Penetration Tests.

**KAJIAN KAWASAN CENDERUNG TANAH RUNTUH, BUKIT TINGGI,
MALAYSIA DENGAN PENGGUNAAN PENGINTEGRASIAN
KEJURUTERAAN GEOFIZIKAL DAN TEKNIK ISOTOP ALAM SEKITAR**

ABSTRAK

Pertumbuhan populasi dan pembesaran penempatan di kawasan berisiko telah meningkatkan kesan bencana alam. Oleh itu, kegagalan cerun, tanah runtuh dan penenggelaman tapak asas telah dikenalpasti sebagai bencana alam yang paling kerap berlaku selepas banjir. Sebaliknya, analisis terperinci terhadap faktor pencetus seringkali terhalang disebabkan oleh kurangnya maklumat yang dikumpul daripada lapangan ukuran. Kawasan sekitar Sekolah Menengah Kebangsaan Bukit Tinggi di wilayah Pahang dianggap sebagai salah satu kawasan rupa bumi semulajadi (granit yang terdedah kepada elemen cuaca) yang terdedah kepada bahaya tanah runtuh dan seharusnya di pantau secara efektif sebelum berlaku amaran awal tentang pergerakan cerun. Kajian ini dibuat bagi meningkatkan pemahaman tentang faktor pencetus tanah runtuh dan kaedah-kaedah pencegahan yang sesuai dengan menggunakan teknik-teknik bersepadu geofizikal, geoteknikal, dan isotop alam sekitar. Hasil-hasil penyongsangan 2D teknik kerintangan menunjukkan kewujudan model struktur. Juga, pecahan ketara yang wujud di dalam unit menandakan terdapatnya zon retak yang lemah. Seperti yang juga telah di tunjukkan secara jelas oleh data pembiasan seismik, kedalaman menuju batuan dasar (penghubung sempadan tepat pada kedalaman lebih kurang 15 m) adalah pelbagai, dan kepelbagaian ini adalah secara umumnya disebabkan oleh ketebalan bahan pemimbuk yang melitupi. Tambahan pula, hasil-hasil yang didapati daripada isotop Hidrogen and Oksigen menunjukkan garis regresi yang mewakili garis air meteorik tempatan seperti berikut: $\delta D = 7.416 \delta^{18}O + 7.428$ ($R^2 = 0.88$). LMWL ini adalah menyerupai garis air meteorik global (GMWL) dan juga menyerupai hubungan global terkini seperti berikut: $\delta D = (8.17 \pm 0.07) \delta^{18}O + (11.27 \pm 0.65)$. Data isotop permukaan dan air bawah tanah yang digunakan dalam kajian ini kesemuanya

disebarkan sepanjang garis air meteorik tempatan, dan ini menandakan bahawa isotop stabil kedua-dua permukaan dan air bawah tanah tidak mempunyai kesan pengwapan dan oleh itu boleh dianggap sebagai konservatif. Daripada kajian ini, satu hubungan baik di antara ciri elektrik (kerintangan) dan ciri geoteknikal (kekuatan tanah) dengan persamaan empirikal $RS = 31.733 (N60) - 165.88$ dan koefisien regresi $R^2 = 0.77$ telah dilihat. Sementara itu, berdasarkan korelasi di antara ciri elastik dan profil peluluhawaan (weathering) bahan bawah permukaan telah dibahagikan kepada tiga zon seperti berikut: tanah sisa, granit yang sangat terdedah kepada elemen cuaca, dan granit yang terdedah kepada elemen cuaca tahap sederhana dengan halaju p-wave masing-masing $300 - 900 \text{ ms}^{-1}$, $900 - 1800 \text{ ms}^{-1}$, $1800 - 3000 \text{ ms}^{-1}$. Juga, berdasarkan keputusan bersepadu yang didapati dari teknik berbeza, zon 'slip surface' adalah diletakkan pada kedalaman 15- 23 m daripada permukaan tanah di mana bahan-bahan menunjukkan sejumlah perbezaan besar ciri berdasarkan halaju utama yang terhasil. Zon lemah berkemungkinan berlaku disebabkan oleh penyusupan air ke bawah melalui rekahan permukaan, di mana ini sangat melemahkan bahan-bahan sub-permukaan terutamanya melalui luluhawa kimia. Oleh itu, kajian ini membantu kita menyiasat dan meramal pelbagai sifat-sifat fizikal bahan sub-permukaan (tanah-tanah dan batu-batan) dengan kos yang lebih rendah dan mengaplikasikannya dalam memahami ciri-ciri struktur bawah tanah kawasan yang terdedah kepada risiko tanah runtuh.

Kata kunci: Tanah runtuh, Lubang Gerudi, Pembiasan Seismik, Tomografi Kerintangan Elektrik, Wenner –Schlumberger, Ujian Penembusan Piawai.

ACKNOWLEDGEMENTS

Firstly, all praises to Allah for giving me the strength and patience to complete this work and may peace be upon our Prophet and Messenger Mohammed SAW. It would not have been possible to write this thesis without the help and support of the kind and wonderful people around me, to some of whom it is possible to give particular mention here.

I would like to express my best thanks to my supervisor Prof. Dr. Ismail Bin Yusoff and co-advisors, Dr. Lakam Mejus and Dr. Rahman Yaccup for their support, direction, encouragement, and which enabled me to complete this study. I offer my regards and blessings to my family especially to my parents, my wife, my brothers and sisters for their encouragement and support.

I would like to thank several members of the Department of Geology, and Faculty of Science for their encouragement, discussion, critical evaluation and invaluable advice on different procedures of my thesis. Other than that, many thanks to the University Of Malaya for funding this work under the IPPP grant number PG214-2014B.

My gratitude goes to the Ministry Of Science Technology and Innovation (MOSTI) for funding the site visit and survey under the project number PKA0514D003.

Finally, I would like to thank my colleagues, friends and everyone who had contributed and helped to finish this work.

TABLE OF CONTENTS

ABSTRACT	iii
ABSTRAK	v
ACKNOWLEDGEMENTS	vii
TABLE OF CONTENTS	viii
LIST OF FIGURES	xii
LISTS OF TABLE	xv
LIST OF SYMBLOS AND ABBREVIATIONS	xvii
LIST OF APPENDICES	xix
CHAPTER 1: INTRODUCTION	1
1.1 Background	1
1.2 The Significance of the Site Selection.....	4
1.3 Research Aims and Objectives	6
1.4 Topography and Hydrology of the Study Area	8
1.5 Geology and Tectonic of the Study Area	9
1.5.1 Regional Geology	9
1.5.1.1 Site Engineering Geology	14
1.5.1.2 Bukit Tinggi Fault Zone.....	14
1.6 Outline of the Thesis	16
CHAPTER 2: LITERATURE REVIEW	18
2.1 Introduction	18
2.2 An Overview of Landslide Occurrence	18
2.3 Landslides Events in Malaysia	22
4.2 Classification of Slope Movements	26
2.5 Landslide Assessment.....	27
	viii

2.5.1	Geological Terrain Mapping.....	28
2.5.2	The Role of Geophysical Methods in Slope Stability Studies.....	29
2.5.2.1	Lithological Imaging Using Geoelectrical Measurements	31
2.5.2.2	Application of Seismic Refraction Imaging in Landslide Investigation	32
2.5.3	Isotopes Technique in Slope Study.....	33
2.5.3.1	The Use of Isotope Technique in Addressing Landslide Problems	34
2.5.4	Geotechnical Investigation	35
2.5.4.1	Hydrologic Boundary Determination Using Geotechnical Parameters	36
2.6	Joint Application of Geotechnical, Geophysical and Conventional Methods	37
2.7	Summary.....	40
CHAPTER 3: METHODOLOGY.....		41
3.1	Introduction:.....	41
3.2	Preliminary Field Investigation	42
3.2.1	Geological Terrain Mapping.....	45
3.3	Geophysical Techniques.....	47
3.3.1	Electrical Resistivity Tomography	47
3.3.2	Seismic Refraction.....	49
3.4	Geotechnical Methods	51
3.4.1	Standard Penetration Test	51
3.4.2	Rock Quality Designation.....	53
3.4.3	Consistency of Soil (Atterberg Limits).....	54
3.4.4	Point Load Index.....	56
3.4.5	Colloidal Borescope.....	56

3.4.6	Standpipe Piezometers	57
3.5	Environmental Isotopes	59
3.6	Summary	60
CHAPTER 4: RESULTS AND DISCUSSIONS		61
4.1	Introduction	61
4.2	GIS Application for Identifying Terrain Features	61
4.2.1	Slope Map	62
4.2.2	Terrain Component Map	63
4.2.3	Slope Activity Map	64
4.2.4	Erosion and Instability Map	65
4.2.5	Construction Suitability Map	66
4.3	Field Results and Interpretations	67
4.3.1	Joint Interpretation of Geophysical Dataset	68
4.3.2	Field-based Geophysical-Lithological Relationships	71
4.3.3	Groundwater Origin, Source and Flow Direction	77
4.4	Field and Laboratory-Based Results and Interpretations	84
4.4.1	SPT values	84
4.4.2	Atterberg limit	85
4.4.3	Rock mass Quality of Granitic Rock	87
4.5	Discussions	90
4.5.1	Significance of the Geological Terrain Mapping	90
4.5.2	Evaluating the relationships between geophysical and geotechnical properties	92
4.5.3	Weathering Zone Interpretation	105
4.5.4	Groundwater Dynamics and Flow Behaviour	105
4.6	Identification of Weakness Plane (Slip surface)	106

4.7	Summary.....	109
CHAPTER 5: CONCLUSIONS.....		111
5.1	Introduction.....	111
5.2	Conclusions.....	111
5.3	Recommendations and Future Work.....	113
REFERENCES.....		115
LIST OF PUBLICATIONS AND PAPERS PRESENTED.....		128
APPENDICES.....		130

University of Malaya

LIST OF FIGURES

Figure 1.1	: The main damages in the school compound. (A) elongated cracks on the retaining channel walls. (B & C) elongated cracks on the major school walls.	5
Figure 1.2	: Location of the study area in Pahang province, Malaysia. (a) plan view of the school compound and preliminary areas of investigation using geophysics (modified and based on Google Maps, 2018).	6
Figure 1.3	: The main river in the study area (Sungai Tanglir River).....	9
Figure 1.4	: Schematic geological map of the focus area (modified from Mineral and Geoscience Department 2015).	10
Figure 1.5	: The engineering geological map for the study area.	15
Figure 1.6	: Map showing the spatial relationship between the Bukit Tinggi earthquakes and the lineaments of the surrounding area (after Mustaffa Kamal, 2009).	16
Figure 3.1	: The general views of the methodological approaches used in this study.....	42
Figure 3.2	: Small scale slope failure can be observed near the SMK Bukit Tinggi area.	43
Figure 3.3	: The visual observation of elongated cracks in SMK site.....	44
Figure 3.4	: Initial conceptual model of the study area.	45
Figure 3.5	: A plan view of the school compound and preliminary areas of investigation using geophysical techniques (modified from Google Maps, 2018).	48
Figure 3.6	: Schematic diagram showing the basic principle of DC resistivity measurements (adaptation from Loke, 2004).	49
Figure 3.7	: The electrode array for Wenner - Schlumberger Configuration.....	49
Figure 3.8	: Creating seismic energy by vertically striking a solid metal plate with a sledgehammer.	50
Figure 3.9	: The image showing the skid drilling machine.	51
Figure 3.10	: The image showing a standard penetration test.	53
Figure 3.11	: The rock core sample. (a) The rock core for borehole (OW3), (b) the rock core sample for borehole (OW2).	54
Figure 3.12	: The collected soil samples.	55

Figure 3.13	: The equipment and procedure for Atterberg limits. (A, b, c) the liquid limit procedure. (F, g, h) the plastic limit procedure.....	55
Figure 3.14	: The Colloidal Borescope System instrument.	58
Figure 3.15	: Water level monitoring using a dipmeter.	59
Figure 3.16	: Collection of water samples by a manual bailer.....	60
Figure 4.1	: The slope maps percentage and degree of the study area.....	63
Figure 4.2	: Terrain Component Map of the study area.	64
Figure 4.3	: The slope activity map of the study area.	65
Figure 4.4	: The Erosion and Instability Map of the study area.....	66
Figure 4.5	: The construction suitability map of SMK Bukit Tinggi area.	67
Figure 4.6	: Plan view of the school compound and location of geophysical investigations (modified and based on Google Maps, 2018).	68
Figure 4.7	: The inversion results of the ERT surveys.....	70
Figure 4.8	: The results of seismic refraction tomography.	71
Figure 4.9	: The Correlation between SR Line 1 and borehole OW3.....	72
Figure 4.10	: The correlation between SR Line 2 and borehole OW5.....	73
Figure 4.11	: The correlation between SR Line 3 and borehole OW2.....	74
Figure 4.12	: The correlation between SR Line 4 and borehole TDR1.	75
Figure 4.13	: The correlation between RES 1 and borehole Log OW3.....	76
Figure 4.14	: The correlation between RES 4 and borehole Log OW5.....	77
Figure 4.15	: Variation of the water table in the study area.	78
Figure 4.16	: (a) Groundwater direction and velocity at OW-2. (b) Groundwater direction and velocity at OW-3.....	79
Figure 4.17	: Plot of δD versus $\delta 18O$ of water samples.....	80
Figure 4.18	: A comparison of seasonal changes of $\delta 18O$, δD and precipitation.	82
Figure 4.19	: The relationship between liquid limit with the depth of the sample.....	86

Figure 4.20	: The relationship between plastic limit with the depth of the sample.	87
Figure 4.21	: The relationship between plastic indexes with the depth of the sample.	87
Figure 4.22	: The relationship between RQD and depth in the study area.....	89
Figure 4.23	: The relationship between ERT and SPT values.	96
Figure 4.24	: (a) The SPT values generated from profile RES 1. (b) The SPT values generated from profile RES 2. (c) The SPT values generated from profile RES 4.	98
Figure 4.25	: The relationship between SR and SPT values.	99
Figure 4.26	: The relationship between ERT and SR values.	100
Figure 4.27	: The empirical relationship for UCS –P-wave values for SMK Bukkit Tinggi area.	101
Figure 4.28	: The relationship between SR, SPT, UCS and weathering grade for SR1.....	102
Figure 4.29	: The relationship between SR, SPT, UCS and weathering grade for SR2.....	104
Figure 4.30	: The Cross sections for SMK Bukit Tinggi area, showing predicted depths of assume slip surface, and weathered granite.	107
Figure 4.31	: The developed conceptual model for landslide prone area.	109

LISTS OF TABLE

Table 1.1	: The major landslides occurred reported in Malaysia from 1990 to 2016 (Haliza & Jabil Mapjabil, 2017).	3
Table 2.1	: The leading causes of landslides (USGS, 2004).	19
Table 2.2	: Classification of landslide movements (Varnes, 1978).	27
Table 3.1	: The geological terrain classification (JMG, 2006).	46
Table 3.2	: Construction suitability classification system (after Brand, 1988).	46
Table 3.3	: Construction suitability classes and types of site investigation (after Mohamad& Chow, 2003).	47
Table 4.1	: The velocity and direction of groundwater.	78
Table 4.2	: The rainfall amount in the study area.	80
Table 4.3	: The results of Oxygen and Hydrogen Isotopes.	83
Table 4.4	: The results of SPT values respect to the Depth.	84
Table 4.5	: The values of Atterberg limit with depth (LL is for liquid limit, PL for plastic limit and PI for plasticity index).	85
Table 4.6	: Rock Mass Classification from RQD Index (Deere et al., 1967).	88
Table 4.7	: The results of RQD with depth in the study area.	88
Table 4.8	: The Geological Classification of Granitic Rocks in the Study Area.	89
Table 4.9	: The results of the point load test index.	90
Table 4.10	: Weathered granite rock mass classification in Peninsular Malaysia. (Source: Extracted and adapted from Islamic Rofiqul@ Zaw Win 2005).	93
Table 4.11	: The obtained values for SPT, SR and ERT.	96
Table 4.12	: Listing of the UCS and PLI values from previous studies.	101
Table 4.13	: The relationship between UCS and weathering grade.	102

Table 4.14	: The relationship between P-wave velocity and Rock weathering grade obtained in the study area.....	105
Table 4.15	: Summary of the physical properties obtained from this study for SMK Bukit Tinggi area.	108

University of Malaya

LIST OF SYMBLOS AND ABBREVIATIONS

δ	: Delta
$\mu\text{m/s}$: Micrometers per second
Ωm	: Ohm-m
ASL	: Above sea level
ASTM	: American Society for Testing and Materials
CBS	: Colloidal Borescope System
DEM	: Digital elevation model
ERT	: Electrical Resistivity Tomography
GIS	: Geographic Information System
GPS	: Global positioning system
GRA	: Geohazards Risk Assessment
IRMS	: Isotope ratio mass spectrometer
LL	: liquid limit
LMWL	: Local Meteoric Water Lines
M	: meter
m/s	: meter per second
mA	: Milliampere
ML	: milliliter
Mm	: millimeter
MPa	: mega Pascal
N(60)	: Corrected SPT value
NW	: North West
PI	: plastic index
PL	: plastic index
PLI	: point load index

PWD	: Public Works Department
RQD	: Rock quality designations
SE	: South East
SMK	: Sekolah Menengah Kebangsaan
SPT	: Standard Penetration Test
SR	: Seismic Refraction
UCS	: Uniaxial compressive strength
V _p	: Primary velocity

University of Malaya

LIST OF APPENDICES

Appendix (A) : Field geophysical process.....	130
Appendix (B) : Sign of instability observation in the school compound.....	132
Appendix (C) : The summarized the Borehole Logs and tests.....	135

University of Malaya

CHAPTER 1: INTRODUCTION

1.1 Background

As a result of population growth and the extension of settlements over risky areas, the impact of natural disasters has increased. Slope failures, landslides and subsidence of foundation have been identified as the most commonly occurring natural disaster after floods. Slopes form either naturally due to the addition of materials on the topsoil, or artificially (man-made) due to the removal of materials by civil construction works. Slopes should remain stable as they appear; however, they are usually dynamic. The slopes possess an evolving system since the materials there are continually moving down at the rates that vary from the imperceptible creep of soil and rock to rock falls.

Landslide is defined as "the movement of a mass of rock, earth or debris down a slope" under the process of gravity (Rahman & Mapjabli, 2017). It can also be referred as mass movements, slope failures, slope and terrain instability. These processes will occur when the driving force is greater than the resistance force under the influence of gravity. Slope failures and landslides are considered as naturally-occurring disasters worldwide. These hazardous problems are high causes various levels of damages to properties and higher death toll to human.

In Malaysia, almost every year, especially during the monsoon season, the occurrence of slope failures and landslides are frequently observed and have been reported as the second most destructive natural disaster (Ismail & Wan Yaacob, 2018; Qasim *et al.*, 2013; Matori *et al.*, 2012). These naturally-occurring disasters cause the closure of roads, affect the foundation stability of the residential building, and in worse cases, cause casualties and huge economic losses (Jamaluddin, 2015; Lee & Abdul Talib, 2006; Sew, 2002). According to Pradhan and Lee (2010), landslide occurrence in Malaysia presents a significant limitation threat to development in many areas, and the

most triggering factor of these landslides is the heavy rainfall. Slope failures and landslide occurrences have resulted in a large number of casualties and huge economic losses especially in hilly and mountainous areas (Public Works Department, 2009). From 1993 to 2011 (Table 1.1), six major landslide occurrences (cuttings and natural slopes) have been recorded near to or within densely populated cities in Malaysia. These landslides resulted in more than 100 fatalities (Rahman & Mapjabli, 2017; Huat *et al.*, 2012).

Landslides normally happen due to intense infiltration during transient rainfall and under partially saturated conditions (Godt *et al.*, 2009). Most of the slope stability and landslide monitoring activities involve the detection of certain parameters that how they change over time. The two important parameters in monitoring landslide area are groundwater levels and ground movement. With the sudden uprising and lowering of groundwater table (pore water changes remarkably), changes in subsurface water and the presence of waterlogged or seepage against a slope in the vicinity of the suspected sliding zone tend to decrease the strength of cohesive soils, which may lead to land sliding.

The rainfall influence on landslides varies significantly depending on their extent, type, and materials, etc. Slope failures are frequently triggered by short intense storms (Paronuzzi *et al.*, 2002; Flentje *et al.*, 2000; Corominas & Moya, 1999; Crosta, 1998; Morgan *et al.*, 1997; Polloni *et al.*, 1992), while most deep-seated landslides are affected by long term variation of annual rainfall, which last for several years (Aleotti *et al.*, 2002; Bonnard & Noverraz, 2001).

Table 1.1: The major landslides occurred reported in Malaysia from 1990 to 2016 (Haliza & Jabil Mapjabil, 2017).

Date	Location	Impacts	Reports
December 11, 1993	Highland Towers Condominium, Kuala Lumpur	Block 1 collapsed, killing 48 people	There had been ten days of continuous rainfall
January 6, 1996	North-South Expressway, Kampar, Perak	Swept a container truck off the road, killing the co-driver of the truck	There was some accumulation of water at the top of the slope due to earlier rainfall
November 28, 1998	Paya Terubong, Penang	Blocked Jalan Bukit Kukus and 17 cars were buried	There were massive land clearances the top of the hill
January 28, 2002	Ruan Changkul, Simunjan, Sarawak	10 houses were destroyed, claiming 16 lives	The district has suffered from bad weather for more than one week
November 26, 2003	Bukit Lanjan, New Klang Valley Expressway, Kuala Lumpur	Blocked the entire expressway to the public for more than six months	Landslide occurred immediately after a period of heavy rainfall
May 31, 2006	Kampung Pasir, Ulu Klang, Selangor	Four people were killed	There was failure of a retaining wall
December 27, 2007	Kampung Baru Cina, Kapit, Sarawak	Three people were killed and nine families were made homeless	Landslide occurred after two hours of heavy rainfall
November 30, 2008	Bungalow in Ulu Yam Perdana, Selangor	Two sisters were buried alive	The incident has been caused by heavy rainfall
December 4, 2008	CIMB Commerce Square and Amanah Raya	Three hundred people were forced to evacuate the buildings	Heavy rain one day before had caused landslide at an adjacent hill
December 6, 2008	Taman Bukit Mewah, Bukit Antarabangsa, Ulu Klang, Selangor	14 bungalow houses were destroyed, five fatalities and injury to 14 people	Prolonged rainfall during the months of October and November
May 21, 2011	Madrasah Al-Taqwa orphanage, Hulu Langat, Selangor	Sixteen people (fifteen children and a caretaker) of an orphanage were killed	Landslide caused by heavy rainfall
29 Dec 2012	Kuala Lumpur		Landslide caused by heavy rainfall and soil movement
11 November 2015	Bukit Tinggi, Pahang and Gombak-Bentong		
January 2016	Bukit Tinggi, Pahang		
February 2016	Puncak Borneo area		

The task of predicting the exact causes of failure is often difficult as the point of ultimate failure is dependent on a number of factors such as slope condition, amount of rainfall, and rainfall intensity, geological condition, and land cover. The best-documented sign of impending failure is the assessment of the increase in the rate of

ground movement of any unstable / potentially risk slope area (localized zone) and how they change with time. Detailed analysis of the triggering factors is often hindered by the lack of information gathered from the field measurements (Tsai & Chen, 2010).

Risk assessment and evaluation in the landslide prone area can provide efficient and rigorous processes to enhance slope management. Moreover, risk assessment and evaluation are very important for engineering structures and are considered as powerful tools for understanding the kinematic aspects of mass movements through correct analysis and interpretation. Therefore, it would be useful to gather significant information for identifying the main causes and mechanism of landslides. The next section will identify the main problem chosen for this study and the significance of applying it in landslide research.

1.2 The Significance of the Site Selection

The study area encompasses an area of 10.09 acres (4.08 hectares) located at Secondary School Bukit Tinggi, Bentong, Pahang (Figure 1.2). The site is located close to Selesa Resort with the geographic coordinates 3°21'16.95"N 101°50'24.9"E. The site itself is easy to access, however, the area near the western boundary is hard to access due to the steep slope and moderate vegetation.

The Bukit Tinggi-Bentong area has a high probability of landslide occurrence. Historically, frequent occurrences of landslides have been reported from several places in Kampong Bharu, Bukit Tinggi-Bentong and Sg Tanglir - the Sg Benus catchment area since 2003. Furthermore, based on a geological survey conducted by Department of Mineral and Geosciences Pahang in 2015, the vicinity of Sekolah Menengah Kebangsaan (SMK) Bukit Tinggi in Pahang province, Bentong Pahang is considered as one of the natural terrain areas (weathered granite) prone to landslide hazards and should be effectively monitored prior to any future slope movements.

Early field observations in the study area revealed the occurrence of elongated cracks on damaged walls, parking lot and roadside (Figure 1.1) within the school premise. These indications are believed to be associated with ground movement at the vicinity of the school compound.

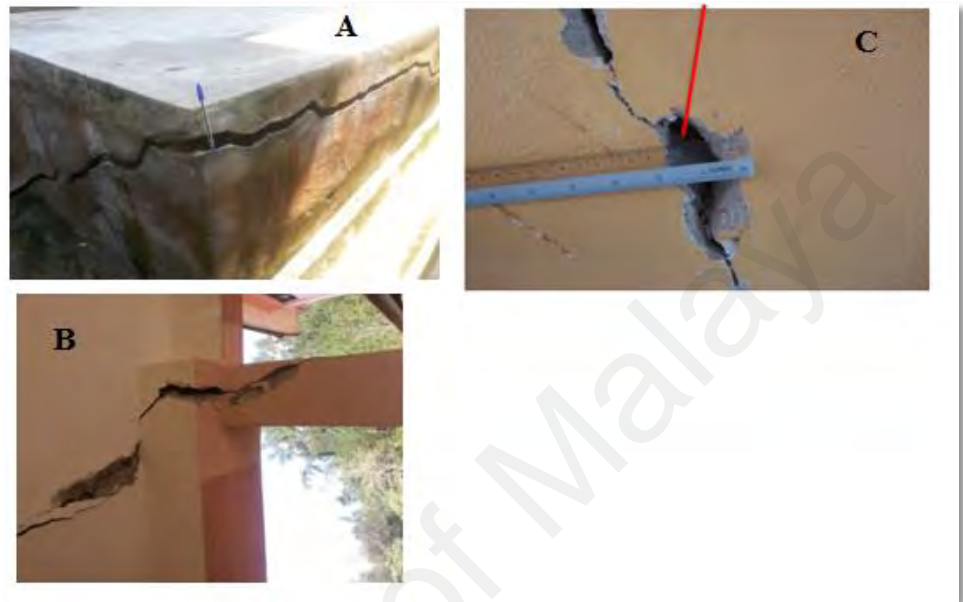


Figure 1.1: The main damages in the school compound. (A) elongated cracks on the retaining channel walls. (B & C) elongated cracks on the major school walls.



Figure 1.2: Location of the study area in Pahang province, Malaysia. (a) plan view of the school compound and preliminary areas of investigation using geophysics (modified and based on Google Maps, 2018).

This study provides an understanding about the triggering factors of a landslide in SMK Bukit Tinggi area and the suitable prevention methods. Additionally, this study gives some recommendations for future research works in the area.

1.3 Research Aims and Objectives

The aims of this study: 1) to assess and evaluate the current condition or the potential hazard caused by the ground settlement and movement in the school area by using the geotechnical, geophysical and environmental isotopes methods, 2) to understand and

predict the subsurface behavior that probably triggers landslide activities, 3) to suggest any protection action for reducing landslide hazards.

These aims are fulfilled by taking into account the following three main objectives:

1. To determine the geotechnical properties of soil and rock in the problematic location of the study area.
2. To determine groundwater dynamics and flow behaviour (origin, source and direction).
3. To define the efficiency of Combined Electrical Resistivity Tomography (ERT) and Seismic Refraction (SR) techniques with the geotechnical properties.

Geotechnical investigations are performed in order to obtain lithological sequence of the subsurface materials as well as to determine physical parameters of subsurface materials. These physical parameters such as standard penetration test (SPT), Rock quality designations (RQD) and point load test are important for defining the subsurface characteristics.

The standard penetration test (SPT) is an in-situ field test of soil, which presents an idea concerning the soil's shear strength. Meanwhile, the rock quality designation (RQD) is used as a standard parameter in drill core logging to provide a quantitative estimate of rock mass quality.

Recently, geophysical investigation has been widely used to assist other underground characteristics (Lapenna et al., 2003; Bruno & Marillier, 2000; Gallipoli et al., 2000; Hack, 2000; Mauritsch et al., 2000; McCann & Forster, 1990). Geophysical investigation has been widely employed for studying landslide since 1970s (Havenith et al., 2000; Hack, 2000; Caris & Van Ash, 1991; Bogoslovsky & Ogilvy, 1977) in order

to determine its physical characteristics and to provide useful information before planning constructions in the areas prone to landslide.

The isotopic fingerprinting was used to assess the origin of groundwater in the landslide prone areas, and to qualify and quantify the aliquot of groundwater from deep water inflow to prevent an area from becoming prone to landslide.

1.4 Topography and Hydrology of the Study Area

The main topography of the site is mostly categorised as an excavated platform at the centre and surrounded by a cut and fills within the school's boundary based on the data collected during construction's period. Based on topographical survey plan provided by a licensed surveyor, the highest point of the proposed development site is approximately 310 m ASL(above sea level), and it is located in the south of the study area. The lowest point is approximately 262 m ASL and is located in the eastern part of the study area.

Field mapping (terrain and geological) was carried out during dry season, and visible surface runoffs were observed within the study area. About two meters wide stream was observed at the western boundary of the study area (Figure 1.3). This suggests that the groundwater table is relatively high in that particular area, especially during rainy seasons. The main river (Sungai Tanglir) is observed to be adjacent to the proposed development area.



Figure 1.3: The main river in the study area (Sungai Tanglir River).

1.5 Geology and Tectonic of the Study Area

1.5.1 Regional Geology

The study area is situated in the central part of Pahang State, east side of the main range of Peninsular Malaysia. The regional geology of Bentong and the surrounding areas are summarised in the simplified map shown in Figure 1.4. The surrounding areas of the studied location are underlain by strongly folded and, thermally metamorphosed argillaceous and arenaceous Lower Devonian rocks along with a sequence of folded Middle to Upper Triassic sedimentary rocks. The rocks are in turn by Late Triassic granite. Quaternary alluvial deposits occur in the river valleys and floodplains.

The Karak Formation, approximately 6 km width, is the oldest rock unit in the region; which flanks the eastern side of the Main Range Granite. It was earlier mapped as ‘Arenaceous Formation’ (Richardson, 1939), ‘Foothills Formation’ (Richardson, 1950) and ‘Lower Arenaceous Series’ (Alexander, 1950). The formation is tightly folded and faulted, with the strata dip steeply to the west towards the Main Range granite. The stratified Karak Formation comprises predominantly of argillite with

interbeds of conglomerate, chert, quartzite and subgreywacke, in the upper part of the formation there are minor occurrences of bedded rhyolite tuff and crystalline limestone. Adjacent to the granite contact, a narrow aureole of metamorphosed slate, phyllite, low-grade schists and hornfelses occur (Shu, 1968).

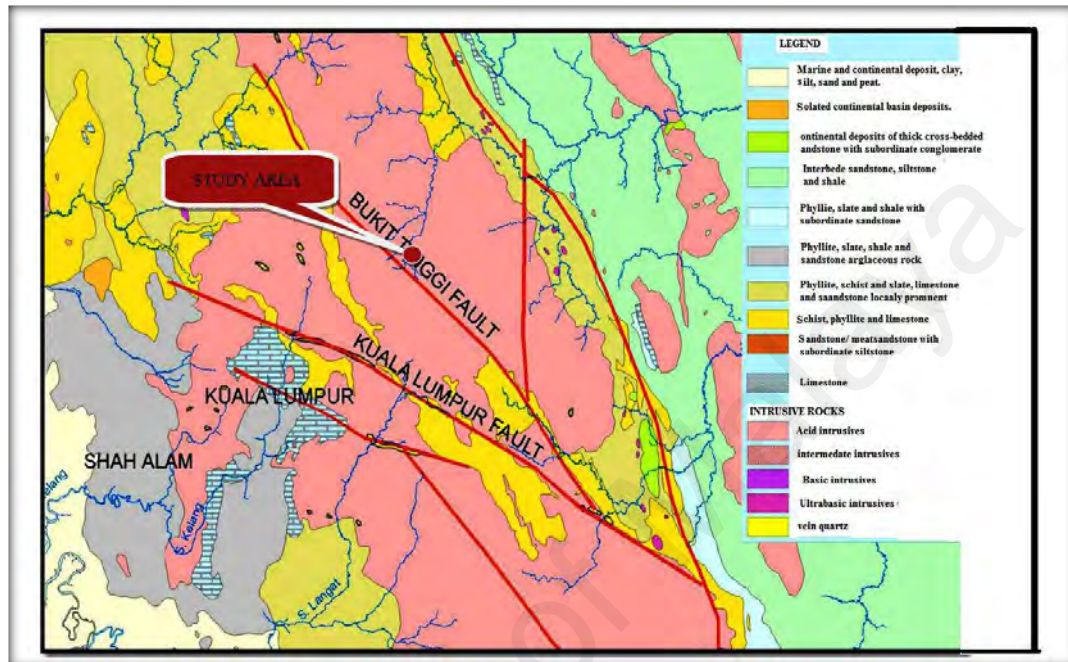


Figure 1.4: Schematic geological map of the focus area (modified from Mineral and Geoscience Department 2015).

The following rock unit in the area is Raub Group that consists of two formations: The Semantan Formation, made up mainly of carbonaceous shale interbedded with rhyolite tuff and minor intercalations of limestone, chert, and sandstone; and the Kaling Formation which is made up of sandstone and conglomerate with subordinate amounts of shale and rhyolitic tuff. Intrusive igneous rocks of mid-Palaeozoic times are represented by basic and ultrabasic bodies, which make interfoliated with the schists and quartzite of the Karak Formation. The second period of intrusive igneous activity resulted in the emplacement of the Main Range and Manhis granite batholiths, the Bukit Besar sodium-rich igneous complex, and the Bukit Woh porphyries. The granite batholiths consist mainly of coarse-grained material, with numerous minor occurrences of fine-grained late-phase differentiates. The Bukit Besar igneous complex comprises a

suite of rocks ranging in composition from diorite to adamellite. The Bukit Woh igneous mass is essentially intrusive acidic porphyries, and also include a subordinate extrusives phase of the rhyolitic composition. The emplacement of the igneous bodies caused wide-spread earth movement, resulting in fracturing and shearing in the solidified rocks. Pneumatolytic and hydrothermal activity related to the intrusion of the Main Range and Manchis granitic magmas then resulted in the deposition of tin-bearing mineralisation along with the fractures in the granitic rocks and adjacent metamorphosed sediment. In the Bukit Woh porphyries, these late stages of magmatic activity are associated with lead and zinc mineralisation (Hutchinson & Tan, 2009).

River alluvium which comprises beds of unconsolidated gravel, sand, and clay (products of erosion of the older rock formations), are found unconformably overlying the older rock formations. They are most extensive in the plains of river valleys including Sungai Bentong, Sungai Semantan, Sungai Perting and Sungai Pahang. The average thickness of the alluvium is less than 4.5 m. The alluvium is often stanniferous and has been largely mined in the past. Hence, some of the area covered by alluvium is presently consisting of the mined-out area with tailings and mining ponds. In some parts, the mining ponds and low-lying mined-out areas are filled with recent sediments. A lesser widespread occurrence is the superficial deposit recognised as loosely consolidated rhyolite ash that was found by Alexander (1939).

The stratified rocks in the region have been folded into a series of anticlines and synclines, and in general, the fold axes strike NNW-SSE, with local variations in the strike near the margins of the igneous bodies. Meanwhile, faults occur more commonly in igneous bodies. The Main Range Granite and the Karak Formation are cut by a major north-south normal fault with dextral displacement.

The main outcropping rocks are different from the western part toward the east, and the rocks are presented as Karak formation, Bukit Tinggi Granite, Genting Sempah

pluton, and Bentong-Raub suture zone. The following is a brief description of these rocks:

Karak formation is developed immediately to the east of the main range granite (Alexander, 1968). These rocks characterized by well developed foliation, SSE striking and steeply dipping. The dominant rock types are mica schist, quartz-mica schist and metaquartzite. The garnet crystals are large and occur locally in Bentong area. These series commonly contain phyllite and slate. And the sweat-outs feature is the occurrence of quartz, the fine-grained aggregates of quartz, biotite, and chlorite are the main components of hard compacted rocks in the granite contact area (Cobbing & Mallick, 1986). *Bukit Tinggi Pluton* is elongated in NW-SE directions with a diameter of 90x20 km and situated between Bukit Tinggi Fault and Bukit Sempah plutonic. This pluton is bounded by Lower Paleozoic strata in the eastern and western sides. Some of the pluton rocks are affected by cataclastic deformation and overlain by large alluvial deposit on both sides of the pluton. This widely distributed pluton is represented by the Gap Granite Unit, Ulu Kali Unit, Senaling Unit, and Rodah Microgranite Unit. *The Gap Granite Unit* is widely distributed and mainly concentrated in the margin region. Additionally, this unit forms most of the outcropping plutonic rocks, and in which extreme appear in the western part near Kuala Kubu Bharu. The rocks are mainly dark grey and consist of brown single crystals of biotite (5-15%) and chlorite with varying degree of intensity, quartz (25-35%), which is surrounded k-feldspar megacrysts which give the rock a nodular appearance, white euhedral of plagioclase (15-25%) crystal which were replaced by muscovite and k-feldspar (Cobbing & Mallick, 1986). The over texture is allotriomorphic granular with the unehedral, intergrown junction between k-feldspar and quartz. The outcrop of *Ulu Kali Granite Unit* are observed in the Genting High Land Road, Karak Highway, the quarry of Bentong, and the stream section in the south of Karak. Most rocks of this unit are affected by cataclastic

deformation, as well marked in the Genting Highland section, but in the Karak Highway, foliated granite dykes cut the Gap Granite and incorporate xenoliths of those rocks. *The Senaling Granite Unit* is exposed in the upper part of stream courses to the west of Telemong, in which the rocks are mainly weathered, and have medium-grained equigranular granite with sporadic k- feldspar megacrysts and groundmass of separate speckly appearance. The minerals of these rocks are mainly; bright black biotite (7-10%), subhedral grey-white k-feldspar (5%), a single globular cluster of quartz (25-35%), and brown euhedral plagioclase (2-10%) (Cobbing & Mallick, 1986). *Rodah Microgranite* is widespread and found as dykes or sills, and as a small pluton. Because of poor exposure, limited access and security issue, the dimensions of these bodies could not be established. Nevertheless, it has been established that small bodies of these rocks cut the gap granite at the eastern end of the Karak highway section and also the Ulu Kali unit to the north-west of Bentong. These rocks appear not to be foliated, but major cataclastic deformation has been observed in the Sg Preting and Karak highway areas. It contains biotite (5%), euhedral tabular k-feldspar (5-25%), blue rounded and corroded quartz (5-10%), brownish plagioclase (5-10%), and quartz and plagioclase megacrysts (50-80%) in grey groundmass. *The Genting Sempah Pluton* is a major body which is approximately 10x35 km in size and occupies the central part of the main range batholiths to the east of Kuala Lumpur. It is located between two major faults, the Bukit Tinggi Fault on the northeast flank and the Kong Koi fault to the south-west. In this pluton, microgranite changes to rhyolite near to contact, and identical rhyolite dykes were observed to have cut the Sempah conglomerate (Haile, 1970). *The Genting Sempah Unit* is a very massive fine to medium grained body with small fractured megacrysts of quartz, feldspar, and biotite. The petrography of this unit consists of quartz, k-feldspar, and plagioclase minerals which are commonly irregular or angular in shape. The groundmass is very fine grained and appears to be composed of small

rounded quartzes. *Bentong-Raub Suture Zone* is representing the Palaeo-Tethys in Peninsular Malaysia. It is a southward extension of Nan-Uttaradit and Sra Kaeo suture of Thailand. This zone contains ribbon chert, which has been dated from the Upper Devonian to Upper Permian period (Metcalf, 1999). Graptolite in the associated slate of Tuah Estate in the south of Karak is dated back to the Lower Devonian period (Jones, 1970). Limestone clasts in *mélange* are from the Lower and Upper Permian ages.

1.5.1.1 Site Engineering Geology

The geology of the site consists essentially of granitic rock. Mainly consist of highly porphyritic very coarse-grained biotite granite, medium porphyritic coarse-grained biotite granite, porphyritic medium coarse-grained biotite granite and non-porphyritic fine-grained biotite granite. The granite boulders have been observed along the school boundary.

The site is covered mostly by the weathered granite and backfills material (Figure 1.5). Moreover, the terrain has undergone weathering to form residual soils of varying thickness. The color of the zone is generally reddish brown and the texture dominated by silty sand that covers the surface of the entire area.

1.5.1.2 Bukit Tinggi Fault Zone

The Bukit Tinggi Fault is a sinistral fault trending NW-SE; and mainly situated in the north of the Kuala Lumpur Fault Zone (Stauffer, 1968). This fault is traced up to Kuala Kubu Bharu (Shu, 1969). In contrast to the Kuala Lumpur Fault Zone, curvilinear trace of this fault zone is separated and strongly expressed. On the radar shuttle radar topography mission (SRTM DEM) and satellite Synthetic-aperture radar (StereoSAR) imageries, this fault zone is clearly visible and extended up to 120 km. covering an area northwards along the boundary between granite and country rock up to Perak.

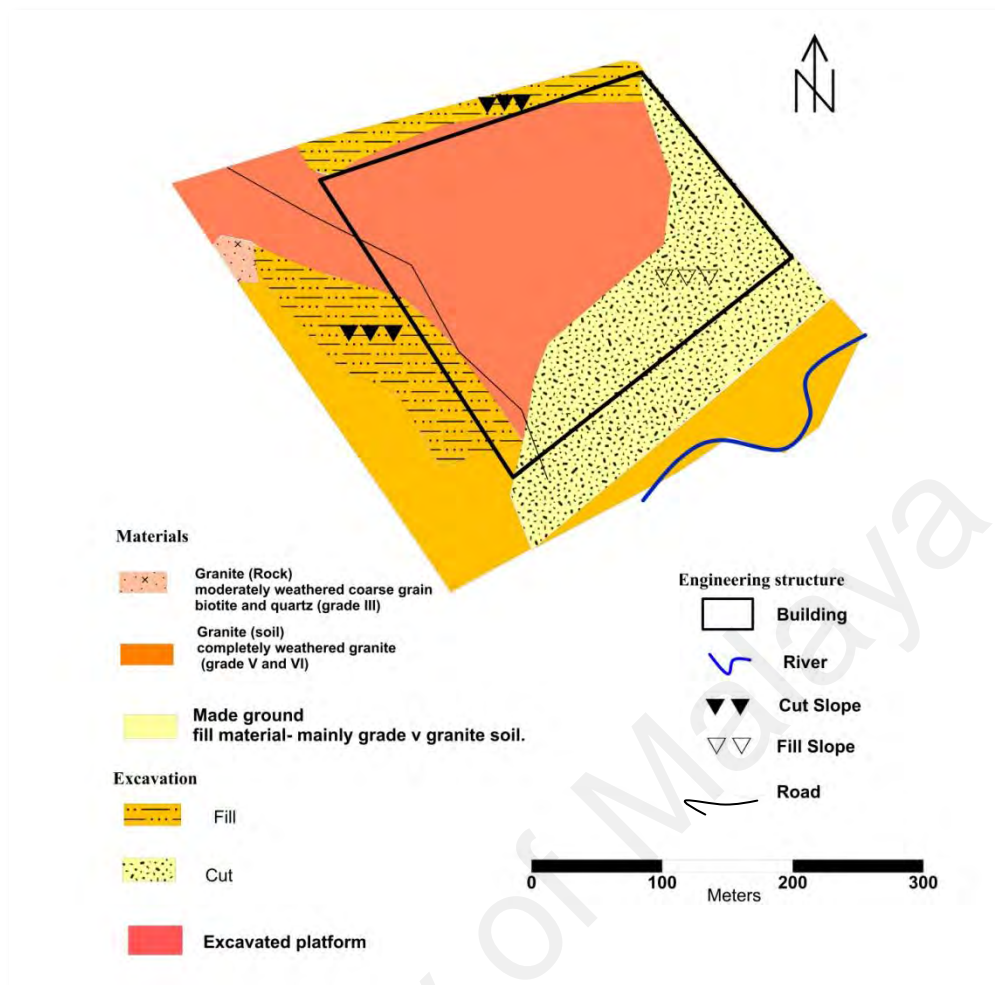


Figure 1.5: The engineering geological map for the study area.

This fault zone is distinguished by mylonites, large quartz veins and fault breccias. Field and microscopic studies on the mylonites confirm that the early ductile microstructures were greatly imprinted by younger brittle-ductile structures. Inside the mylonites, a stretching lineation and distinct foliation appeared as elongated quartz and symmetric to asymmetric lenses of feldspar. The inclined stretching lineation in the mylonites along this fault illustrates it as a strike-slip with the essential dip-slip element (Shib, 2009).

Previous research on the Bukit Tinggi fault mylonite indicated that the initial ductile motion had a dextral sense of shear (Ng, 1994) except along the Karak Highway and Kuala Kelawang, in which the movements were sinistral (Zaiton Haron, 2002). Moreover, this fault has several active strands as evident from several hazardous

earthquakes were recorded in Bukit Tinggi area (Shuib et al., 2017). Such earthquake strands in future can thus trigger a landslide in this area.

Since 30 November 2007, 23 earthquakes have occurred in Bukit Tinggi and the surrounding areas (Figure 1.6). Although these earthquakes were mild, and no signs of damages were reported, but any future tremors can trigger landslide hazards in the area.

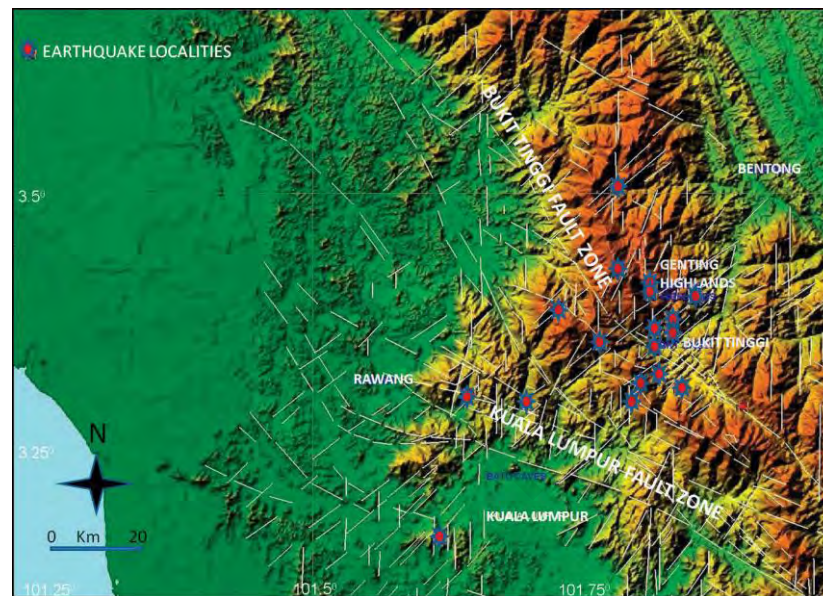


Figure 1.6: Map showing the spatial relationship between the Bukit Tinggi earthquakes and the lineaments of the surrounding area (after Mustaffa Kamal, 2009).

1.6 Outline of the Thesis

The main goal of this thesis is to assess and evaluate the ground and underground condition within and around the school area by using different methods. To achieve this goal, an integrated geotechnical, geophysical and environmental isotopes methods are used to investigate and mitigate potential landslide hazard in the area.

In order to document the findings and achievements of this research project, the thesis is divided into five chapters as follows:

Chapter-2 explain the status of a landslide occurring and investigation by the geotechnical, geophysical, and environmental techniques. This chapter also presents the mechanism of landslide triggering factors and the methods used in previous research to mitigate the landslide hazard.

Chapter-3 presents the methods and materials used for this study in Bukit Tinggi area, and the procedure to identify subsurface structures, particularly weak zones in the area.

Chapter-4 describes the results and the interpretation of the obtained data that has been used in evaluating and assessing the Bukit Tinggi area. Moreover, this chapter can assist for the estimation and prediction of the properties of the subsurface material (soils and rocks), especially in reducing the cost of investigation and increasing the understanding of the Earth's subsurface characterizations physical parameters.

Chapter-5 focuses on the conclusion for this study and recommendations for future work.

University of Malaya

CHAPTER 2: LITERATURE REVIEW

2.1 Introduction

This chapter presents a broad overview of the landslide related problems globally and specifically in Malaysia along with the strategies to assess and reduce their adverse impacts. The mechanisms that triggered landslides and their contributing factors are also included and discussed in detail. Moreover, this chapter presents examples of various studies accomplished on broader overview of the topic, to achieve a certain level of understanding on the matter, and to identify the current state of research on the issue.

2.2 An Overview of Landslide Occurrence

Landslide is a major naturally-occurring disaster, which causes significant socioeconomic damage and losses. One of the main factors that accelerated their occurrence globally is climate change (Bennett *et al.*, 2016). The Centre for Research on Epidemiology of Disasters (CRED) 2015) recorded that landslides account for more than 17% of the deaths from most of the natural hazard events. The occurrences of landslides have caused billions of dollars damages and have left thousands of people dead and injured each year (Rahman & Mapjabli, 2017; Laccase & Nadim, 2009). Globally, a total of 4862 fatal landslide events were recorded between 2004 and 2016, excluding those triggered by earthquakes (Froude & Petley, 2018). The spatial distributions of landslide events have no clear pattern, but the countries that have significantly higher rates of landslide incidences are Central America, the Caribbean Islands, South America, East Africa, Asia (making up to 75% of the total landslides), Turkey, Iran and the European Alps (Froude & Petley, 2018).

Table 2.1 lists the possible triggering causes of landslides events, including heavy rainfall, snowmelt, water level changes, volcanic eruption, earthquakes and slope geometry changes. In some cases, landslides may occur due to numerous causal factors (PWD, 2009).

Vast amounts of research that have been documented in the literature examined multiple issues associated with landslides and the possible prevention or reduction in their frequency and intensity (Wu *et al.*, 2015; Kalkan *et al.*, 2005; Hartinger *et al.*, 2000; Vichas *et al.*, 2000; Ahmad *et al.*, 1999; Çelik *et al.*, 1999).

Table 2.1: The leading causes of landslides (USGS, 2004).

Geological Causes	Morphological Causes	Human Causes
Poor/Susceptible materials	Weathering effects Freeze/thaw shrink/swell	Digging of slope
Splitting, Jointing, Shearing in materials	Tectonic/Volcanic pressure	Pumping out Leakages, Irrigation Mining
Negatively acquainted (Faults/Bedding etc.)	Accumulation loading slope/crest	Cutting of forests
Contrast to permeability, Material stiffness	Piping/Erosion Removal of vegetation	Encroachments on slopes

In the last thirty years, landslide studies have been carried out in various regions of the world. For instance, Tang (1991) carried out a study on outcropping weathered granitic rocks in the Kartum Stream in Sudan and correlated it to the possible landslides occurrences. The author reported that a typical landslide observed in the stream was affected by the climate conditions, especially during the wet season due to rainfall which raises the water level in the stream embankment, thus increasing the pore water pressure in the embankment rocks, and increasing the possibility of landslide occurrence. Moreover, in China, Wu and Tianchi (2001) identified the mechanics, characteristics, types and dynamics of debris flows and the damage they cause to infrastructure and agriculture. Their classification is based on viscosity, composition, triggering factors, origin, and scale. Their study also assisted in differentiating between debris flows, landslides and similar phenomena. Five different approaches were suggested to classify the debris flows rooted in the viscosity, composition, triggering factors, origin, and scale. The authors also summarised variations between debris flows

and other related phenomena, for instance, landslides and floods. Carey *et al* (2018) studied the displacement mechanisms of slow-moving landslides in response to changes in pore water pressure and dynamic stress in New Zealand. The authors used laboratory experiments to evaluate the pore water pressure and stress for collected samples. The results indicated that the displacement rates are influenced by an absolute stress state component and a transient stress state component.

Many landslides triggering factors including both natural and human-made were studied by different researchers. For example, Nutalaya (1991) identified several factors contributing to landslides and sheet flooding, especially during the rainstorm event: (1) significant deforestation of areas, which caused the erosion of steep slopes; (2) a slope gradient exceeding 35% resulted in the deposition of alluvial causing flooding; and (3) and the granitic rocks were deeply saturated with residual sand. Bronnimann *et al.* (2011) studied the landslide triggering mechanisms based on geological, geotechnical and geophysical datasets. The datasets for the slope stability analysis were collected from topographic investigations and geological mapping whereas the soil geotechnical parameters were collected from a series of in-situ tests. A geophysical survey was applied using a vertical electrical soundings method in order to detect the existence and continuity of a potential sliding surface. The authors found that landslide occurrences are due to quick groundwater flow through the fractured rocks, which increased the hydraulic head and build up the pore water pressure in the fractured rocks. Furthermore, Owen *et al.* (1995) examined the landslide induced by earthquake using landscape maps to evaluate their responsibility as natural hazards. The authors concluded that avalanching was the major landslide process that occurred during the earthquake. On the other hand, the heavy monsoonal rains were most devastating in the lower reaches of the valleys where the rivers actively eroded steep rocks and debris slopes, and road construction had created cut into slopes. The ground conditions, geology and

geomorphology of the area were studied for their role in the distribution of mass movements, a hazard map was produced, and high-risk areas were identified. Kuo *et al.* (2018) studied the critical rainfall conditions for large-scale landslides in Taiwan. The authors analysed the seismic record against the intensity of rainfall records. The results indicated that three general rainfall threshold models and the vital factors of an estimate warning model were found to be the duration and effective rainfall.

The landslide risk assessment and methods were studied in different forms, Tingsanchali (1989) suggested two methods for controlling big landslide in Thailand. The author used structural control measures and non-structural control measures to avoid the possible impact of the hazard. Structural control measures applied the engineering techniques while non-structural measures used knowledge, practice or agreement. The author attempted to determine which method was best suited for controlling the debris flow depending on the extent and geo-material characteristics of the area. In addition, socioeconomic, financial and political factors were also important considerations. The evaluation landslide methodology was developed by Morgan *et al.* (1997) in Medison Country, Virginia, United States. The author's works resulted in the development of a method to identify areas subjected to debris flow hazards, i.e. Carbon-14 dated method was used to understand the repetition interval of the debris flow proceedings and, was verified based on the stratigraphy study for recurrent intervals interpreted from the carbon-14 dating of the prehistoric debris flows. The authors also suggested strategies for reducing debris-flow hazards and the studied location and its surrounding area. Additionally, Fathani *et al.* (2016) suggested an integrated methodology to develop a standard for landslide evaluation by using seven early warning sub-systems. These included risk assessment and mapping, dissemination and communication, the establishment of the disaster preparedness and response team, development of an evacuation map, standardised operating procedures, installation of

monitoring and warning services, and local commitment for operating and maintaining the programme. The authors found that the implementation of an early warning system is effective in a risky area and can be applied, but with some limitation such as sustainment of the device during the landslide event.

The geographic information system (GIS) method is the most commonly used for analysing landslide characteristics due to its efficiency and broad coverage. It supports subsurface mapping of soil slopes for predicting the weak zones (Broeckx *et al.*, 2017; Alvioli *et al.*, 2016; Pradhan *et al.*, 2012; Oh & Lee, 2011; Sezer *et al.*, 2011; Pradhan, 2010; Ayalew *et al.*, 2005; Syed Omar *et al.*, 2004; Dai & Lee, 2002; Gritzner *et al.*, 2001). GIS also has been proven effective in identifying regions with a high likelihood of slope failure (Ali *et al.*, 2018; Oh & Lee, 2011). However, A limitation of using GIS is that it collects only surface horizontal motion data for the topographical expression of slope failure, whereas motion data concerning within the rock and soil cannot be accessed (Zhu *et al.*, 2011; Jongmans & Garambois, 2007). The next section of this review introduces the Malaysian experience for assessing and evaluating the triggering factors of landslides and the methods used to do so.

2.3 Landslides Events in Malaysia

Landslides are major causes of fatalities in Malaysia and the second most damaging natural disaster after floods (Kazmi *et al.*, 2016; Matori *et al.*, 2012). According to the Malaysian Public Works Department (PWD) (2009), the total economic loss due to landslides was estimated at approximately 5 billion US dollar. The first major recorded landslides in Malaysia occurred in 1919 at Bukit Tunggul, Perak State. This landslide caused 12 fatalities and damaged properties. Landslides often become serious threats to residential and commercial structures including transportation, highways, waterways, pipelines, and other structures (Pradhan & Youssef, 2009). This list indicates that landslide can cause large socioeconomic damage and losses. Additionally, large-scale

landslides usually occur only after the areas have been developed. Unnecessary disasters and significant economic losses could have been avoided if the geohazards that caused the large-scale landslides were identified and assessed prior to the development. Hence, prior to any infrastructural development, the planners should consider the influencing factors of the large-scale landslides in their development plans (Jamaluddin, 2015).

Landslides in Malaysia are often triggered by heavy rainfall which varies with changing water level and with slope geometry. The primary factors causing slope failure in hillside developments in Malaysia are rainfall and stormwater activity (Matori *et al.*, 2012; Lee *et al.*, 2011; Sezer *et al.*, 2011; Huang *et al.*, 2008; Friedel *et al.*, 2006). The most common types of landslides in Malaysia are shallow slides where the slide surface is usually less than four metres deep, and their occurrence is usually during or immediately after intense rainfall (Ting, 1984, Jamaludin, 2015). Malaysia has an estimated 21,000 landslide-prone areas of which 16,000 or 76% are in Peninsular Malaysia while 3,000 are in Sabah and 2,000 in Sarawak State (Rahman & Mapjabli, 2017). Majority of the landslides occurred on cut slopes or embankments alongside roads and highways in mountainous areas. Some landslides also occurred near high-rise apartments and residential areas.

Furthermore, over the last decade, there have been several catastrophic landslides as reported by Lee & Pradhan (2006). Malaysian PWD has identified more than 100 hill slopes as being at high risk of possible landslides (Mukhlisin *et al.*, 2010). Jaapar (2006) compiled a list of landslides in Malaysia from 1990 to 2004 and found that most of them were classified as highly risky to human life.

Due to the high occurrence of landslide events in Malaysia, many geological and geotechnical studies have been carried out to address this problem. Most of these studies used GIS to create a final hazard map for the areas prone to landslides. For example,

Sew and Tan (2006) studied the causes of slope failure using abuses of the prescriptive method and found that 60% of the 49 cases from 2000 to 2006 of slope failure in Malaysia are man-made, which were due to either design or construction errors. Most cases of slope failures in Malaysia are attributed to human factors such as unregulated construction, incompetence, lack of maintenance system, ignorance of geological elements, unethical practice and various harmful human attitudes (Jamaluddin, 2006). Based on the study conducted by Jamaludin and Hussien (2006), the slope assessment projects carried out in Malaysia can be divided into large-scale or medium- to small-scale assessments. Large-scale assessments are broadly used in prioritizing slope maintenance along roads and highways, while medium- to small-scale assessments are used for controlling development in hilly areas. Meanwhile, Roslee *et al.* (2010) studied the importance of geological engineering inputs to landslide hazard occurrences in the Trusmadi Formation slopes, Sabah state, Malaysia. The authors used the engineering properties of soil samples, which indicated that the failing materials consist mainly of poorly graded silty clay soils characterised by low to intermediate plasticity content. The authors also recommended that the geological factor evaluation should be prioritised and included in the initial steps of all infrastructure programmes; which may play a vital role in landslide hazard and risk assessment to ensure public safety. Chigira *et al.* (2011) compared landslides in weathered granitic rocks from Japan and Malaysia. According to them, many landslides have been induced in weathered granitic rock areas by rainstorms in Japan, killing nearly 1500 people since 1938. Some major landslides in Malaysia are also associated with weathered granitic terrain, which killed more than 200 people.

The landslide characteristics have further been analysed by Pradhan and Lee (2010), which focus on landslide risk analysis using an artificial neural network model on different training sites. The landslide hazard indices were calculated using the trained

back-propagation weights, and the landslide hazard map was created using GIS tools. According to the authors, the hazard map could be used to estimate the risk to population, property and existing infrastructure. Moreover, the susceptibility map of landslides at Klang Valley was produced by Pradhan (2010). The author's susceptibility map was based on the calculated fuzzy membership values and fuzzy algebraic operators, which was verified by comparing it with the existing landslide locations for calculating the prediction accuracy. Among the fuzzy operators, the author found that the gamma operator ($\lambda = 0.8$) showed the best accuracy (91%) while the fuzzy algebraic product showed the worst accuracy (79%) in the prediction of landslide locations.

According to the previous study (Shuib, 2009); landslide in the study area was probably caused by the Bukit Tinggi fault. The author explored the role of geological structures and their relationship to the earthquake events using the SRTM digital elevation model. The author's results show that the source of earthquakes is located at or near to the intersection of three sets of major lineaments trending N-S, NW-SE and NE-SW. This corresponds to the N-S faults, the NW-SE Bukit Tinggi and Kuala Lumpur fault zones and the NE-SW faults, respectively. This study thus indicates an evident and direct relationship between the earthquakes and the geological structures of the area. Furthermore, Shuib *et al.* (2017) studied the active faults in Peninsular Malaysia with an emphasis on the active geomorphic features of the Bukit Tinggi region using IFSAR and field verification. They found that several segments of the Bukit Tinggi fault are active and can be considered as potential sources of earthquakes in the area. Any future activity along this fault can thus result in significant damage by earthquake tremors in the future.

It is, therefore, recommended that concrete, many actions should be taken to mitigate hazards in landslide-prone areas, such as modified land-use planning; standardizing codes for excavation, construction; and protecting the existing developments. National

Slope Master Plan (2009-2023) provides an integrated and efficient action plan for mitigating risk from landslides on slopes nationwide. Since 2013, the works have begun on an early warning system that can send out alerts at least two hours before a landslide occurs (Rahman & Mapjabli, 2017).

2.4 Classification of Slope Movements

Gravity produces stress in downward on the material in natural and artificial slope. The geometry of the slope contributes to the downward force as steeper gradients place more pressure on the materials for greater displacement, thereby making the landslide more likely and intense. Geomorphologists characterise these processes as mass wasting or mass movement, otherwise known as landslides. These terms can be confusing if they are not defined each time they are used. Varnes (1987) suggested that slope movement can be used as a comprehensive term for any downslope movement of earth materials.

There are several classifications of slope instability proposed by different researchers (Hutchinson, 1988; Varnes, 1978; Sharpe, 1938). These classifications are based on the grouping of characteristics such as the material, geometry, mechanics, deformation, and movement, among and some others. These characteristics constitute vital factors for understanding, predicting, and preventing slope failures.

Additionally, Varnes (1978) suggested a classification system of landslides based on the type of movement (Table 2.2), with the type of material being used as a secondary classification tool. The advantage of this classification is the recording of movement and materials of landslides, which can be used to classify past events. It also detects the mechanism of deformation, which is important in the analysis of slope stability.

Table 2.2: Classification of landslide movements (Varnes, 1978).

Movement type	Material classification		
	Bed rock	Engineering soils	
		Mainly coarse	Mainly fine
Falls	Rock fall	Debris fall	Earth fall
Topples	Rock topple	Debris topple	Earth topple
Slides	Rotational	Rock slide	Debris slide
	Translational		
Lateral spreading	Rock spread	Debris spread	Earth spread
Flows	Rock flow	Debris flow	Earth flow

2.5 Landslide Assessment

Landslides refer to the likelihood of slope failures for a specific area and period (Canli *et al.*, 2018; Guzzetti *et al.*, 1996). There is a scientific reason for each landslide, and it does not occur without warning if the failed or potentially unstable slope area is well monitored.

In recent years, landslide assessment has become a leading subject for researchers and decision-makers to understand the natural phenomena, and it is used as an approach to predict hazards in the future (Aleotti & Chowdhury, 1999). Many studies are conducted to assess landslides and probable reduction in losses of life (Kalkan *et al.*, 2005; Vichas *et al.*, 2001; Hartinger *et al.*, 2000; Çelik *et al.*, 1999; Barberalla *et al.*, 1988). Moreover, deformation measurement and analysis are used together to evaluate the site risk, deformations are directly concerned with human life and safety (Kalkan, 2007, Kalkan & Alkan, 2006).

The landslide hazard assessment is one of the most useful tools to predict and reduce the magnitude of hazards. A national research centre in Italy conducted a review in the year 2000 about the experiences of landslide assessment and monitoring; the

instruments used and discussed some example of landslides and the main problem in the installation of instruments.

Zaki *et al.* (2014) monitored and evaluated the stability of soil slopes, methods and feasibility of acoustic emission technique. Prior to this technique, several other techniques have been used to monitor the stability of slopes, such as the global positioning system (GPS), the GIS, aerial photography, Acoustic emission (AE) and inclinometers. The authors found that by using AE, the prediction for the stability of soil slopes can be more precise. The authors further stated that the acoustic emission could provide an effective solution for detecting early activities related to landslide development and provide early warning of such failures. Several landslide risk assessment methods which are the focus of this study were presented in their report.

2.5.1 Geological Terrain Mapping

Terrain mapping is defined as a process of dividing the landscape into polygons based on a terrain classification system. It provides information about present-day geomorphological processes (Abd Manap *et al.*, 2010; ESTFBC, 1996). In the geological terrain mapping approach, data is captured for the terrain parameters based on field survey by taking into consideration the slope morphology and components such as slope gradient, terrain profiles, erosion and instability. On the other hand, the terrain can be evaluated by examining its features and landforms. This helps recognise the limitation of a given area and its suitability for various uses. The terrain should be considered as part of the geotechnical engineering plans prior to any development. It involves the systematic collection and characterisation of terrain properties and their suitability for the intended development.

There are many terrain assessments that were used all over the world for various aims of land use, for example, the American system which points out on land

management and soil erosion (Newell, 1978; Spangle *et al.*, 1976), the British system on geology and landforms (Mohamad & Chow, 2003), the Canadian system on landcover (Vold, 1981) whereas the Australians system on engineering geology and related subjects (Mohamad & Chow, 2003).

Furthermore, the Geotechnical Engineering Office of Hong Kong had created a terrain mapping system. According to this system, the Mineral and Geoscience Department Malaysia has created a modified system of the Hong Kong model keeping in view a climatic similarity between Malaysia and Hong Kong (Mohamad & Chow, 2003).

Moreover, the Department of Mineral and Geosciences (JMG) had conducted a study in (2010) the Cameron Highland using remote sensing application to identify the terrain mapping features. The authors found that features such as side slope hillcrest, foot slope, straight slope, convex slope, and concave slope were defined using aerial photographs with conjunction with digital elevation model (DEM). Another such study conducted study was carried out in Genting Highland by Mohamad and Chow (2003). The authors used the thematic maps and attributes table for slope gradient, slope activity, erosion, and morphology. The authors then created construction maps for the study area to plan and develop the project area.

2.5.2 The Role of Geophysical Methods in Slope Stability Studies

In recent years, geophysical methods have been used to assist in the investigation of slope stability movements and groundwater flows (Gelisli & Ersoy, 2017; Chen *et al.*, 2014; Dostal *et al.* 2014; Lapenna *et al.*, 2003; Bruno & Marillier, 2000; Gallipoli *et al.*, 2000; Hack, 2000; Mauritsch *et al.*, 2000; McCann & Forster, 1990). It has been used in landslide investigations since the late 1970s (Hack, 2000; Havenith *et al.*, 2000; Caris & Van Ash, 1991; Bogoslovsky & Ogilvy, 1977) to determine landslides characteristics,

for example, the major body, geometry and surface break. Among the surface geophysical techniques, ERT and SR methods are considered promising geophysical approaches for landslide studies (Hazreek *et al.*, 2017; Bichler *et al.*, 2004; Batayneh & Al-Diabat, 2002). Furthermore, geophysical methods have been applied to investigate slope stability based on their ability to provide additional information about subsurface physical properties. Geophysical application to such studies has been growing rapidly as a result of latest developments in computer expertise software and in mathematical methods.

Additionally, in evaluating the stability of a landslide prone area, it is vital to identify the thickness of the slipped materials and the slip surface. The depth is often estimated from borehole information. However, during the last five decades, geophysical methods have been used widely to identify materials geometry in landslide area (Malehmir *et al.*, 2013; De Vita *et al.*, 2006; Cummings & Clark, 1988; Bogosklovsky & Ogilvy, 1977; Denness *et al.*, 1975). Most geophysics textbooks describe the basic principles of geophysical methods as a tool for investigation. Geophysical methods (especially the SR and ERT) are used to locate slip surface because materials above and below the slip surface give a significantly different response to seismic velocity and resistivity due to the changes in lithology.

Seismic refraction is a surface technique with staged data acquisition stages that can protect the site condition and environment. There are numerous advantages in applying the SR method due to its effectiveness in terms of cost, time and environment. Moreover, SR is a useful technique to investigate landslides by interpreting the first arrivals in the seismic signals, and it is assumed that the velocity increases with depth (Kearey *et al.*, 2002). Both of these geophysical techniques are widely used in engineering geology characterised by relatively fast field data acquisition and low costs. At the same time, electrical resistivity tomography is a useful technique used to obtain

high-resolution images for shallow subsurface investigation (Reynolds, 1997). It can also be applied to study landslide characteristics and it is a standard approach for geophysical prospecting as a solution to solve geological problems. It is also useful to determine characteristics of landslides such as main body, geometry, the surface of a break, (Yalmaz & Kamaci, 2018; Yang *et al.*, 2004; Hack, 2000; Havenith *et al.*, 2000).

2.5.2.1 Lithological Imaging Using Geoelectrical Measurements

In electrical resistivity tomography (ERT) field survey, different electrode configurations can be used (dipole-dipole, Schlumberger, Wenner, etc.) to send the electric currents into the subsurface to measure the produced voltage signals. Theoretically, this is performed by inserting an electric current from two electrodes into the subsurface to measure the potential fall between two other electrodes (Sharma, 1997).

Many studies have been conducted to determine the lithological condition in the landslide prone area. For example, 2D electrical resistivity tomography was applied to investigate the cause of landslide in Garhwal Himalaya (Sastry *et al.*, 2006). Three representative Wenner-Schlumberger profiles spanning the landslide were surveyed. Generally, resistivity tomograms showed the presence of slip zones at a depth range of 10 to 20 m from ground level. The inferred lithological depth sections underscore the importance of resistivity tomography in landslide studies, especially in hazard assessment on a detailed scale. Also, Saad *et al.* (2008) studied the slope failure area using 2D electrical resistivity imaging in Pahang, Malaysia. The results show that there are three different regions made up of completely weathered gravelly clayey sand, highly or moderately weathered gravelly silty sand and unweathered boulder. The results also show that the factors causing landslides include subsurface boulders and the saturated zone that caused subsidence of the surface. Hazreek *et al.* (2017) studied the forensic assessment on near-surface landslide using ERI at Kenyir Lake area in

Terengganu. They used an integrated analysis of ERI and borehole data to assess landslides. The results showed a combination of heavy rainfall and an existing weak zone as the major factors that triggered this failed slope. This result assisted the geotechnical engineer in designing a less costly and speedy remediation procedure for the failed slope.

2.5.2.2 Application of Seismic Refraction Imaging in Landslide Investigation

Seismic refraction is widely applied in engineering geology as a useful geophysical tool for investigating landslides. The velocity structure of a landslide mass, depth to bedrock and failure surface, and lateral extent of a landslide can be estimated using seismic refraction. This method is applicable as both shear and compression wave velocities are generally lower in the landslide body than in the unaffected groundmass. McCann & Forster (1990) documented several case histories showing the use of seismic refraction for locating undisturbed bedrock below landslides.

Furthermore, seismic refraction is a useful technique to investigate subsurface geological structures. By this method, one can identify the depth of bedrock and the seismic velocity of layers (Ferrucci *et al.*, 2000). Seismic refraction can also be effectively used in the determination of landslide characteristics such as the depth and dip of a slip surface/shear plane (Carpentier *et al.*, 2012; Al-Saigh *et al.*, 2008).

In a landslide, the materials above the slip surface are usually deteriorated, weakened, and weathered, while the materials below the slip surface remain intact (Al-Saigh, 1993). Hutchinson (1982) noted that changes in lithology corresponded well with the position of shear surface. Al-Dabbagh (1985) noted a poor core recovery from the zone of the material above the slip surface due to weathering effect above the slip surface, whereas, a well-developed core recovery and unweathered rock were noted below the slip surface.

Many authors used the seismic refraction imaging to evaluate the landslide area, for example, Abidin *et al.* (2012) investigated the near surface landslides in the Kundasang area of Sabah State using 2D seismic refraction tomography technique. The results showed that the primary velocity (V_p) values range between 330 to 600 m/s covering of topsoil/residual soil, a weathered zone with a mixture of soil, boulder and rock fractured (500–1900 m/s) and fresh rock/bedrock (> 2300 m/s). Malet *et al.* (2012) used 3D seismic refraction travel time tomography to investigate the La Valette landslide in south French Alps. Based on borehole geotechnical data and geophysical investigations, the authors suggested that an interface corresponding to an internal slip surface can be suspected (value of (1200 m.s^{-1}) at a depth of -10 to -15 m. The stable substratum is characterized by higher values of P-wave velocity of $1800\text{--}3000 \text{ m.s}^{-1}$. Moreover, Yalmaz & Kamaci (2018) used the seismic refraction method on Kısıklı Landslide in Turkey. The results indicated that relatively low velocity and elastic parameters correspond to highly porous and permeable materials in near-surface with a thickness of about 4-5 m.

2.5.3 Isotopes Technique in Slope Study

In addition to the slope gradient and geological structure, water plays a vital role in slope failure and mass movement in landslide-prone area. Water in a slope provides not only a mass load, but also a lubricant between particles or strata (Peng 2010; Lee & Kim, 2007). Severe slope failure is usual during a heavy raining as fast infiltrated rainwater enhances the slope's load and provides additional pore water pressure to devastate the slope stability. Instability of hill slopes is normally triggered by hydrological and hydrogeological causes leading to infiltration, a rise of pore water pressure, and decreases effective stress in the soil (Peng *et al.*, 2007; Van Asch *et al.*, 1999; Wiczorek, 1996).

Furthermore, stable isotopes of hydrogen and oxygen have been used extensively for the development of conceptual models, characterisation of the hydrological system, understanding the changing of water quality, discovering origins of water, determining groundwater residence time and performing palaeohydrology research. In addition, oxygen and hydrogen isotopes of water are extensively used as tracers to recognize hydrogeological processes such as precipitation, and groundwater recharge, (Syakir *et al.*, 2018; Li *et al.*, 2008; Gibson *et al.*, 2005). A comparison of oxygen and hydrogen isotopes composition in precipitation and groundwater helps to evaluate the recharge process and source of groundwater recharge.

2.5.3.1 The Use of Isotope Technique in Addressing Landslide Problems

Environmental isotopes are normally used in geochemical and hydro-geological investigations. Stable isotopic compositions of water are constantly fractionated by temperature, topography, season, and evaporation. Different water sources and environments result in unique hydrogen and oxygen isotopic signatures (Vandenschrick *et al.*, 2002; Yurtsever & Gat 1981). Hydrogen and oxygen isotope compositions in water are barely affected by water-rock reaction in normal temperatures (Lee *et al.*, 1999; Gat, 1996; Gat, 1981). Moreover, the use of environmental isotopes to determine the origin of groundwater sources in slope has been proven to be useful in studying landslide (Peng *et al.*, 2007). In this regard, Tullen *et al.* (2006) used the O18 time series of two springs to determine the hydrogeological system of the translational Hohberg landslide in Switzerland. According to them, the rapid response of springs on snowmelt and rain events could be explained by water flow through the high permeable morainic deposits.

Furthermore, Yeh *et al.* (2011) studied environmental isotopes (oxygen and hydrogen) in the Chih-Pen Creek basin, Taiwan, to determine the groundwater recharge mechanism. They collected 177 samples from rivers and groundwater and found two

different Local Meteoric Water Lines (LMWL) from different seasons. Moreover, they compared the deuterium excess using the mass-balance equation and found that the analyzed groundwater consists of 76% wet season precipitation and 24% dry season precipitation. This means that there is a distinct seasonal variation of groundwater recharge in the study area. i. e., About 79% of the groundwater is recharged from the river water, while 21% is from the rain that falls on the basin.

Recently, Syakir *et al.* (2018) conducted a review of environmental isotopes application in disaster risk management. The authors found that climate change, urban expansion, deforestation, and an increase in population are thought to be the main factors of water-related disasters. Understanding these factors and the hydrological processes is important to reduce the impact of humanity impose on the regional ecosystem. They have further mentioned that using isotopic signatures for ecosystem studies could provide useful information in understanding potential natural hazards.

2.5.4 Geotechnical Investigation

The role of geotechnical engineer in design and construction varies according to distribution of responsibilities in an organisation. Nevertheless, by definition, the geotechnical engineer is responsible for acquiring and interpreting soil, rock, and foundation data for the designing and construction of various types of structures. The proper execution of this role requires a thorough understanding of the principles and practices of geotechnical engineering, subsurface investigation techniques and principles, design procedures, construction methods and planned facility utilisation supplemented along with a working knowledge of geology and hydrology. The proper discharge of the geotechnical engineer's duties requires that he or she be involved from the very beginning of the planning stage of a project. Based on prior knowledge and understanding, geotechnical engineer can provide guidance on the location of a proposed tunnel or road project with reduced cost, improved constructability, and other

advantages. If the services of a geotechnical engineer are taken after the final project location is determined, serious deficiency may arise in the structure at the execution stage.

Several studies were carried out in different locations of Malaysia to assess geotechnical characteristics of soil and rocks. Ng (1992a) studied granite Schleroscope Shore hardness in the eastern part of Kuala Lumpur and found that hardness (Hs) of Kuala Lumpur granite is between 85 and 100. Kausarian (2014) have reported that the granite along the SILK highway is grade I and I-II in properties, while its texture is ranging from coarse to medium. The author also found that the Rock Quality Designation (RQD) is 87.73%.

Also Kausarian have reported that the granite in Kajang quarry consists of five types i. e., medium-coarse-grained porphyry granite, moderately coarse-grained granite, biotite granite, fine grain and sheared white granite, and chlorite sheared granite. The author reported that the analysis of rock mass characterisation quality found this area in range from very low (V) to very good (I), but mostly are concentrated in low quality (IV) to moderate (III) range. Furthermore, rock mass classification system based on Bieniawski (1979) found 44% of the rock mass as good quality (class II) and 56% as average quality (Class III).

2.5.4.1 Hydrologic Boundary Determination Using Geotechnical Parameters

In geotechnical engineering, field tests are vital for identifying underground conditions. An important test among them is the standard penetration test (SPT) which is perhaps the most common geotechnical test because can estimate the soil's resistance parameters or shear strength (Humyra *et al.*, 2012). Most laboratory tests must be performed on moulded samples of soils. These tests are laborious and time-consuming, and sometimes the results are not accurate due to poor laboratory conditions

(Siswosoebrotho *et al.*, 2005; Venkatasubramanian & Dhinakaran, 2011). Meanwhile, the SPT has been used widely for subsurface investigation in many parts of the world (Souza *et al.*, 2012). It measures the resistance of a hollow core being hammered with a 63.5kg weight. The hollow core receives a soil sample during the process which is logged for soil identification purposes. Also, the relative density can be estimated from this test (Silva, 2010).

Furthermore, natural rock mass differs from most other engineering materials because it contains structure discontinuities such as joints, bedding planes, folds, sheared zones and faults (Zhang, 2016). Because of the discontinuous nature of rock masses, it is important to choose the correct domain that is representative of the rock mass affected by the structure analysed when determining the engineering properties. If the structure is significantly larger than the rock blocks formed by the discontinuities, the rock mass may be simply treated as an equivalent continuum for the analysis (Zhang, 2010). For this purpose, different empirical correlations have been proposed for estimating the engineering properties of jointed rock masses based on the classification indices such as Rock Quality Designation (Zhang, 2010; Zhang & Einstein, 2004; Deere *et al.*, 1967).

Several studies of geotechnical application have been conducted to assess and investigate the subsurface conditions. Gui *et al.* (2002) conducted a series of instrumented borehole drilling beneath Kennington Park in London. The degree of matching varied among six borehole data with poor correlation, which may be due to the local soil heterogeneity against the sampling interval of different site.

2.6 Joint Application of Geotechnical, Geophysical and Conventional Methods

In a tropical environment, weathering process is considered as the main reason for decomposition and breakdown of granitic rock minerals, thus reducing its physical

properties. The conventional method of classification adopted for weathered granite is becoming less useful now due to low sample recovery (Nordin & Zainab, 2013). Therefore, advance techniques are now used to assess in-situ condition through correlation between the geophysical and geotechnical techniques.

Accordingly, the correlation of geophysical results with engineering results is considered important to determine the signature of engineering parameters from the infield data (Oyediran & Falae, 2018).

Notably, soils have complicated in-situ behaviour because of many factors. Hence, in order to have the right comprehension, soils need to be analyzed using geophysical and geotechnical engineering skills, in addition to other related disciplines such as geology, geomorphology, climatology and other earth and atmosphere sciences discipline (Bery & Saad, 2012). Moreover, the rock strength is an important property for rock classification. The Uniaxial Compressive Strength (UCS) is one of the most important property of rocks, which has been used extensively in the geological analysis for over 30 years (ISRM, 1985). Since determining the UCS in the lab is costly and time-consuming, the Point Load Index (PLI) is used as an indirect method for estimating uniaxial compressive strengths (Tsiambaos & Sabatakakis, 2004; Quane & Russel, 2003). Zein and Sandal (2018) have studied the correlation between PLI and UCS in samples collected from Nubian sandstone formation in Sudan by using the lab tests. They found that a reliable linear regression equation between UCS and PLI is $UCS = 10.18 \times PLI + 50$ with a conversion factor of 10.18 and applied it to estimate the strength of the collected sandstone samples.

Many researchers used the correlation between combined geophysical and geotechnical methods to assess the landslide area. The correlation is found useful due to its effectiveness in terms of cost, time and environment preserve. Also, the correlation

between P-wave velocities (VP) and core samples can show the level of weathering for rock layer.

Bery and Saad (2012) studied the correlation of Seismic P-Wave Velocities with Engineering Parameters (N Value and Rock Quality) in an area with Tropical Environment. They used the results of P-wave velocities of materials (soils and rocks) from laboratory and field measurement to compare physical parameters like N value and RQD. They found the empirical correlation for N value in the tropical environmental:

$$V_p = 23.605 (N) - 160.43 \quad (2.1)$$

where the correlation regression is 0.9315 (93.15%). Meanwhile, the empirical correlation between P-wave velocities and RQD values is:

$$V_p = 21.951 (RQD) + 0.1368 \quad (2.2)$$

Where the correlation regression is 0.8377 (83.77%). The correlation between apparent P-wave velocities with penetration strength for study sites is:

$$V_p (\text{app}) = 292.59 (P_s) + 474.69 \quad (2.3)$$

Where the correlation regression is 0.97. In addition, Kausarian *et al.*, (2014) conducted a study for evaluating weathering grade of granitic rocks at Kajang Quarry. The authors used the seismic refraction method and RQD results of boreholes from four locations. They found that the first location consists of five weathering zones with Vp ranging from 200 to 5400 m/s. The second location consists of four weathering zones with Vp ranging from 600 to 5600 m/s. The third location consists of four weathering zones with Vp ranging from 800 to 5250 m/s, while the fourth location consists of five weathering grades with Vp ranging from 250 to 5000m/s. Meanwhile, the authors further stated that the RQD in the first location shows excellent rock quality (98.63%), and in the second location, RQD shows that the rock is good quality (98.38%), whereas,

in the third location, RQD shows that the rock is excellent quality (99.03%), and lastly, in the fourth location, RQD shows that the rock is excellent quality (96.43%).

Moreover, Gho *et al.* (2014) conducted an empirical correlation study between the V_p and UCS for Malaysian granite. They used the laboratory ultrasound test and UCS for 77 collected samples. They found an empirical correlation between UCS and V_p for granite as the following:

$$UCS = (2.55 \times 10^{-5}) \cdot V_p^{1.7658} \quad (2.4)$$

Where a coefficient of determination (R^2) is 0.90. This correlation offered a simple and quick estimation for granitic rock in Malaysia.

According to the previous studies, this study was selected in order to enhance the possible empirical correlation for soil and rock parameters in the landslide-prone area by using integrated techniques.

2.7 Summary

This chapter highlighted findings from the previous studies conducted in many parts of the world. This chapter also discussed the conventional and advanced techniques that were used in landslides research. A case study of using geotechnical methods was discussed in order to get a good perspective about the geology and hydrology and to assess the geotechnical characteristics of soil and rocks. Moreover, the isotopic signatures are discussed to provide useful information in understanding the potential natural hazards. Furthermore, the methods and findings explained in this chapter enhance the understanding of landslide triggering factors, mechanism and hazard mitigation.

CHAPTER 3: METHODOLOGY

3.1 Introduction:

This chapter presents an outline of the research methods used in the finest way to scientifically overcome landslide related problems. This chapter includes also different steps generally designed to solve the related research problems and understand the logic behind them. Furthermore, this chapter presents a set of techniques such as geophysical, geotechnical, geological terrain mapping, laboratory tests (SPT, RQD, Atterberg limit), and environmental isotopes techniques which are best suited to achieve the research objectives.

This chapter begins with field-based geological mapping, geophysical and engineering methods, and stable isotopes approach that are relevant to this study. This is followed by introducing the geophysical, engineering and stable isotopes data processing steps. The use of geophysical approaches is considered as non-destructive methods, but it may not provide enough information about the subsurface features. Therefore, additional information in the shape of engineering parameters is needed to overcome the lack of information. Meanwhile, engineering methods only give single point information, but geophysical methods can provide a spatial distribution of the interest required parameters. The isotopes methods are used to determine the dynamic and flow behaviour and to confirm, which can support the geophysical and engineering information significantly.

Lastly, the preliminary results and interpretations from the early observations are presented in the next section. The general views of the approaches that are used in this research are shown in (Figure 3.1).

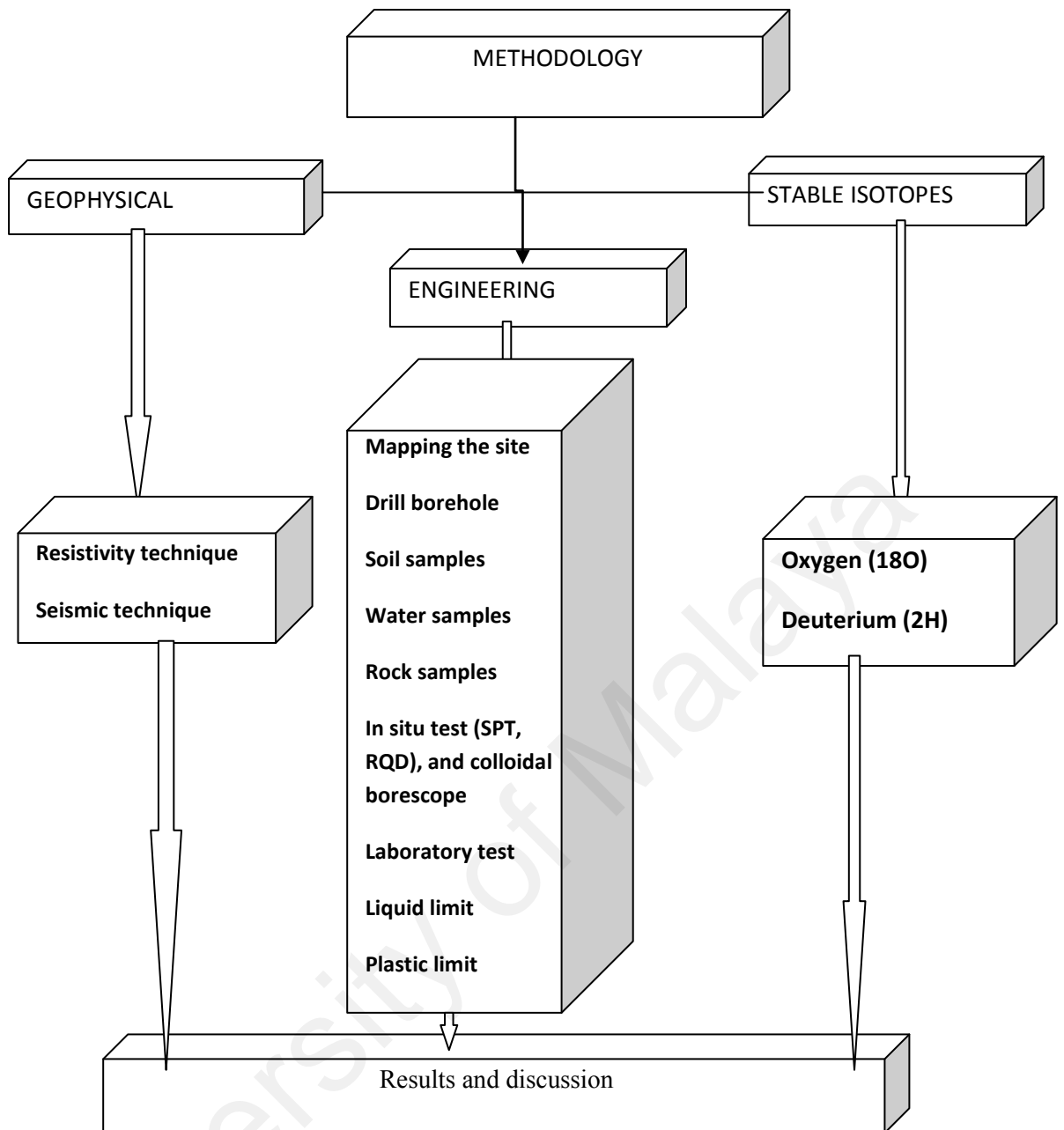


Figure 3.1: The general views of the methodological approaches used in this study.

3.2 Preliminary Field Investigation

The preliminary site investigation consists of many activities such as topographical, geological, terrain and engineering mapping. A digital thematic map for the area based on the survey map was provided by a licensed surveyor. The equipment used in the investigation includes a Suunto compass and clinometer, Garmin Etrex 12 channels Global Positioning System (GPS), Bushnell laser range finder, Bushnell binocular, a geological hammer, and digital camera and measurement tapes. This is followed by a site visit conducted in 2016 to verify the thematic map.

A visual inspection was conducted using the GRA (Geohazards Risk Assessment) form in order to identify and locate the problematic area. Accordingly, any signs of cracks, settlement, and slope instability were recorded in the details (Figure 3.2, 3.3). Geological terrain mapping was conducted in accordance with the Guideline for Highland Development, Ministry of Natural Resources and Environment, 2006.



Figure 3.2: Small scale slope failure can be observed near the SMK Bukit Tinggi area.



Figure 3.3: The visual observation of elongated cracks in SMK site.

The initial conceptual model (Figure 3.4) of the site was developed from the perspective of potentially risky area. Preliminary field observation, along with datasets of solid bedrock and hydrogeological characteristics were used to construct a 3D hydrogeological block model. Also, a list of assumptions is outlined, for example, the presence of thick loose material that may contribute to ground settlements, the presence

of fractures and fissures, and the broken water pipe can be an important feature for the occurrence of the settlement.

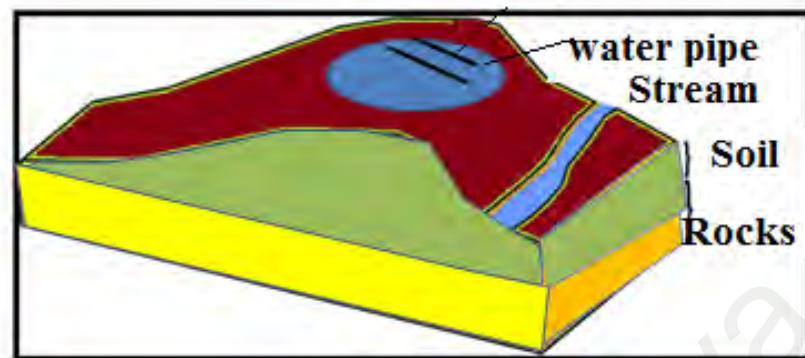


Figure 3.4: Initial conceptual model of the study area.

3.2.1 Geological Terrain Mapping

Terrain evaluation involves the investigation of landform and related features. This technique is used to identify the limitations of land use and to broadly assess the overall suitability of land use. It is used widely as a planning tool and has a major application in the field of geotechnical engineering. In this study, a systematic approach is taken to collect, characterize and rationalize the natural variations across the terrain.

The mapping is performed by field observation using slope map (generated by using GIS software) as a guide, by following the procedure and job specification produced by Mineral and Geosciences Department Malaysia (2006) stated in Table 3.1.

The data processing analyses include transferring field surveyed data to digital map attributes using GIS application. The production of the digital map had been validated with field survey map for terrain attributes and boundary inspection. Finally, a construction suitability map was created for the study area with respect to geological terrain classification (Table 3.2 and 3.3).

Table 3.1: The geological terrain classification (JMG, 2006).

SLOPE	TERRAIN CODE	ACTIVITY CODE	EROSION AND INSTABILITY	COVER + TREE			
0°-5°	1 Hillcrest/Ridge: A	Natural slope: -rock 1	No appreciable erosion: 0	Soil Slope	Dense Vegetation	No water seepage a	
		-soil 2				Minor water seepage b	
6°-15°	2 Sideslope: -straight B	-soil & rock 3	Sheet erosion: -minor 1			Moderate water seepage c	
	-concave C		-moderate 2			High water seepage d	
16°-25°	3 -convex D	Cut slope: -rock 4	-severe 3			No water seepage e	
		-soil 5				Minor water seepage f	
26°-35°	4 Footslope: -straight E	-soil & rock 6	Rill erosion: -minor 4			Moderate water seepage g	
	-concave F		-moderate 5			High water seepage h	
36°-60°	5 -convex G	Fill: -rock 7	-severe 6			No water seepage i	
		-soil 8				Minor water seepage j	
>60°	6 Drainage valley: H	-rock & soil 9	Gully erosion: -minor 7	Partly Soil Partly Covered	Sparse Vegetation (Partially Barren)	Moderate water seepage k	
			-moderate 8			High water seepage l	
	Flood plain: I	Terraces: -rock a	-severe 9			No water seepage m	
		-soil b				Minor water seepage n	
	Costal plain: K	-rock & soil c	Well defined recent landslide: (diameters)			Moderate water seepage p	
			< 10m a			High water seepage q	
	Litoral Zone: L	Reclamation: d	- 10m-50m b				
	Marsly/ swampy: S		> 50m c			Partially covered with concrete/bitumen etc. Dense vegetation in uncovered part	No water seepage R
	Wave cut platform: W	Mined-out: e				Minor water seepage s	
			Development of general instability:			Moderate water seepage t	
	Alluvium plain: X	Water bodies: -natural stream f	-recent n		High water seepage u		
		-man-made channel g	-relict r		No water seepage v		
	Undulating hill: Y	-water storage h			Partially covered with concrete/bitumen etc. Moderate vegetation in uncovered part	Minor water seepage w	
		-pond l	Coastal instability: w		Moderate water seepage x		
		Colluvium: m			High water seepage y		
		Excavated platform: p			No water seepage A		
					Minor water seepage B		
					Moderate water seepage D		
					High water seepage E		
					No water seepage F		
					Minor water seepage G		
					Moderate water seepage H		
					High water seepage I		
					No water seepage J		
					Minor water seepage L		
					Moderate water seepage M		
					High water seepage N		

Table 3.2: Construction suitability classification system (after Brand, 1988).

Class Characteristics	Class I	Class II	Class III	Class IV
Geotechnical Limitations	Low	Moderate	High	Extreme
Suitability for Development	High	Moderate	Low	Probably Unsuitable
Engineering Costs for Development	Low	Normal	High	Very high
Intensity of Site Investigation Required	Normal	Normal	Intensive	Very Intensive
Examples of Terrain	1.Insitu terrain <15° minor erosion 2.Cut platforms in insitu terrain	1.Insitu terrain 15° - 25°, no instability or severe erosion 2.Insitu terrain <15°, severe erosion 3.Colluvium <15°, no instability or severe erosion	1.Insitu terrain 25° - 35° no instability or severe erosion 2.Insitu terrain 15° - 25°, history of landslips 3.Colluvium 15° - 25°, general instability	1.Insitu terrain >35° 2.Insitu terrain 25° - 35°, instability or severe erosion 3.Colluvium 25° - 35°, moderate erosion

Table 3.3: Construction suitability classes and types of site investigation (after Mohamad& Chow, 2003).

Risk Category	Description of Site Investigation	Description of Site Investigation		
		Classes I,II	Class III	Class IV
Category a. Loss of life b. Economic loss Negligible a. None expected (no occupied premises) b. Minimal structural damage. Loss of access on minor roads Low a. Few (only small occupied premises threatened). b. Appreciable structural damage. Loss of access on sole access roads. High a. More than a few b. Excessive structural damage to residential and industrial structures. Loss of access on regional trunk routes.	Assessment of surrounding geology and topography for indication of stability. Visual examination of soil and rock forming the site or to be used for the embankment. Specialist Advice – Requirement (A) Geology and topography survey of site and surroundings area. Soil and rock joint strength parameters for foundation and cut slopes. For embankments steeper than 1 on 3, recompacted strength parameters of fill. For cut, information on groundwater level. Specialist Advice – Requirement (B) Detailed geology and topography survey of site and surrounding area. Soil and rock joint strength parameters for foundation and cut slopes. Recompacted strength parameters for fill. For cut, information on ground water level. Specialist Advice – (B)	As for Class I and II. More detailed geology and topography survey. For the steeper slopes, information on soil and rock joint strength parameters. Survey of hydrological features affecting the site. Specialist Advice – Requirement (B) As for Class I and II. Survey of hydrological features affecting the site. Specialist Advice – Requirement (B) As for Class I and II. Survey of hydrological features affecting the site. Extend investigations locally outside limits of the site to permit analyses of slopes above and below the site. Specialist Advice – Requirement (C)	As for Class I and II. Area outside confines of site to be examined for instability of soil, rock and boulders above the site. Specialist Advice – Requirement (B) As for Class I and II. Extend outside limits of site to permit analyses of slopes above and below the site. Specialist Advice – Requirement (C) As for Class I and II. Extend investigations more widely outside limits of site to permit analyses of stability of slopes above and below the site. Specialist Advice – Requirement (C)	
Note : Requirement for Specialist Advice: A) Services for an experienced geotechnical engineer or engineering geologist not necessary B) Services for an experienced geotechnical engineer or engineering geologist to depend on location relative to developed or developable land C) Services for an experienced geotechnical engineer or engineering geologist essential				

3.3 Geophysical Techniques

Geophysical techniques used for this study includes Electrical Resistivity Imaging and the Seismic Refraction (Figure 3.5). The decision to choose these techniques in this study is due to their attribute, which reflects some important physical properties (electrical conductivity, seismic wave velocities, and density) of subsurface material. In addition, simple correlation can be made between the data for each technique. Compared to other conventional techniques such as drilling and auguring, the geophysical techniques provide higher data coverage in a short time.

3.3.1 Electrical Resistivity Tomography

The electrical resistivity tomography (ERT) survey has been carried out by using the ABEM Terrameter SAS 4000 system, LUND electrode selector system (ES464), 4 multi-core cable and electrodes. Two short stainless steel rods (electrodes) are inserted about 15 – 30 cm deep into the Earth surface through which current is sent into the ground. Two additional electrodes are used to measure the Earth Voltage (or electrical

potential) generated by the current. The depth of investigation is a function of the electrode spacing used. The greater the spacing between the outer current electrodes, the deeper the electrical currents will flow in the Earth, hence the greater the depth of exploration.



Figure 3.5: A plan view of the school compound and preliminary areas of investigation using geophysical techniques (modified from Google Maps, 2018).

A total of five ERT profiles were measured by employing a Wenner-Schlumberger quadrupole configuration. A number of 60 electrodes layout made in a straight line with constant 2 m spacing. Then, the equipment automatically selected the active electrodes for each measurement based on selected array input. The resistivity of the subsurface materials was measured by injecting a certain amount of electrical current (10-50 mA) into the ground through a pair of electrodes and the resulting voltage (potential) measured at a different pair of electrodes on the ground surface. The RES2DINV software is used to process and determine a two-dimensional (2D) resistivity model for the subsurface from the data obtained by an electrical resistivity survey. A detailed explanation about the survey (Figure 3.6) and method of interpretations can be found in the published papers by Loke (2004), Dahlin (2001), and Keller and Frischknecht (1966).

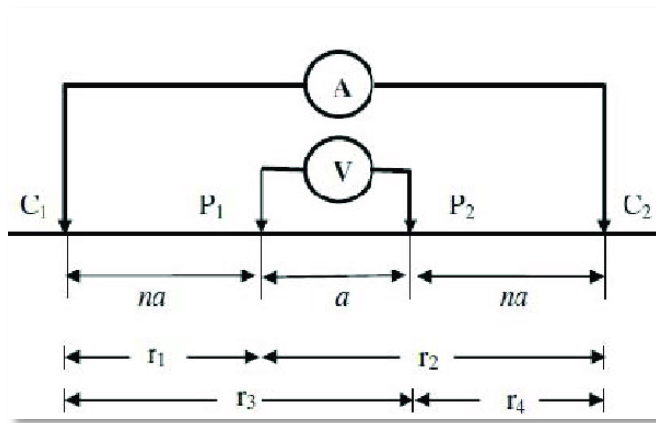


Figure 3.6: Schematic diagram showing the basic principle of DC resistivity measurements (adaptation from Loke, 2004).

Wenner-Schlumberger quadrupole configuration (Figure 3.7) was used in this study in order to determine the vertical layered changes. Also, this method enhanced data resolution.

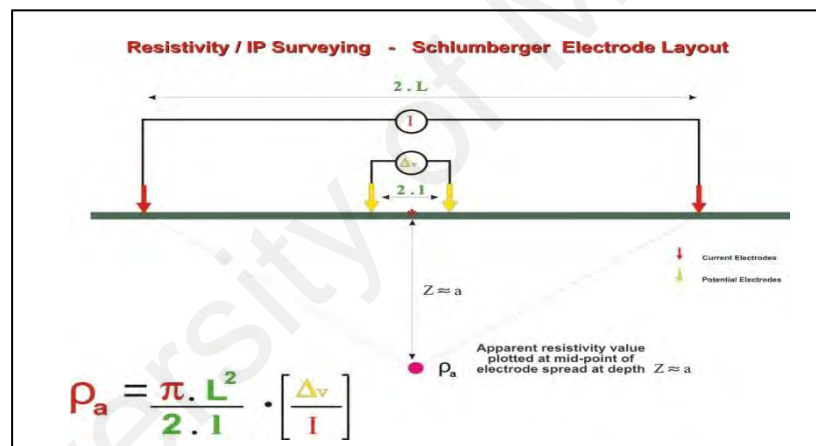


Figure 3.7: The electrode array for Wenner - Schlumberger Configuration.

3.3.2 Seismic Refraction

Seismic refraction surveys were conducted using a 24-channel Geometrics StrataVisor NZ instrument (Figure 3.8). Geophones, functioning as the receivers, with a frequency of 40 Hz were spaced at 5 m intervals making a total profile length of 115 m. A total of six seismic refraction profiles were collected. The manual trigger mode was by creating seismic energy by vertically striking a solid metal plate with a sledgehammer. The seismic refraction data were processed and interpreted using ReflexW software program (Sandmeier Scientific Software, Karlsruhe, Germany).

Regardless of the technique used to process and interpret the data, multiple shot-points were performed along the survey profile to provide greater data coverage and potentially more accurate models. In total, 7 shot-points were made along each of the survey profile to build a subsurface velocity model. The seismic refraction method uses travel times of refracted arrivals to derive: 1) depths to velocity contrast, and 2) shapes of refracting boundaries.



Figure 3.8: Creating seismic energy by vertically striking a solid metal plate with a sledgehammer.

The geophysical results utilize data from drilling program for enhanced clarification about the geotechnical significance of the observed geophysical units. Meanwhile, laboratory analysis of drill samples allows the establishment of petrophysical relationships and thus, permits more quantitative use of the geophysical data in the context of hydrological-geotechnical model conceptualization. The next section will discuss all field and laboratory-based methods and material used in this study to obtain the required results.

3.4 Geotechnical Methods

Geotechnical investigations are performed in order to obtain the lithological sequence and the physical parameters of the subsurface materials. The principle of soil and rock mechanics is used to investigate subsurface conditions and related materials.

A total of four boreholes were drilled in the selected area by using a wash boring machine (Figure 3.9), which includes power rotation of the drilling bit and removal of recovered core materials by the circulation of fluid. The size of these holes was 100 mm in diameter (30 meters deep) and rock coring was carried out in accordance with the American Society for Testing and Materials (ASTM) D 2113.

Samples consisting of rock quality designation (RQD) test, Atterberg limits and point load index (PLI) test were applied to borehole materials through for laboratory experiments. Field-based measurements such as standard penetration test (SPT) and colloidal borescope were applied on this borehole. These tests are applied to enhance and support the perspective of geophysical methods.



Figure 3.9: The image showing the skid drilling machine.

3.4.1 Standard Penetration Test

Standard Penetration Test (N- value) was performed, utilizing a split barrel sampler and a self-tripping hammer of approved design (Figure 3.10). The value of the N was

reported with the number of blow counts for each 75mm penetration of the sampling tube. For the first 150mm penetration (the seating drive), the blow counts that do not contribute to the value of N were also included. Generally, this is carried out in all types of soil (except very soft silt and soft clays), at 1.5m intervals or at change of strata. Also, the soil samples recovered from the split barrel were preserved as disturbed samples for subsequent tests.

There are numerous factors other than the hammer type that are affecting the N value. Relevantly, many authors have proposed the correction factors including drill stem's length and type, type of anvil, blow rate, usage of liners or borehole fluid and the hammer type. The corrected SPT values are computable from general equation of the field measured N_f from the general equation (excluding the corrections made to overburden) (Aggour & Radding, 2001) shown below:

$$N(60) = N_{(Field)} * n1 * n2 * n3 * n4 * n5 * n6 \quad (3.1)$$

Where $n1$ the energy correction factor, $n2$ the rod length correction factor, $n3$ the liner correction factor, $n4$ the borehole diameter correction factor, $n5$ denotes the anvil correction factor and $n6$ the blow count frequency correction factor. The average values of correction factors, as proposed by Aggour & Radding (2001) as follows: $n1 = 1.67$, $n2 = 1.0$, $n3 = 1.0$, $n4 = 1.0$, $n5 = 0.7$, $n6 = 1.0$.



Figure 3.10: The image showing a standard penetration test.

3.4.2 Rock Quality Designation

The rock quality designation is applied as a standard parameter in drill core logging to provide a quantitative estimate of rock mass quality. A total of four core samples were described to furnish the study with additional information concerning the quality of the subsurface rocks in the study area (Figure 3.11).

The procedure for rock drilling is in accordance with British Standard 5930: (1999). The core barrel used for this study produces a rock core of 70 mm in diameter. The Rock Quality Designation (RQD) was also reported for each core run. The RQD is the ratio of the total length of the good quality core each exceeding 100mm in length divided over the length of the core run. The classification of RQD values and Rock mass quality is displayed according to Deere *et al.*, (1967).

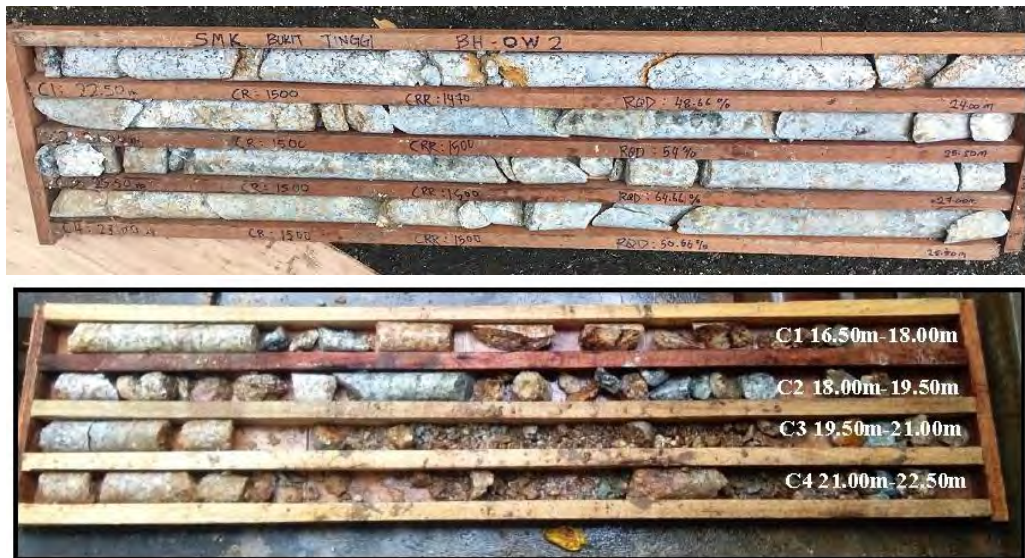


Figure 3.11: The rock core sample. (a) The rock core for borehole (OW3), (b) the rock core sample for borehole (OW2).

3.4.3 Consistency of Soil (Atterberg Limits)

Clays and silts can be classified based on their behaviour and different water content, thus reflecting some of the engineering properties of the earth material. Consistency is a term that is frequently used to describe the degree of firmness (e.g., soft, medium, firm, or hard). The Atterberg limits, which include liquid- and plastic limits as well as the plasticity index, were measured to determine the plasticity of the collected soil samples using the Casagrande method. Eight samples were taken from the site and labelled clearly such as the borehole name, depth of sampling, date of the sample taken, and the type of sample. These samples were placed inside the polyethene bag and marked with the sample number and borehole name. Moreover, all samples were stored orderly on the site in protective boxes in a dry place until their dispatched to the laboratory (Figure 3.12).

Furthermore, in this study, the ASTM D 4318 - Standard Test Method for Liquid Limit, Plastic Limit, and Plasticity Index of Soils were used for the collected samples as shown in Figure 3.13.



Figure 3.12: The collected soil samples.

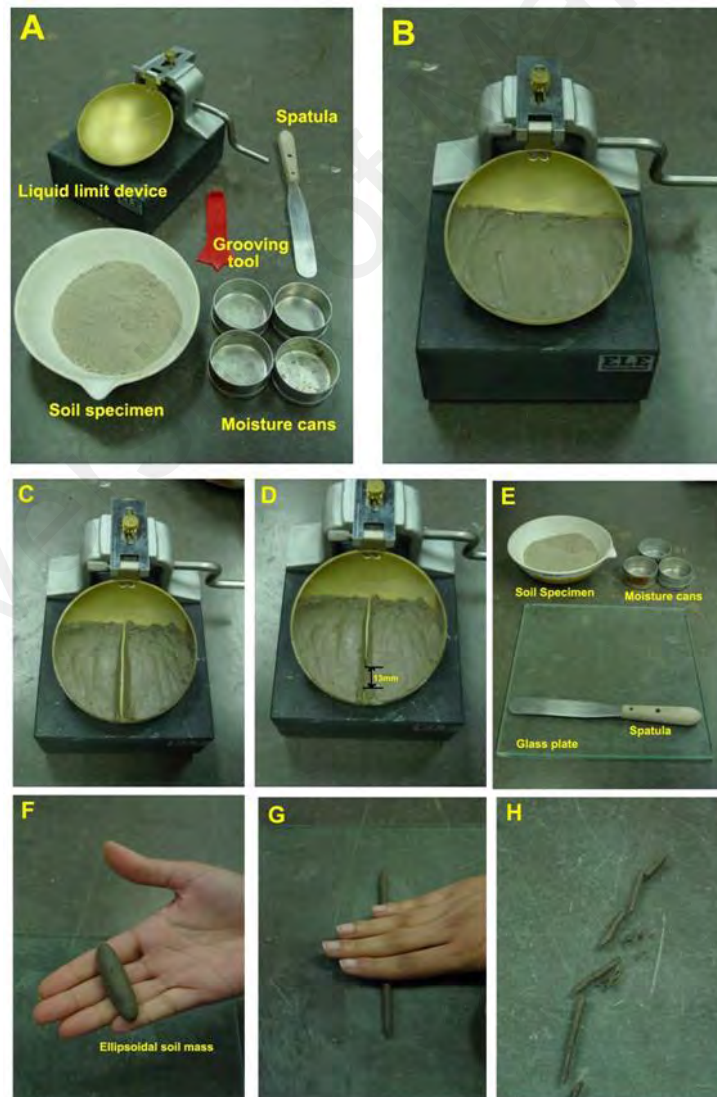


Figure 3.13: The equipment and procedure for Atterberg limits. (A, b, c) the liquid limit procedure. (F, g, h) the plastic limit procedure.

The plastic index calculated using the following equation

$$PI=LL-PL \quad (3.2)$$

3.4.4 Point Load Index

This test is used as an important method for rock classification (Kaya & Karaman, 2016; Norbury, 1986). This method shed light on failure of rock occurred as a result of tensile stress. In addition, this test is a useful alternative to indirectly obtain USC and can be conducted on a rock sample without using any special sample preparation.

In this study, the point load index test was conducted on nine samples collected from granitic rocks. Depths of coring of rock samples are varied from 15 to about 28m from the ground level. Preparation of samples was carried out according to ASTM D4543-08. Rock core was cut and polished to achieve desired dimensions.

3.4.5 Colloidal Borescope

Colloidal Borescope System (CBS) is an in-situ measurement system that is developed by Oak Ridge National Laboratory consisting of Charged Couple Device (CCD) camera, a fluxgate compass, an optical magnification lens, an illumination source and stainless steel housing (Kearl 1997). This instrument is capable to measure directly the suspended colloid particles size (1-50 μ m) and to determine the real-time groundwater direction and velocity in open borehole or in monitoring well (Figure 3.14). The measurement of velocity and direction are based on movement of the particles in the groundwater system. Upon the measurement in the well, an electronic magnified image (140x) is transmitted to the surface, where it is viewed and analyzed. The fluxgate compass will align with the direction of boroscope in the well, while the source of illumination is a source of lighting for the lens to capture the movement of particles in the groundwater. All the particles flow and direction that has been captured will be transmitted to the video digitizer and analyzed using the software.

The colloidal borescope is inserted into a screen zone in the borehole to obtain consistent horizontal laminar flow in a steady direction over time. This zone is classified as preferential flow zones rather than low flow zone because the latter case exhibit swirling directional flow that does not permit a linear velocity measurement (Kearl 1997, Kearl & Roamer 1998). Due to insertion of the instrument into the borehole, the flow is initially swirling and multidirectional. Normally, it takes about 20-30 minute to obtain the laminar horizontal flow in the screen zone. Consequently, it is necessary to secure the instrument cable at the surface. The observation continued until one and a half hour to get consistent velocity and direction. During the observation, Aqualite software is used to record the direction and velocity in real time. In this study, CBS was conducted in three boreholes.

3.4.6 Standpipe Piezometers

Standpipe piezometers are used to evaluate the piezometric water level in soil and rock (construction control, stability monitoring, dams and reservoir). Five numbers of Standpipe piezometers of 50 mm diameter were installed to get reliable measurements of groundwater level (Figure 3.15). Theses standpipes were measured once a month by using dipmeter instruments from October 2017 to September 2018.



Figure 3.14: The Colloidal Borescope System instrument.



Figure 3.15: Water level monitoring using a dipmeter.

The next section presents the optimal methods used on collected water samples (surface and groundwater) and the analysis of oxygen and hydrogen isotopes.

3.5 Environmental Isotopes

A total of 60 water samples were collected from precipitation, stream water, tap water and groundwater. These samples were collected at one-month interval between October 2017 and September 2018 for stable isotopic analyses. The groundwater samples were collected from boreholes by using manual bailer (Figure 3.16). Samples were stored in 30 mL and 1000 mL polyethene bottles. The samples were then transferred to nuclear laboratory of Malaysia for analyses. The hydrogen and oxygen isotopes were determined using SERCON 20-20 isotope ratio mass spectrometer (IRMS).

All isotopic ratio results are presented as the d-notation (‰) relative to the international VSMOW (Vienna Standard Mean Ocean Water) standard.



Figure 3.16: Collection of water samples by a manual bailer.

3.6 Summary

The main objective of this chapter is to examine the capacity of geophysical, engineering, geological and isotope techniques to characterize the subsurface condition in the landslide-prone area. Furthermore, the selected methods for this study enhance the understanding of landslide slip surface, triggering factors, and hazard mitigation.

CHAPTER 4: RESULTS AND DISCUSSIONS

4.1 Introduction

The focus of this chapter is to highlight the contributions of the used integrated methods in providing logical explanations of the chosen research problems i.e., assessment of the landslide prone area. The relationships between geotechnical and geophysical properties (if any) are presented in order to highlight the capability of geophysical techniques in solving geotechnical problems. In addition, the implications of integrated datasets for shallow subsurface problems are discussed, to prepare conceptualization of the site. The importance of using stable isotopes in a landslide-prone area is presented as a guide to enhance the conceptualization of groundwater movement and origin in a problematic area. Finally, the findings of this research are presented, which will help future researchers to determine the subsurface problems with lower cost and effort.

4.2 GIS Application for Identifying Terrain Features

Field geological terrain mapping was conducted and performed by field observation using the slope map (generated by using GIS software) as a guide. The whole procedure has been done according to job specification introduced by Mineral and Geosciences Department Malaysia (Mohamad & Sum, 2003). Data processing and analyses include transferring of field surveyed data to digital map attributes using GIS software. Production of the digital map has been validated with field survey map for terrain attributes and boundary inspection.

Desk study involves the review of maps and satellite imagery to confirm the exact location of the proposed development site. Limited to the finance of this study, the used maps including the survey and layout plan which was produced by using GIS application. Thematic maps were created such as slope map, slope activity map, terrain component Map, and Construction Suitability map. These maps are used for

interpretations of a geological feature within the landslide prone areas, which serve as a useful guide for zoning of the area that can be developed.

These maps provide essential information for topographic features in the study site, which can help enhance the assumptions.

4.2.1 Slope Map

The slope map is created from topography survey data using GIS application. The slope gradient is given in degrees and divided into six groups as shown in Figure 4.1. The slope angle of each terrain unit is measured along the direction of the greatest declivity. This direction, which is normal to the contour, enables the identification of the most limiting slope angle. Each slope gradient was grouped based on JMG and the field observation and the classification grading were given accordingly to their respective attributes. Figure 4.1 presents the slope angle for SMK Bukit Tinggi area. The results show that 60.14 % of the study area is occupied by slope of less than 5 degrees, 4 % is with a slope of 6- 15 degree, 10.45 % is with slope of 15- 25 degree, 19.39 % is with slope of 26- 35 degree, and 5.6 % is with slope of 36 – 45 degree. These results aid to an assumption that the variation of slope gradient has a direct effect on the occurrence of a landslide in the study area.

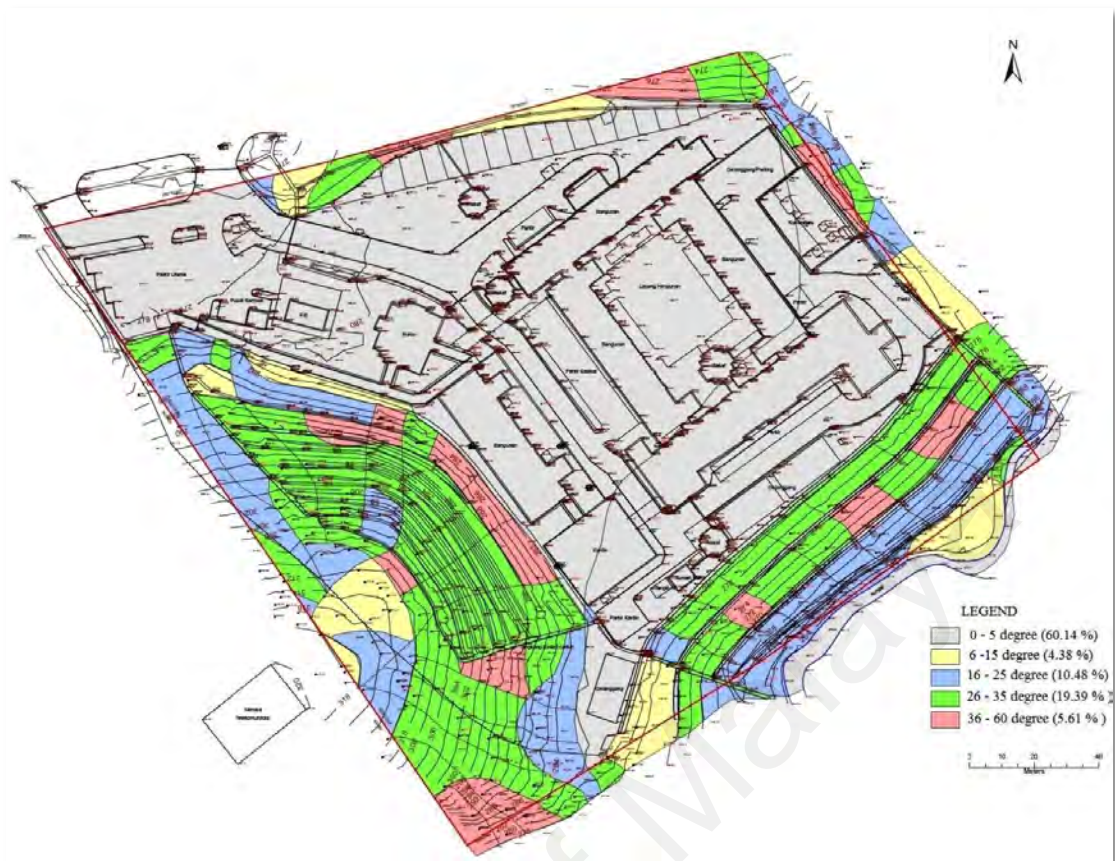


Figure 4.1: The slope maps percentage and degree of the study area.

4.2.2 Terrain Component Map

The terrain component attributes describe the physical appearance and component of the slope. They describe the shape of the existing natural terrain. An indication of the component of the slope in soil and rock are implicit in the class definition as shown in Figure 4.2. The obtained results of the component map show that the 78.31% of the terrain is classified as straight side slope, 12.60% is classified as a convex side slope, while 7.98% is considered as concave side slope of the terrain. Drainage valley covers 1.11% of the total terrain classification.

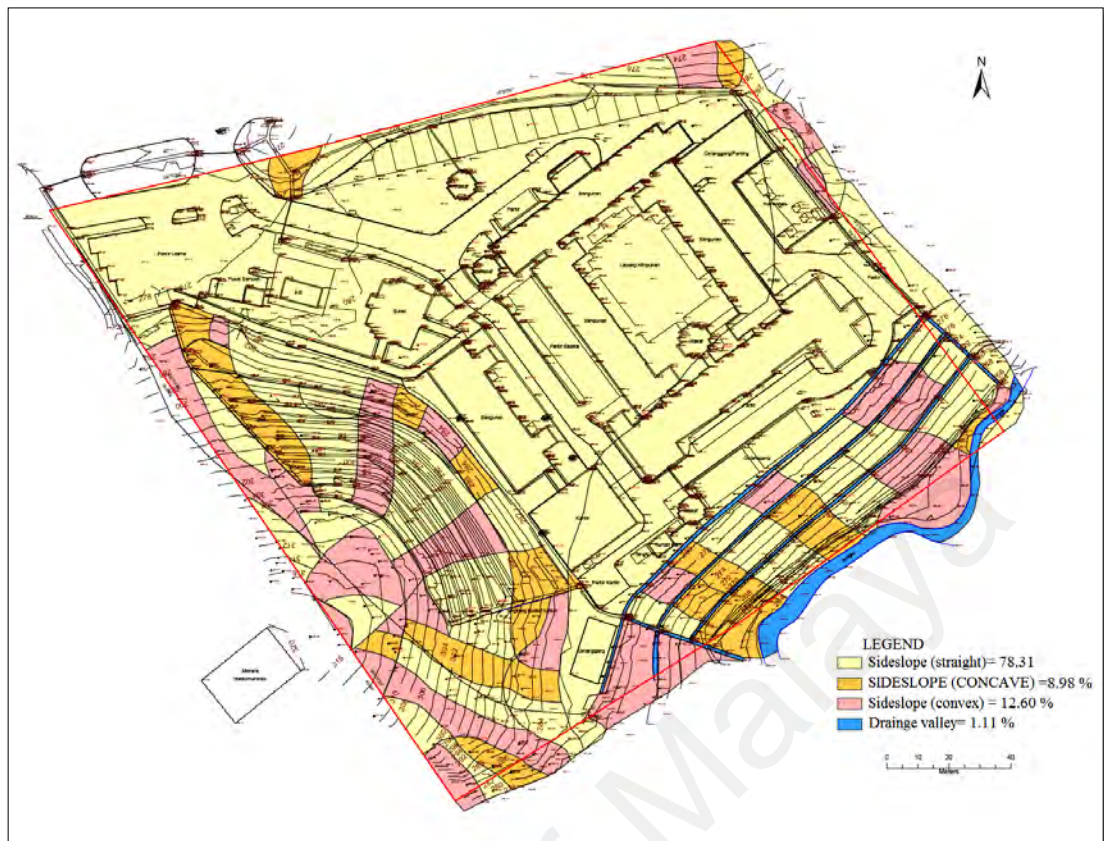


Figure 4.2: Terrain Component Map of the study area.

4.2.3 Slope Activity Map

The slope activity attributes describe the physical appearance of the slope. They describe the situation where the natural terrain and stream have been altered by man-made activities to form cut slopes, fill slopes and channels. Generally, the terrain activity in the study area can be classified into seven classes as presented in Figure 4.3.

As shown in Figure 4.3, the natural water stream (code f) and man-made water channel (code g) represent 1.11% of the study area, natural soil slopes (code 2) and natural rock slopes (code 3) represent 13.48%, Cut slope – soil (code 5) covers 15.16%, while fill slope (code 8) represents 27.30% of the study area. The excavated platform (code p) covered the majority 42.95% of the site.

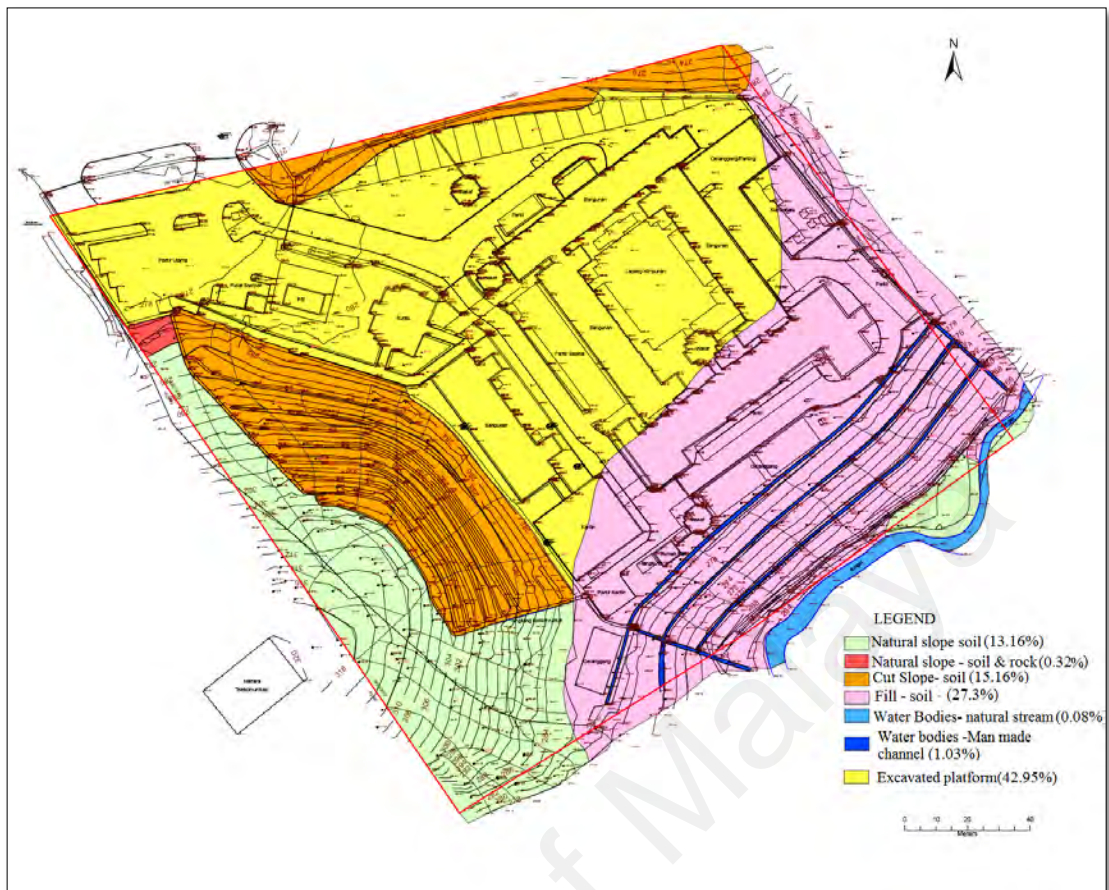


Figure 4.3: The slope activity map of the study area.

4.2.4 Erosion and Instability Map

The erosion and instability classification describes the surface condition of the terrain on the basis of the major forms of terrain denudation. Slope failure and slope instability are indicated by this attribute. Figure 4.4 presents the results of the slope instability map, where the proposed development area is 50.62% classified with no appreciable erosion while minor sheet erosion covers 49.38% of the area.



Figure 4.4: The Erosion and Instability Map of the study area.

4.2.5 Construction Suitability Map

As a result of the abovementioned thematic maps, the Construction Suitability map was created and the proposed development site was classified into the following classes; Class I, Class II, Class III, and class IV (Figure 4.5). The class I areas cover 63.49% of the proposed development site, which is equal to 6.40 acres. In-situ terrain in this area is less than 15 degrees and no instability is recorded. With low geotechnical limitations, these areas are highly suitable for construction due to fewer foundation problems. The class II areas cover 10.48% of the proposed development site. These areas require moderate geotechnical and geological studies due to the geotechnical limitations, and needs the intensity of site investigation. The class III areas cover 19.32% of the proposed development site. The development in these areas requires detailed geotechnical and geological studies due to the geotechnical limitations (soil and rock strength parameters). The terrain slope in these areas ranges from 25 to 35 degrees with potential instability and severe erosion. The class IV areas cover 5.61% of the total area,

and are located as isolated patches in the proposed development site. The in-situ terrains in class IV areas are above 35 degrees. Therefore, development in this area is not suitable. This area also has extreme geotechnical limitations and intensity of site investigation is required. The rest of 1.10% (0.11 acres) of the proposed development site is classified as water bodies.

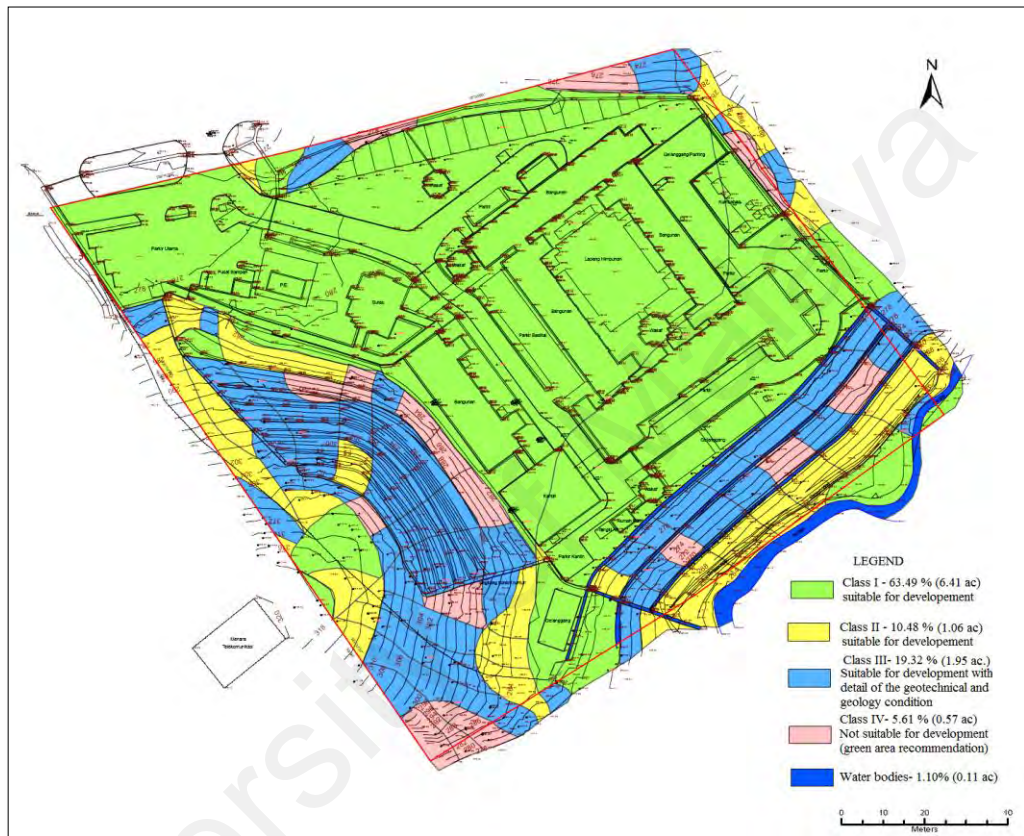


Figure 4.5: The construction suitability map of SMK Bukit Tinggi area.

4.3 Field Results and Interpretations

One of the challenges to develop a comprehensive conceptualization of any site lies in gaining the subsurface physical properties. This is possible to achieve since the strong contrasting subsurface structure can be characterized by different physical properties. For this purpose, the ERT survey has been carried out along five profiles in the study area. Seismic refraction tomography was carried out on six profiles as well (Figure 4.6). Also, a total of 5 boreholes have been drilled within the study area to investigate the lithostratigraphy, collect core samples for laboratory analysis, and install piezometers.

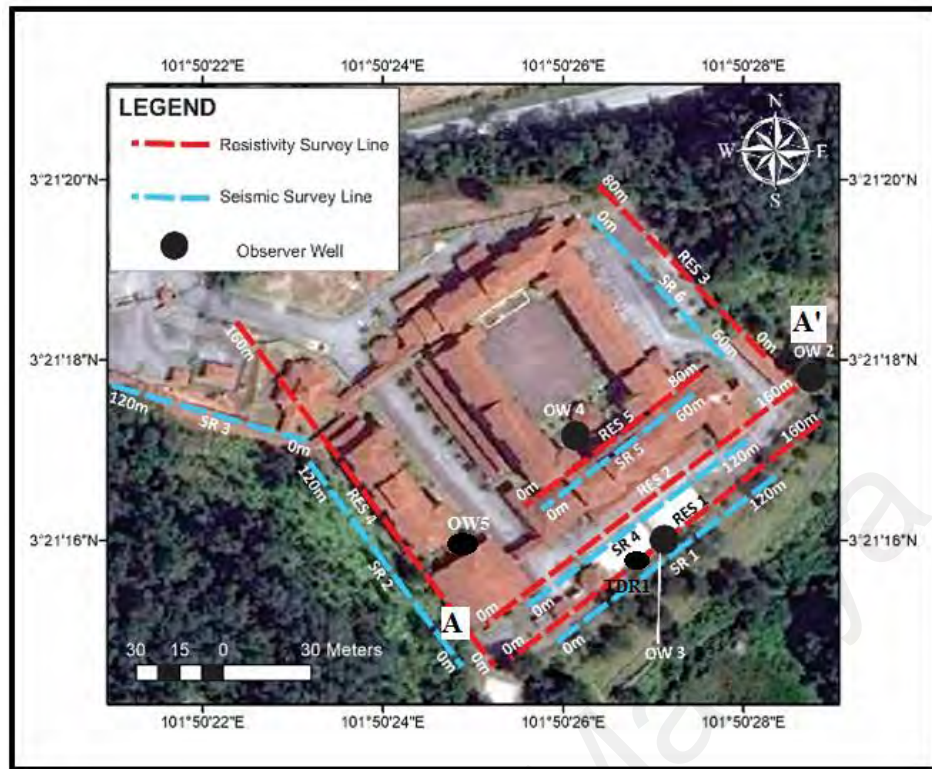


Figure 4.6: Plan view of the school compound and location of geophysical investigations (modified and based on Google Maps, 2018).

4.3.1 Joint Interpretation of Geophysical Dataset

Figure 4.7 shows that the sharp resistivity (ρ) contrasts displayed in most of the 2D inversion results, suggesting the presence of a two-layer structure. The top layer appears to have a variable thickness ranging from 5 m to 15 m (e.g. RES2, RES3 and RES4) below the ground surface, while the second layer appears approximately at a depth of 15 m (e.g. RES4) below the ground surface. It is interesting to note that the second layer does not appear in the RES1 and RES5 images as a result of the thick top layer. Based on the root mean square (RMS) error of the inversion results, the interpretation here is focused on RES1 and RES4 as these profiles have low RMS error compared to RES2, RES3 and RES5.

The most prominent feature in the vertical sections is a clear contrast between the conductive zone ($<500 \text{ Ohm-m}$) and resistive zone ($>2000 \text{ } \Omega\text{m}$). The conductive zone is indicative of clay-rich or sandy and/or gravely materials, while the resistive zone may indicate weathered granitic bedrock. The top layer appears in patches ranging between

20 Ohm-m and 500 Ohm-m. In some parts of the profiles, patches of highly resistive 'boulder' are also present within the top layer (e.g. RES1). Moreover, the 'break' in the unit is apparently noted, indicative of the presence of weak fractured zones. This leads to an assumption that the electrically conductive layer (<500 Ohm-m) is indicative of loose/poorly sorted backfill materials comprising variable quantities of clay, silt, gravel and sand.

The results of the SR tomography are presented in Figure 4.8. The tomography images depict a two-layer structure model (SR1, SR2, SR3, SR4) and thus, confirming a similar observation from electrical resistivity measurements. Based on the seismic tomography images, the upper layer (≤ 15 m) has P-wave velocity ranging from 300 m/s to 1000 m/s, overlying a second layer (≥ 15 m) with P-wave velocity values ranging from 1000 m/s to 3000 m/s. This leads to an assumption that the low P-wave velocity (<15 m) is associated with loose and poorly sorted materials. The tomography images show a sharp boundary interface approximately at a depth of 15 m, which may be due to contrasting elastic properties of the subsurface materials. Based on this boundary interface it is assumed that the slip surface depth starts from 15 m below the ground surface. It is interesting to note that the second layer does not appear in the SR5 and SR6 images as a result of the thick top layer.

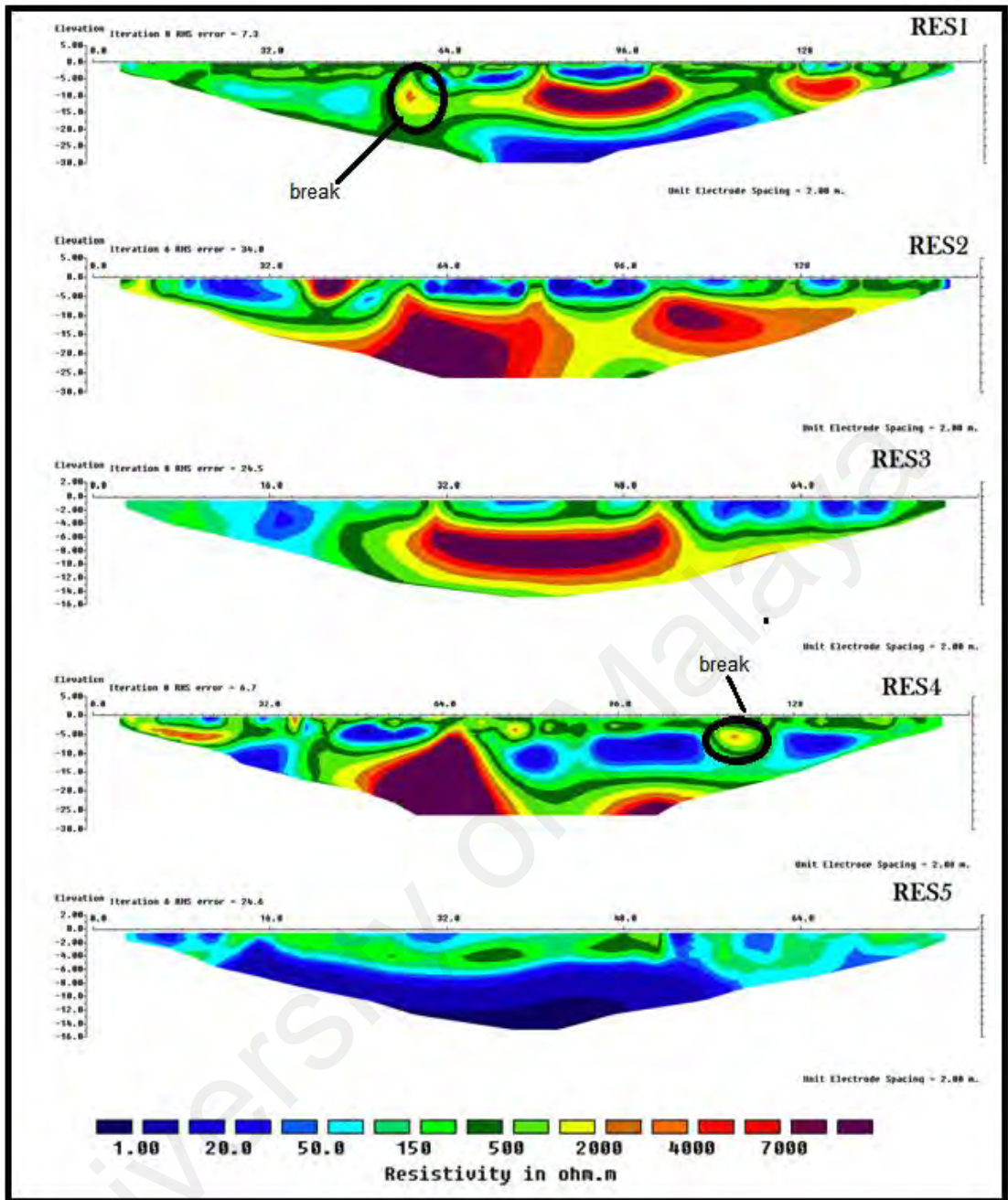


Figure 4.7: The inversion results of the ERT surveys.

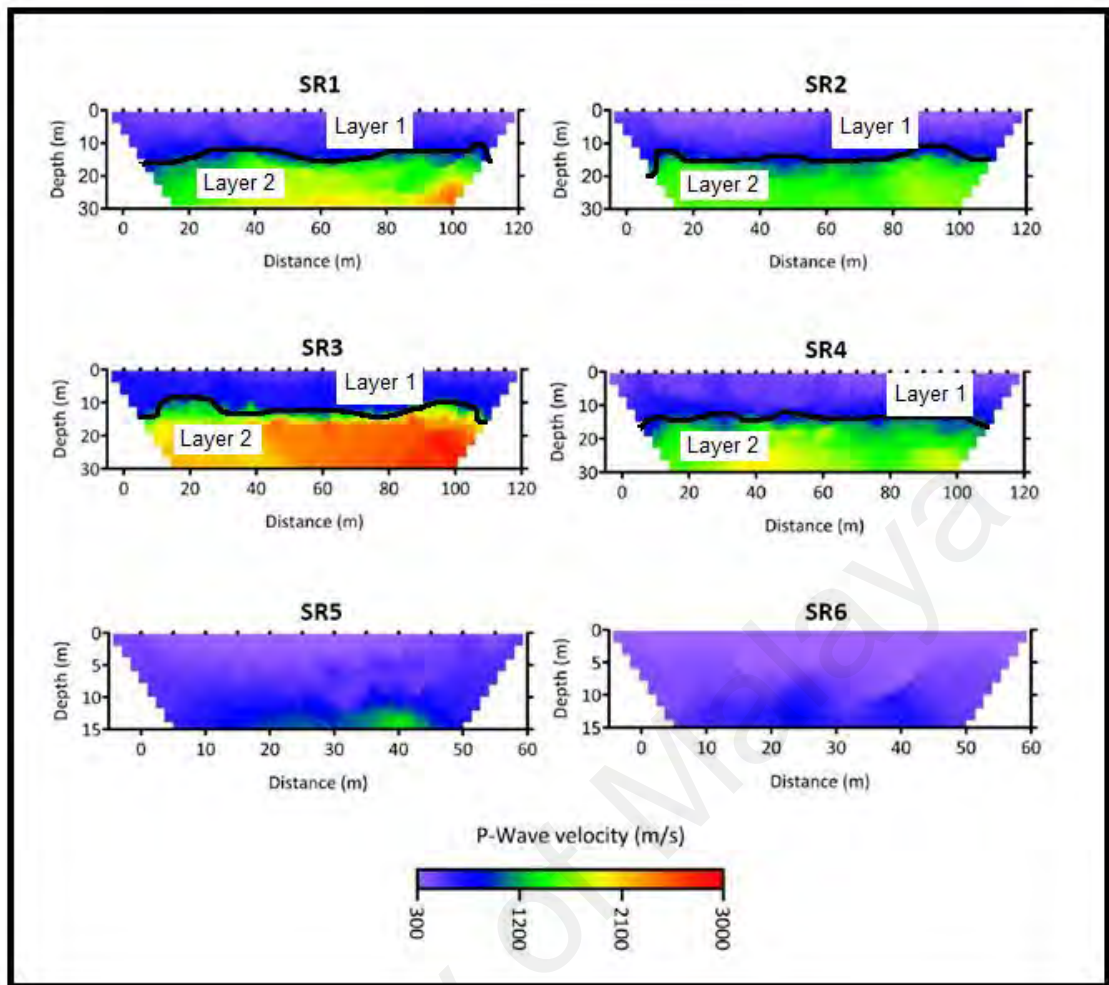


Figure 4.8: The results of seismic refraction tomography.

4.3.2 Field-based Geophysical-Lithological Relationships

The environmental study suggests that countless physical parameters have to be taken into account prior to making a crucial decision for civil construction. The aforementioned physical parameters are integral in denoting their behavior, which is affected by changes in condition with time. Accordingly, in the present study, the data for the SR and ERT are correlated with the borehole data gathered from the study area. Notably, soils have complicated in-situ behaviour because they are highly impacted by many factors. Hence, in order to have the right comprehension, these soils need to be analyzed using geophysical and geotechnical engineering skills, in addition to other related disciplines such as geology, geomorphology, climatology and other earth and atmosphere related discipline (Bery & Saad, 2012).

Figure 4.9 presents the tomography image of the seismic refraction survey profile line 1 linked to borehole OW3 description. As shown in this image, three zones are determined with P-wave velocity values ranging from 300 to 1800 m/s. The first zone, which indicates a P-wave velocity ranges from 300 – 900 m/s consist of silt, sand and clay (loose/ poorly sorted) materials. This zone is classified as a zone of weathering (grade VI to V), which have a thickness from 5 to 15.5 meters under the ground surface. This observation enhances the previous assumption that the electrically conductive layer (<500 Ohm-m) is indicative of loose/poorly sorted backfill materials comprising variable quantities of clay, gravel and sand. The second zone underneath the first zone, which presents P - wave velocities range from 900 to 1800 m/s, consist of weathered granite and designated as grade IV. This zone begins at a depth of 15.5 meters from the ground surface and maintains a thickness from 4 to 8 meters. The third zone consists of weathered granitic rocks of medium-grade III. This zone has a P-wave velocity range of 1800-3000 m/s and has a thickness of 4-6 meters.

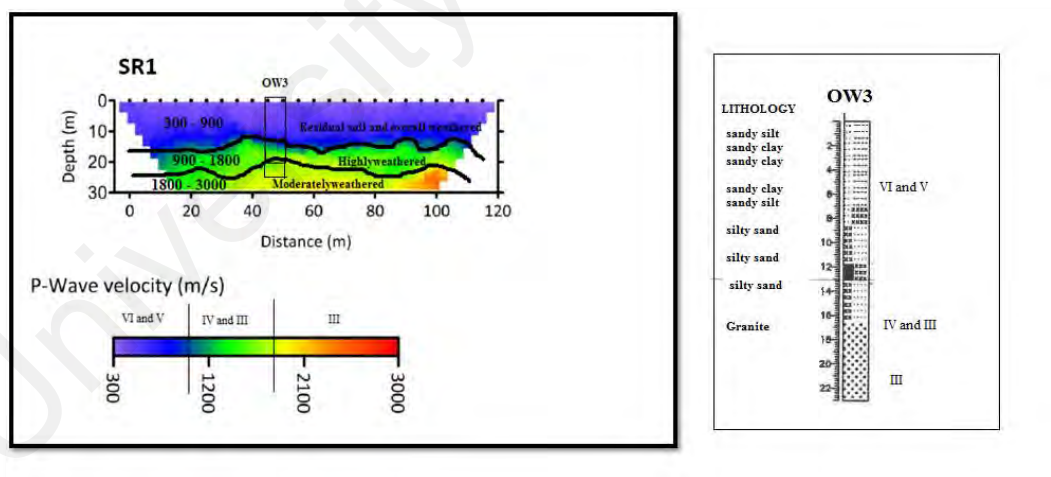


Figure 4.9: The Correlation between SR Line 1 and borehole OW3.

Figure 4.10 presents the tomography image results of the seismic refraction survey in profile line 2 and it is correlation to borehole OW5 description. As shown in this Figure, two zones are indicated with P-wave velocity values ranging from 300 to 1800 m/s. The first zone has an average P-wave velocity from 300 – 900 correspondings to silty-sandy

materials (loose materials) residual soils and extremely weathered granite. This zone is classified as VI to V, which have a thickness of 5 to 14 meters from the ground surface. The second zone underneath the first zone has a P - wave velocities range from 900 to 1800 m/s. This zone of highly weathered granitic rocks is classified as Grad-IV. This zone begins at a depth of 14 meters from the ground surface and the thickness varies from 4 to 8 meters.

Accordingly, the comparison of borehole log and P-wave velocity support the sharp resistivity inversion boundary, which separates the conductive zone of highly sandy composition from the resistive zone of weathered granite bedrock.

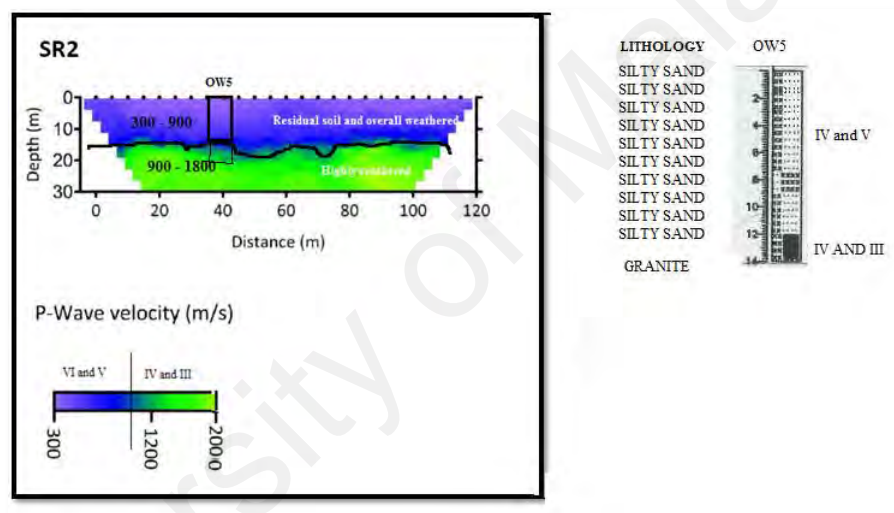


Figure 4.10: The correlation between SR Line 2 and borehole OW5.

The study of P wave velocity related to borehole OW 2 description is presented in Figure 4.11. As shown in Figure, the P-wave velocity of zone 1 ranges from 300 to 900 m/s, corresponding to silty sand. This zone of residual soils and extremely weathered granite is classified into grade VI to V. The thickness of this zone varies from 13 to 15 meters from the surface. Zone 2 underneath of zone 1 which is dominantly occupied by highly weathered granitic rocks is classified as grad-IV. The recorded P-wave velocities here ranged from 900 to 1800 m/s. This zone begins at a depth of 13 meters from the surface and varies in thickness from 7 to 10 meters. The third zone of weathered granitic

rocks of medium-grade III, with a P-wave velocity of 1800-3000 m/s, has a thickness of 10 - 12 meters.

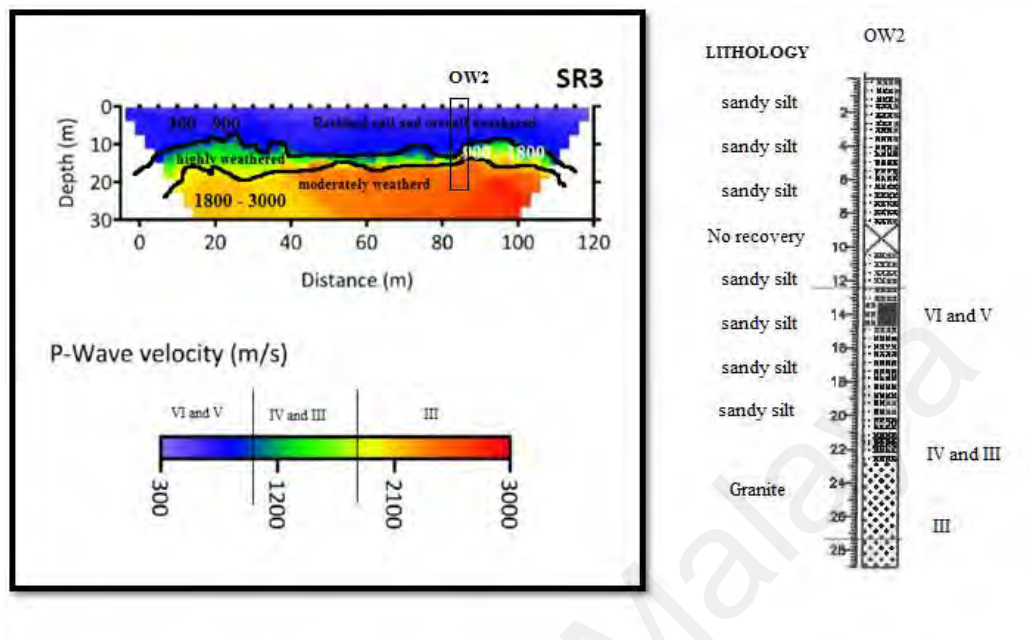


Figure 4.11: The correlation between SR Line 3 and borehole OW2.

Figure 4.12 presents the results of the seismic refraction survey along profile line 2 correlated to borehole TDR 1 description. As shown in this Figure, two zones are presented with P-wave velocity values ranging from 300 to 1800 m/s. The first zone presents an average P-wave velocity range from 300 – 900, corresponding to silty-sand (loose materials) residual soils and extremely weathered granite. This zone is classified as VI to V which has a thickness of 14 to 16 meters from the ground surface. The second zone underneath the first zone has a P-wave velocities range from 900 to 1800 m/s. This zone of high weathered granitic rocks is classified as grade IV. This zone begins at a depth > 16 meters from the ground surface and the thickness varies from 4 to 8 meters.

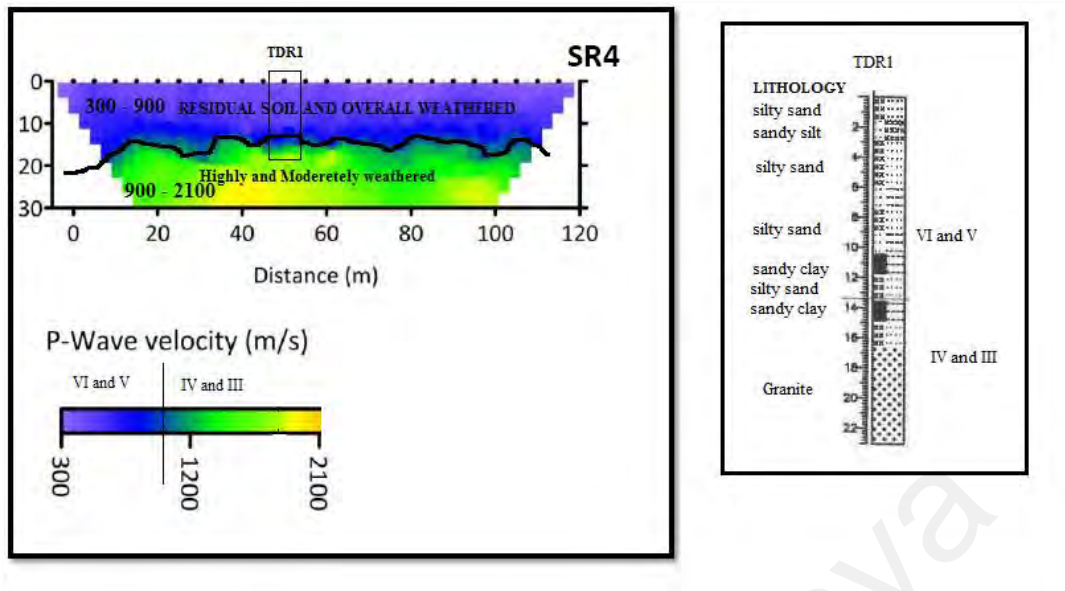


Figure 4.12: The correlation between SR Line 4 and borehole TDR1.

The inversion results of resistivity survey (RES1 and RES4), borehole lithology (OW3 and OW5), and corrected SPT log results (at the same location) are presented in Figure 4.13 and 4.14. The inversion results of Figure 4.13 show the presence of a two-layer structure. The resistivity of the first layer is low (<500 Ohm-m), indicating the appearance of the conductive zone and at 15 m depth below the ground surface. While the second layer is the resistive zone (>2000 Ohm-m) of weathered granite bedrock. The Borehole log confirms the lithological materials (as expected from RES), where the conductive zone (<15 m) contain sandy-silty clay materials along with sandy-silty materials and the resistive zone (15 m) contain granite rocks. The low SPT values are being observed at 3 -5m depth, while from the ERT image it is represented by low resistivity value. It is, therefore, assumed that the low resistivity value can be an indicator of clay-rich loose materials. Moreover, its noted that the 'break' in the unit is an apparent, indication of the presence of weak fractured or cracked zones. Due to the lack of information from the borehole log, it is suspected that the conductive layer that appears after 20 m depth may indicate the loose materials.

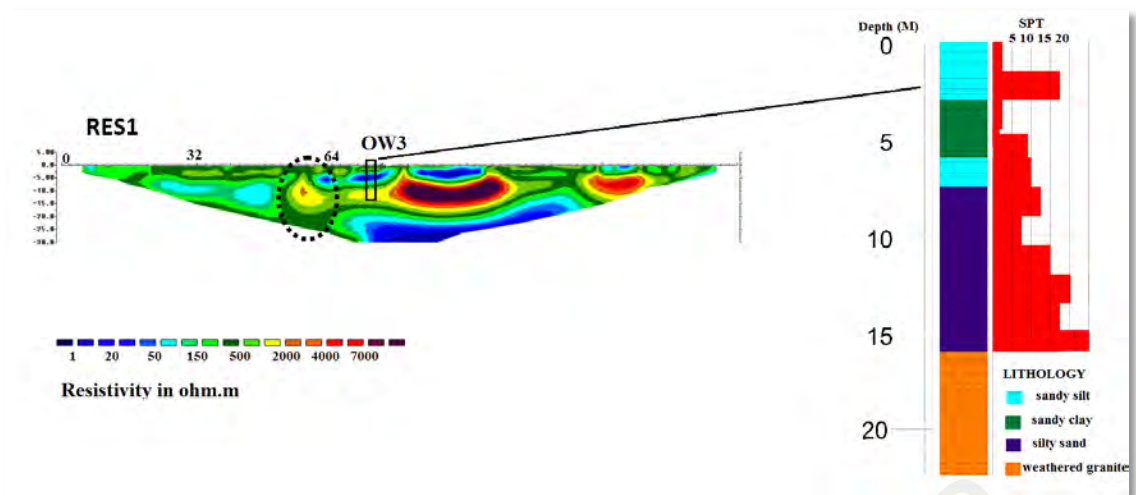


Figure 4.13: The correlation between RES 1 and borehole Log OW3.

The inversion results in Figure 4.14 show the presence of two-geo electrical resistivity layers. The resistivity of the first layer is low (<500 Ohm-m), which suggests a saturated silty-sandy unit with thickness ranging from 2- 13 m. The resistivity of the second layer (>2000 Ohm-m) indicates a granite zone. The corrected SPT values for this layer are 20-50, which appear at depths between 2 m to 13 m, indicating dense to very dense materials. These results are in good agreement with the low SPT value and low resistivity values of this depth zone. Although the SPT result has a relatively higher value (>50) at 13 meters depth, it shows the beginning of a resistive zone (granite rocks). In some part of this profile, the presence of resistive features is associated with the weak and fractured zone.

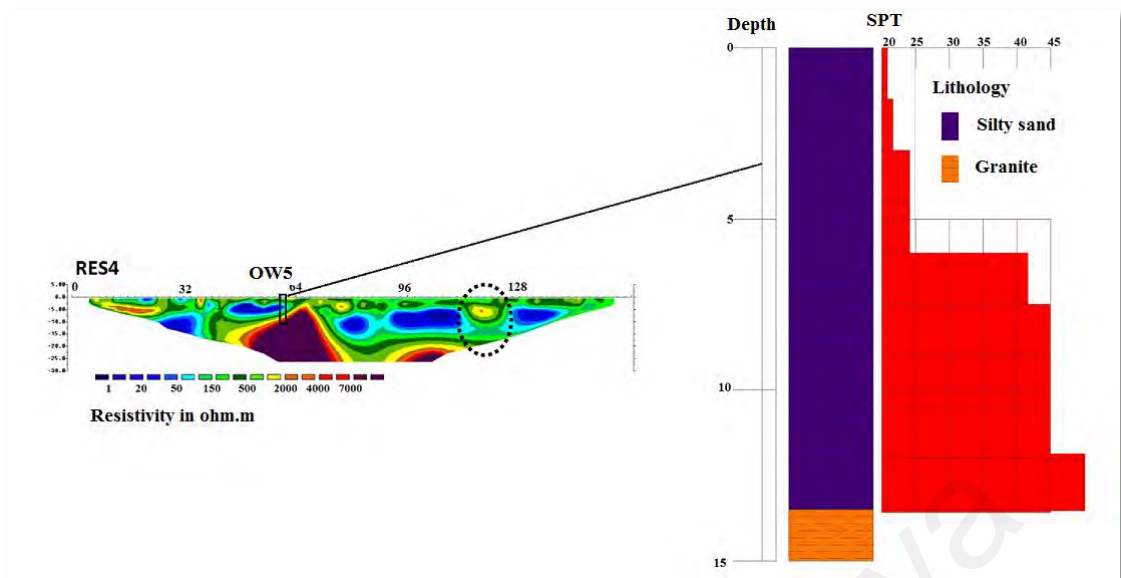


Figure 4.14: The correlation between RES 4 and borehole Log OW5.

4.3.3 Groundwater Origin, Source and Flow Direction

It is a well known fact that water is one of the major factors in slope instability that can act to soften the soils and allow the slope failure or foundation to settle. Fluctuation of groundwater levels in the slope and its movement trend, as well as poor drainage (presence of waterlogged in the subsurface) or seepage in the pathway in a localized topography of the sloping area are among the important parameters that should be closely monitored. Due to a sudden uprising and lowering of groundwater table (pore water changes remarkably), and the presence of waterlogged or seepage against a slope/settlement of a building in the vicinity of the suspected sliding zone tend to decrease the strength of cohesive soils, which may lead to land sliding or collapse. In this study, the average changes in the water table are presented in Figure 4.15.

As shown in Figure 4.15, the water table is approximately at the contact point of soil and granite rocks, indicating the onset of weathering activities. Meanwhile, data obtained from the CBS technique is further analyzed here to assess the possible connection between groundwater and other water sources. The average value was taken to interpret the direction and velocity of the groundwater as shown in table 4.1, and Figure 4.16.

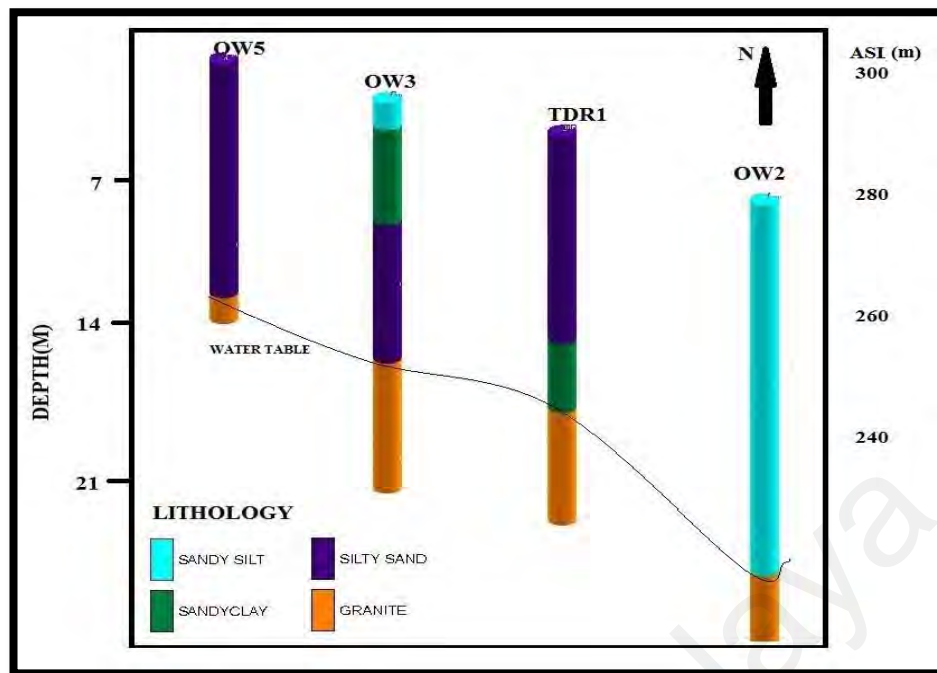


Figure 4.15: Variation of the water table in the study area.

Table 4.1: The velocity and direction of groundwater.

Borehole	Direction (Degree)	Velocity ($\mu\text{m/s}$)
OW-2	191.58	50.78
OW-3	185.11	37.59

These values indicate that OW2 and OW3 have the same flow system. As shown in Figure 4.16, the groundwater in both OW2 and OW3 are moving toward a river in the south of the study area. It shows that the groundwater at OW2 and OW3 is likely discharged to the nearby stream with the same direction as the mass movement, leading to the assumption that the presence of groundwater increases the chemical weathering and thus, triggering a mass movement.

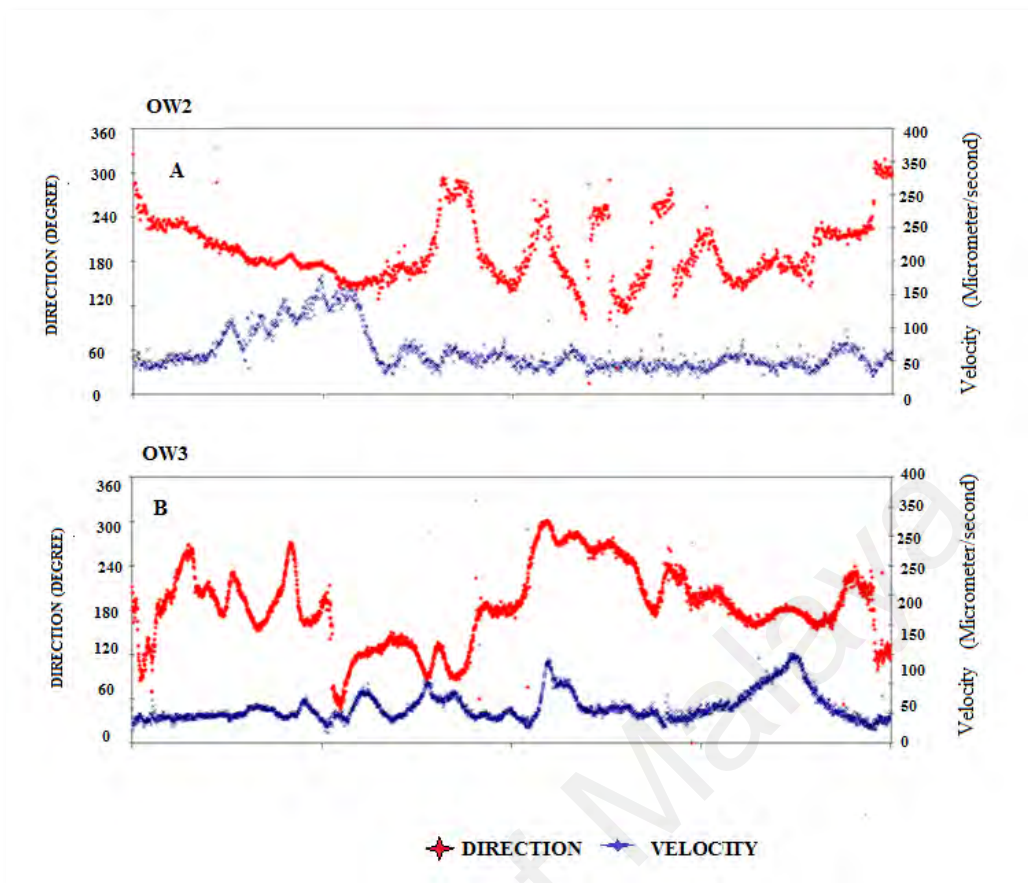


Figure 4.16: (a) Groundwater direction and velocity at OW-2. (b) Groundwater direction and velocity at OW-3.

As mentioned above, most of the landslide events are associated with heavy rainfall record. Rainfall induces fast infiltration of water in slope which increases the pore water pressure and builds up extra pressure underground to destroy the stability of slope. Thus, proper knowledge about the hydrological and hydrogeological aspects is important to enhance an understanding of landslide triggering factors (Wieczorek, 1996).

In the present study, the average amount of rainfall measured in the SMK area between October 2017 and September 2018 are presented in Table 4.2. The maximum rainfall in the study area is 386 mm recorded in September 2018, while the minimum amount is 49 mm recorded in January 2018.

Environmental stable isotopes of oxygen-18 ($\delta^{18}O$) and Deuterium (δD) that are used here to get fingerprinting characteristics of the hydrogeological process that are

affected by meteorological processes. (Kumar *et al.* 2008; Li *et al.* 2008; Blasch & ryson 2007; Palmer *et al.* 2007; Gammons *et al.* 2006; Gibson *et al.* 2005; Deshpande *et al.* 2003; Vandenschrick *et al.* 2002; Clark & Fritz 1997; Gat, 1996). Thus, these isotopes are used to trace the origin of water (Clark & Fritz, 1997) i.e., to get a relative contribution of rainfall to groundwater recharges mechanisms in the SMK. The results of isotopic signature for Oxygen and Hydrogen are summarized in Table 4.3. In addition, the local meteoric regression water line (LMWL) is plotted in Figure 4.17, showing a relationship between the $\delta^{18}\text{O}$ and δD of all the water samples collected from the study area.

Table 4.2: The rainfall amount in the study area.

Month	Rainfall (mm)
Oct-17	290.394
Nov-17	201.11
Dec-17	265.2
Jan-18	160.225
Feb-18	64.5762
Mar-18	147.407
Apr-18	142.545
May-18	188.292
Jun-18	49.062
Jul-18	75.14
Aug-18	235.365
Sep-18	386.75

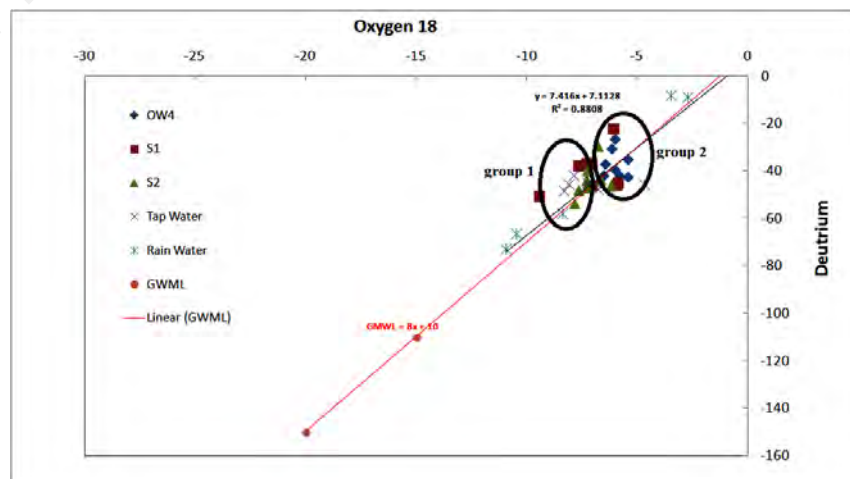


Figure 4.17: Plot of δD versus $\delta^{18}\text{O}$ of water samples.

As shown in Figure 4.17, most of the surface and groundwater are scattered and slightly deviated from GMWL and LMWL, indicating that the water is likely to recharge directly from precipitation (Peling, 2009). The regression line between δD and $\delta^{18}O$ for the collected water samples are determined as the LMWL, were

$$\delta D = 7.416 \delta^{18}O + 7.1128 \quad (4.1)$$

Where the correlation regression is 0.88 (88%). This LMWL is similar to the global meteoric water line (GMWL) defined by Craig (1961), as well as to the recent global relationship of

$$\delta D = (8.17 \pm 0.07) \delta^{18}O + (11.27 \pm 0.65) \quad (4.2)$$

However, groundwater and tap water were divided into two groups. Group 1 comprises of tap water and surface water and Group 2 comprises of groundwater. This suggests that there is no logical connection between groundwater and tap water in the study area.

The long term average rainfall amount recorded in SMK Bukit Tinggi area and it is a correlation with isotopic results for surface and groundwater are presented in Figure 4.18. This Figure clearly shows that the isotopic signatures of monthly precipitation have no significant wide variations with that of the hydrological year. Both $\delta^{18}O$ and δD have significant compatibility with the monthly rainfall amount. The mean weight precipitation of $\delta^{18}O$ and δD during October 2017- September 2018 period is -6.39/00 and -37.05.20/00, respectively.

The mean weight of surface and groundwater for $\delta^{18}O$ and δD during the October 2017- September 2018 period are -6.53 and -38.2, respectively. Positive relationship of mean weight between the rainfall and other water bodies (surface and groundwater) indicates that the local rainfall has directly affected the groundwater recharge, thus changes the water table and the slope stability in the area.

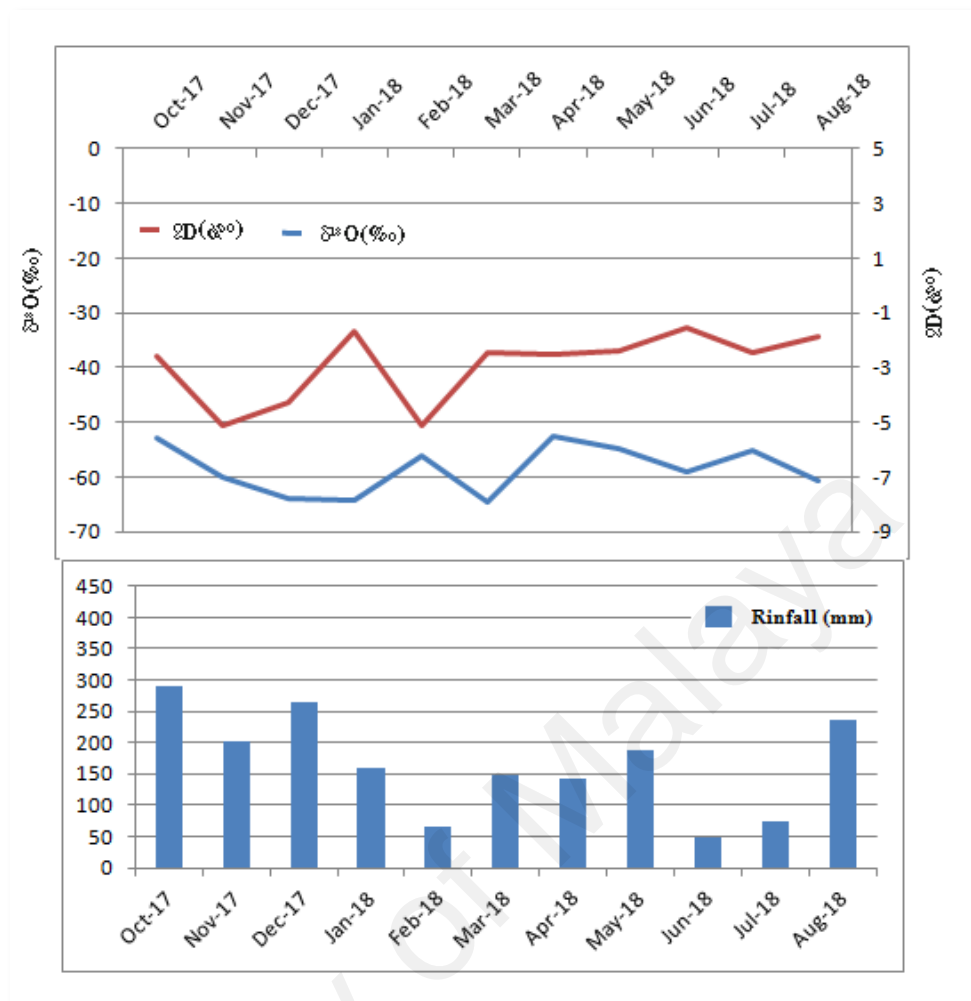


Figure 4.18: A comparison of seasonal changes of $\delta^{18}\text{O}$, δD and precipitation.

Table 4.3: The results of Oxygen and Hydrogen Isotopes.

Month	OW4			Stream 1			stream 2			Tap Water			Rain Water		
	C13	O18	Deut	C13	O18	Deut	C13	O18	Deut	C13	O18	Deut	C13	O18	Deut
Oct-17	-39.84	-6.02	-26.50	-39.52	-7.32	-36.70	-39.34	-7.30	-43.92	-39.06	-7.28	-44.89			
Nov-17	-39.51	-6.52	-41.70	-39.68	-7.10	-46.20	-41.79	-7.33	-47.08	-40.76	-7.19	-44.22	-40.68	-10.95	-73.03
Dec-17	-40.26	-5.42	-34.73	-40.53	-7.67	-37.85	-40.28	-7.70	-48.10	-40.70	-8.13	-45.57	-40.86	-10.48	-66.25
Jan-18	-40.57	-6.18	-30.27	-40.31	-6.12	-22.21	-40.32	-6.82	-29.71	-40.55	-7.44	-38.11	-40.31	-4.71	-45.70
Feb-18	-40.40	-5.44	-42.24	-41.18	-9.46	-50.62	-40.89	-7.85	-53.70	-40.85	-8.34	-48.13	-40.68	-8.41	-58.00
Mar-18	-40.29	-6.01	-39.43	-39.91	-5.90	-44.84	-40.06	-6.22	-46.32	-40.32	-6.82	-47.65	-40.96	-2.74	-8.71
Apr-18	-40.30	-5.79	-42.06	-40.09	-5.98	-45.86	-40.40	-6.71	-43.42	-40.99	-7.92	-41.71	-40.64	-3.47	-14.79
May-18	-40.61	-6.26	-38.85	-41.01	-7.67	-37.99	-40.72	-7.07	-38.96	-40.29	-6.65	-44.71	-40.77	-6.35	-24.70
Jun-18	-40.18	-5.40	-32.06	-40.13	-5.90	-27.90	-40.09	-6.12	-31.60	-40.35	-7.53	-35.64	-40.4167	-5.27333	-36.25
Jul-18	-41.06	-6.38	-38.24	-41.43	-8.76	-41.02	-41.01	-7.51	-39.38	-41.06	-7.31	-42.66	-41.02	-5.63	-24.53
Aug-18	-40.97	-7.05	-35.84	-40.86	-7.54	-38.83	-40.83	-7.18	-35.69	-40.97	-8.02	-42.34	-40.10	-5.87	-18.54

4.4 Field and Laboratory-Based Results and Interpretations

As an integral part of this study, the laboratory testing of materials was performed. In situ and laboratory-based engineering results obtained for this study includes SPT, RQD, Atterberg limit, and PLI.

4.4.1 SPT values

The SPT test is conducted to characterize the strength of soil materials. As the test progresses, soil samples and groundwater information are also collected. The results of SPT with respect to depth are summarized in Table 4.4 (Appendix C).

Table 4.4: The results of SPT values respect to the Depth.

B.H	N60	Depth
OW3	6	1.5
	10	3
	7	4.5
	6	6
	10	7.5
	12	9
TDR1	6	1.5
	8	3
	8	4.5
	13	6
	9	7.5
	10	9
OW4	14	7.5
	15	12.5
	13	12
OW2	15	15.5
	16	15.5
	8	4.5
	9	7.5
	16	1.5
	11	9

As shown in the Table, the minimum value of corrected SPT is 6 and the maximum value is 25 (SPT \geq 50 is refusal). It is observed that the highest value of SPT is related

to depth dense materials (silty sand) located at 15m depth. The lowest value of SPT is due to the presence of loose and poorly sorted materials. Also, the SPT values between 4 and 10 are observed at some depth (< 10 m), indicating the presence of loose materials to dense materials.

4.4.2 Atterberg limit

The critical water contents of a fine-grained soil were measured in the laboratory using the Atterberg limit test. Eight disturbed soil samples were collected from the boreholes in the target area. The results of the Liquid Limit, Plastic Limit and Plastic index tests are shown in Table 4.5.

Table 4.5: The values of Atterberg limit with depth (LL is for liquid limit, PL for plastic limit and PI for plasticity index).

ID	Depth (m)	LL	PL	PI
OW1	1.5			
	3			
	4.5			
	6			
	7.5			
	9			
	10.5			
	12			
OW3	1.5	37	26	11
	3			
	4.5			
	6			
	7.5	55	33	22
	9			
	10.5			
	12	41	29	12
	13.5			
15				
OW2	1.5			
	3	40	28	12
	4.5			
	6			
	7.5			
	9			
	10.5			
	12	35	25	10
	13.5			
	15	51	28	23
OW2	16.5			
	18			
	19.5			
	21			
	1.5	28	24	4
	3			
	4.5			
	6			

Table 4.5, continued.

OW4	7.5			
	9			
	10.5			
	12			
	13.5			
	15	33	25	8

Table 4.5 presents the Atterberg limit values for the collected soil samples from different boreholes. The difference between Liquid Limit and Plastic Limit denoted the plasticity index (PI) of soil. As noted in this table, the majority of PI values are between 7 and 17, revealing the presence of silty soil at a depth between 1.5 and 15 meters below the surface. However, the presence of clay and sand can be noted from the PI value of 23 in borehole OW2, and PI value of 4 in borehole OW4. This information thus suggests that the study area comprises of variable content of clay, silt and sand.

The possible effect of depth underground with physical parameters (Atterberg Limits) for soil is determined. Figures 4.19 to 4.21 show the relationships between the depth of sample (D) below ground surface and the Atterberg limits values i.e., liquid limit (LL), plastic limit (PL) and plastic index (PI), as indicated in these Figures the depth of sample (D) has no effect (correlation is found $R^2 < 0.30$) on the Atterberg limits of soil because they depend on the physical and mechanical properties of soil particles obtained from disturbed samples.

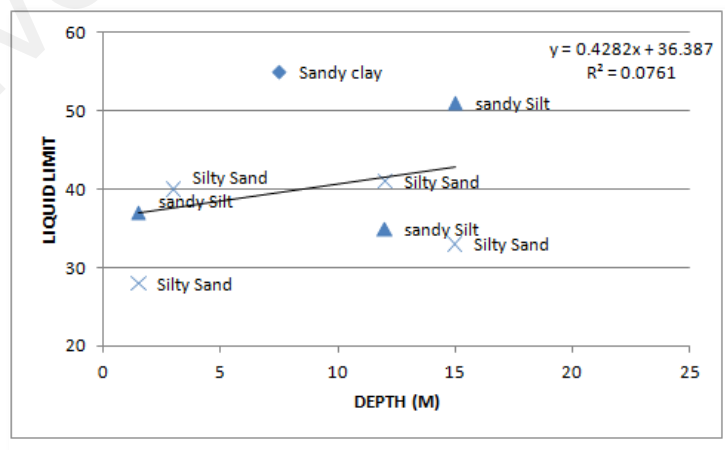


Figure 4.19: The relationship between liquid limit with the depth of the sample.

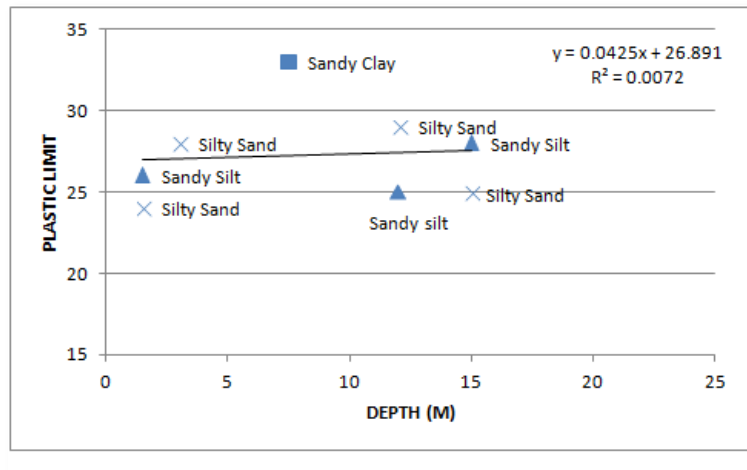


Figure 4.20: The relationship between plastic limit with the depth of the sample.

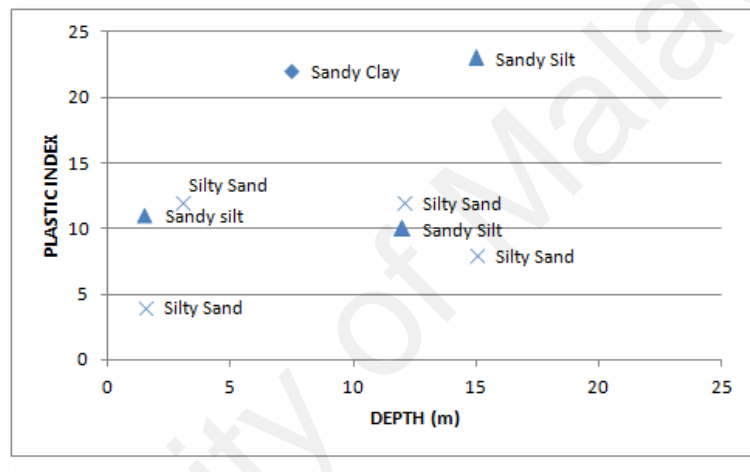


Figure 4.21: The relationship between plastic indexes with the depth of the sample.

4.4.3 Rock mass Quality of Granitic Rock

The rock quality designation and point load index are applied as a standard parameter in drill core logging to provide a quantitative estimate of rock mass quality. The classification of RQD values and Rock mass quality are displayed in Table 4.6. A total of four core samples were made as a description investigated for furnishing good information concerning the quality of underground the granitic rocks in the study area (Table 4.7).

Table 4.6: Rock Mass Classification from RQD Index (Deere et al., 1967).

RQD	Rock mass quality
< 25%	very poor
25% - 50%	poor
50% - 75%	fair
75% - 90%	good
90% - 100%	excellent

Table 4.7: The results of RQD with depth in the study area.

B.H	DEPTH	RQD
	22.5	49
OW2	24	59
	25.5	65
	27	51
	16.5	33
	18	20
OW3	19.5	16
	21	39
	16.5	13
	18	15
OW4	19.5	10
	21	10
	16.5	35
	18	22
TDR1	19.5	20
	21	35

Here, it can be noticed that as listed in Table 4.7 the depth of samples range from 16.5 – 28 meters below the ground surface and the value of RQD ranges between 10 and 65. As observed in Figure 4.22, a good correlation coefficient is found between RQD and Depth of sample with $R^2 = 0.52$ (52%) and a linear relationship between RQD and Depth with the empirical equation:

$$\text{RQD} = 4.5 * (\text{D}) - 50 \quad (4.3)$$

Where: RQD is rock quality designation value, and D is the depth of the sample. Referring to this equation the rock mass quality for the study site with depth less than 23 are classified as very poor in quality.

The RQD values with a depth of samples (Figure 4.22) appear into two groups. The first group has a mean value of around 22 % (very poor) and a depth ranging between 15 and 24 meters below the ground surface. The second group is distinguished with a mean value of about 56 % (Fair) and a depth > 24 meters. This variation of rock mass quality supports our findings from seismic tomography that the depth between 15 - 23 meters are classified as highly weathered granite (grade IV), while the depth > 23 is classified as grad-III (granite).

Table 4.8 summaries the geological classification for SMK Bukit Tinggi.

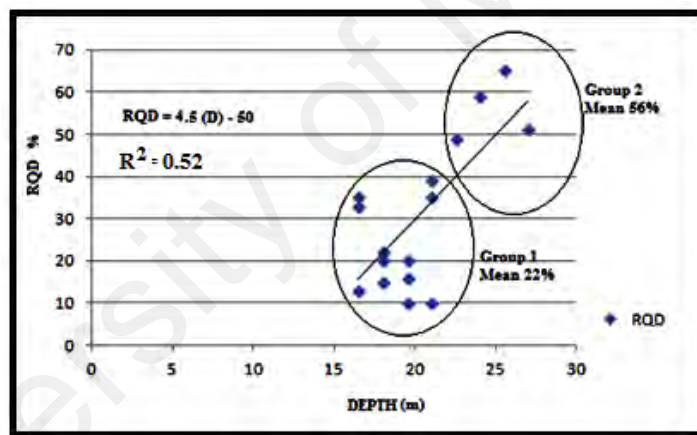


Figure 4.22: The relationship between RQD and depth in the study area.

Table 4.8: The Geological Classification of Granitic Rocks in the Study Area.

DEPTH	RQD	ROCK MASS QUALITY
<15 M	-	VERY POOR
15-23 M	LESS THAN 50	POOR
> 23 M	50- 75	FAIR

The point load index test gives a direct indicator of rock strength and enhances the understanding of other parameters. The results of point load test for nine collected samples are presented in Table 4.9.

Table 4.9: The results of the point load test index.

DEPTH	PLI (MPa)
15	1.47
17	1.67
18	1.81
19	1.7
20	1.66
22	1.85
23	1.91
24	1.77
25	1.84

As shown in the table, the values of point load test for granitic samples ranges between 1.47 to 1.91 MPa with the corresponding depths between 15 and 25 meters below the ground surface. According to these point load results the granitic rocks in the study site are classified as very low - low in strength (Deer, 1968). The results are used in further correlation to enhance final assumptions about the study area.

4.5 Discussions

As mentioned above, the aim of this research project is to assess and evaluate the chance of any potential hazard expected from ground settlement and ground movement in the school area by using geotechnical, geophysical and environmental isotopes methods. This, in turn, will enhance an understanding to predict the subsurface behavior that can trigger landslide activities and to suggest any protection actions to reduce such hazard.

4.5.1 Significance of the Geological Terrain Mapping

As a result of the systematic scientific processes, interpretive maps of geologic features are created. As such, evaluating groundwater, predicting earthquake events, and

assessing landslide hazards are some of the topics of concern in this study. Generally, this study used scientific procedures and methods to achieve the aim by starting with preliminary site investigation such as topographical, geological, terrain and engineering mapping.

Vast part of research that has been documented in the literature mentioned that the terrain features identification is based on systematic field observation (e.g. Manap *et al.*, 2010; Dia & Lee, 2002; Pain, 1985). In this context, the American system which points out focuses on land management and soil erosion (Waynell, 1978; Spangle *et al.*, 1976; the British system on geology and landforms (Dent, 1977; Lawrance, 1972; Bibby & Mackney, 1969), and the Canadian system on land cover (Vold, 1981). On the other hand, the Australians system focuses on engineering geology and related subjects (Grant, 1972, 1982). For this study, the Minerals and Geoscience Department Malaysia evaluation system (2006) is used. The results of the present study show that the SMK Bukit Tinggi area is classified into five classes according to the ability of development. The findings of this study are in agreement with the findings of Mohamad & Chow (2003) by which they created a construction map for Cameron Highland based on thematic maps of slope, activity, erosion and component maps. Moreover, their initial conceptual model of the site was developed from the perspective of potential risk development.

This study thus offers better results for the features under the studied SMK terrain, as evident from the obtained integrated information on landslide-related features. A construction map is the most important thematic map in this study due to a comprehensive understanding of the problematic site and the possible remediation proposal. The slope and component map also plays a vital role in this study. The advantage is that these maps give good information about the terrain features such as hillcrest, slope angle, side slope, foot slope, and concave slope. This information can

provide useful insight about the landslide triggering scientific assumptions building. Moreover, the results of terrain mapping are tallied with the field observation, which plays a vital role in selecting geophysical lines and borehole location. In addition, these results provide information on subsurface properties with low cost relatively large areas.

4.5.2 Evaluating the relationships between geophysical and geotechnical properties

In many cases, due to financial and time limitations in a project, various types of relationships are needed to estimate engineering parameters value (soil and rock strength) from the infield data (ERT and SR). In the present study, the data obtained from seismic refraction and electrical resistivity tomography methods are correlated with the borehole data gathered from different location of the study. An attempt to link the rock quality with seismic velocity has been performed at intervals, in the light of rock engineering and engineering geology information. The SR employed in this study encompasses 4 seismic lines which are comparing with 4 borehole datasets. As shown in Table 4.10, the correlation between P-wave velocities (VP) and the granitic rocks can reveal the level of weathering of the rock layer in peninsular Malaysia as reported by RafiqulIslam and Zaw Win (2005). Electrical Resistivity Tomography and Seismic Refraction methods were used in many types of research to assist landslide investigation (Lapenna *et al.*, 2003, Hack, 2000; Bruno & Marillier, 2000; Gallipoli *et al.*, 2000; Mauritsch *et al.*, 2000; McCann & Forster, 1990). Some studies identified the lithological condition in the landslide prone area (Rambhatla *et al.*, 2006), while some investigated the main bodies, their geometries and the surface breaks (Yang *et al.*, 2004; Hack, 2000; Havenith *et al.*, 2000; Caris & Van, 1991; Bogoslovsky & Ogilvy, 1977).

Table 4.10: Weathered granite rock mass classification in Peninsular Malaysia. (Source: Extracted and adapted from Islamic Rofiqul@ Zaw Win 2005).

Weathered Grade	P Wave Velocity (ms^{-1})	Explanation
VI and V	300-900	Residual soil and overall weathered
IV	900-1500	Highlyweathered
III	1500-2500	Moderatelyweathered
II	2500-4000	Slightlyweathered
I	4000-6000	Freshrock

In the present study, the ERT and SR were used to investigate the lithological boundary of a landslide zone in SMK Bukit Tinggi area. The obtained results show that variations in the electrical resistivity have been successfully used to identify two stratigraphic-structures. The contrasting electrical resistivity properties are used to characterize these stratigraphic units i.e., (1) an electrically conductive layer (variable thickness) with a resistivity value range of 20 Ohm-m to 500 Ohm-m, and (2) a deeper electrically resistive layer with a resistivity value of > 2000 Ohm-m. The results of this study are thus comparable to the previously reported findings by many researchers, by which they explained use of ERT in determining the thickness of landslide materials (De Vita *et al.*, 2006; Cummings & Clark, 1988; Bogosklovsky & Ogilvy, 1977; Denness *et al.*, 1975) as well as the casing of landslide (Hazreek *et al.*, 2017; Saad *et al.*, 2008).

The seismic refraction method has been effectively used in determining the landslide characteristics such as the depth and dip of a slip surface (Al-Saigh *et al.*, 2008), and changes in lithology with the position of slip surface (Hutchinson, 1982). However, these determinations have been made with an assumption that the velocity increases with depth (Kearey *et al.*, 2002). Correlation between data is needed to overcome this limitation. The seismic tomography images depict a two-layer structure model as well, confirming the observation of a two-layer structure from the electrical resistivity measurements. Based on the seismic refraction tomography images, the upper layer (\leq

15 m) has P-wave velocity values range of 300 m/s to 900 m/s, overlying a second layer (≥ 15 m) with P-wave velocity values range of 900 m/s to 3000 m/s. These images show a sharp boundary interface approximately at a depth of 15 m, because of the contrasting elastic properties of the subsurface materials. The here presented results thus agree with the previous studies in which the P-wave velocities values between slip surface and topsoil was attributed to a sharp boundary interface of slip surface (Kamic & Yalmaz, 2018; Malet *et al.*, 2012). Based on the here presented results, the initial conceptual model is improved significantly giving a good perspective for differentiating lithological units in the landslide-prone area for future developments using a set of geophysical methods.

In addition, the geotechnical parameters are investigated to get a proper assessment of soil and rocks as per the previously reported investigations (Kausarian, 2014). Standard penetration test results and Atterberg limits indicate that the materials up to 15 meters are considered loose and weak materials. Meanwhile, there is no correlation between the Atterberg limit and the targeted depth, indicating that the Atterberg limits do not depend on soil depth but on the physical and mechanical properties of soil particles. This study also examined the PI of soils, revealing different contents of clay, silt and sand at a depth range from 1.5 to 15 meters below the ground surface.

Furthermore, the present study determined the rock mass quality for rocks by using RQD and PLI results (Zhang, 2010; Zhang & Einstein, 2004; Serafim & Pereira, 1983; Coon & Merritt, 1970; Deere *et al.*, 1967). These results show the RQD values in a range between 10 and 65%, which classify the studied rocks as poor rocks (Deere *et al.*, 1967). In addition, the granite rocks have various grade of weathering ranging from extreme to moderately weathering. These results are supported by the point load test results (1.47 - 1.91 MPa), which is classified as very low - low in strength (Deer, 1968). The results of this study further indicate that the granitic rocks in the SMK area strongly

affected by weathering processes, thus increasing a chance of developing a slip surface for future landslide hazards in the area. The present results are thus in agreement with the previously conducted investigation (Kausarian, 2014) that classified the granitic rock mass according to RQD values. These results thus enhanced the development of the initial conceptual model and correlated well with other parameters to get a comprehensive understanding about the landslide slip surface.

Many of the documented literature have correlated the P-wave velocity with the borehole data in conjunction with geology, geomorphology, climatology and other related fields (Bery & Saad, 2012). Based on the here presented results the granitic rocks of the study area are classified into 3 zones. The first zone with a P-wave velocity of 300 to 900 m/s is made up of residual soils and extremely weathered granite. This zone, which has a variable thickness between 0 and 15.5 meters, is classified as Grade-VI and V in terms of weathering intensity. The second zone consists of highly weathered granitic rocks (grade IV) and has P-wave velocities ranged from 900 to 1800 m/s. This zone begins at a depth of 15.5 meters from the surface and varies from 9 to 10 meters in thickness. The third zone consists of weathered granitic rocks of medium-grade III with a P-wave velocity of 1800-3000 m/s and a thickness of 4-6 meters. The finding is almost similar to that of Abidin *et al.* (2012) who found the P-wave values of 330 to 600 m/s from topsoil/residual soil, a weathered zone with a mixture of soil, boulder and fractured rock (500 - 1900 m/s) and a fresh rock/bedrock (> 2300 m/s). The difference in P-wave values for two studies may be due to the fact that velocity in the field is heavily influenced by many factors such as the existence of cracks and squats (particularly in granitic rocks), porosity and groundwater conditions.

In the present study, the results of the averages corrected SPT from four boreholes are correlated with geophysical values (at the same locations). The relationship between ERT and corrected SPT are shown in Figure 4.23 and Table 4.11.

Table 4.11: The obtained values for SPT, SR and ERT.

Average N60	Average RES (ohm/m)	Depth (m)	Average SR (m/s)
6	99	1.5	318
10	100	3	345
7	58	4.5	320
6	33	6	350
10	60	7.5	385
12	170	9	400
6	80	1.5	415
8	139	3	418
8	75	4.5	425
11	81	6	450
9	142	7.5	444
10	103	9	595
14	260	11	615
15	335	12.5	615
13	230	14	618
15	350	15.5	620
16	450	15.5	685

As observed in Figure 4.23, a good correlation is found between SPT and ERT parameters with $R^2 = 0.77$ (77%) and a linear relationship between SPT and ERT with the empirical equation:

$$RES = 31.733 (N60) - 165.88 \quad (4.4)$$

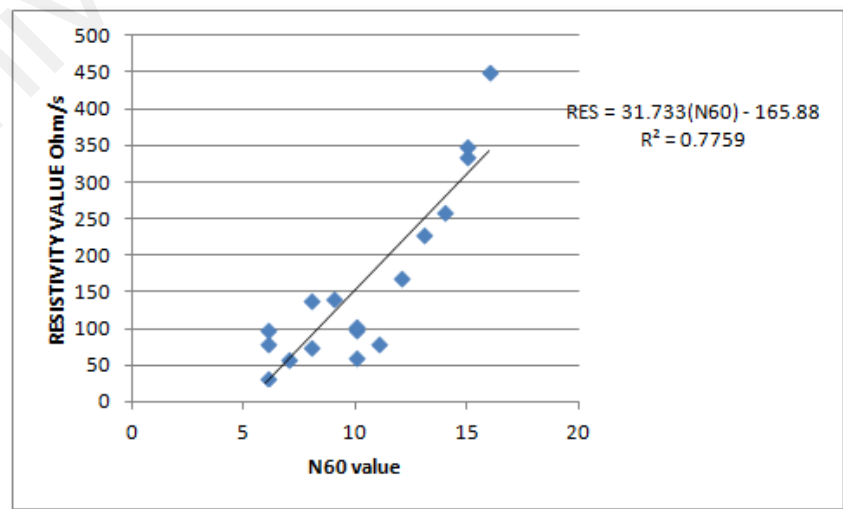


Figure 4.23: The relationship between ERT and SPT values.

The empirical equation (4.4) has been introduced to estimate corrected SPT values directly from resistivity data (Figure 4.23). The accuracy of this equation was verified by correlating the corrected SPT values with the P-wave velocity values and with the conventional method results. Furthermore, the transfer of equation 4.4 to the corrected SPT is made (Figure 4.24) by using Surfer 13 software. The validity of generated SPT is between 0 and 98 m in length and 15 meters in depth.

Figure 4.24 presents the inversion images of resistivity survey and the corrected SPT values generated from RES1, RES2, and RES4. In general, the results of SPT are similar to that of inversion resistivity, indicating the presence of two-layer structure underneath. The thickness of top layer varies from 5 m to 15 m and appears in RES2 and RES4, while the second layer appears approximately at a depth of 15 m (below the ground surface). However, these layers do not appear in the RES1 images because of the thickness of the top layer. The most important feature in the vertical sections is the clear showing of the conductive zone (SPT < 50) and resistive zone (SPT > 50). Moreover, an apparent break is noted in the unit (RES1, Res4) with SPT value >50, indicative of the presence of weak fractured zones.

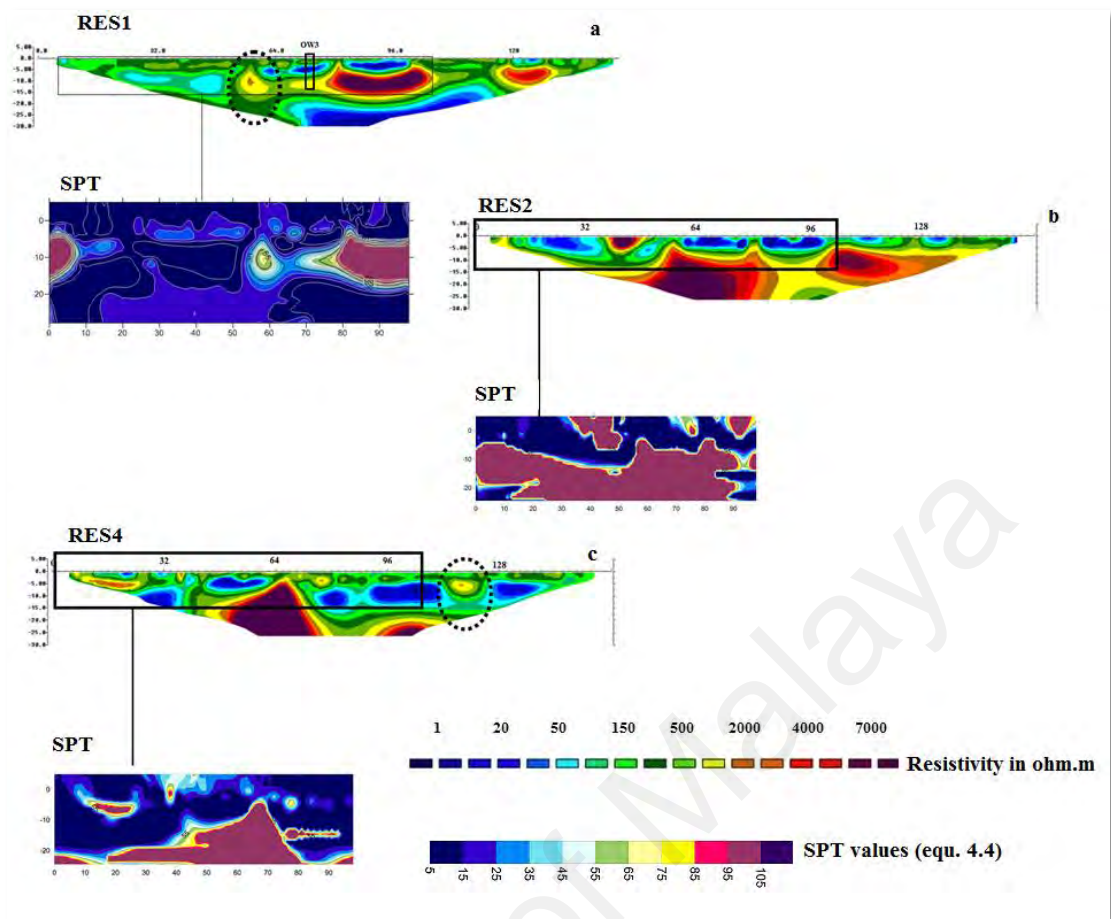


Figure 4.24: (a) The SPT values generated from profile RES 1. (b) The SPT values generated from profile RES 2. (c) The SPT values generated from profile RES 4.

The generated SPT results present a range of values (5 - 10) appear at 5- 15 meters depth, indicating that consists of loose/poorly sorted materials. The values between 10 and 30, which also appear at 5 and 15 meters depth, indicating the presence of dense materials (silty sand). The SPT result has relatively higher values (> 50), which appeared at exactly at 15 m depth, showing the beginning of the resistive zone (weathered granite).

Accordingly, the correlation variation of the P-wave velocity and the SPT with the respective depth is presented in Figure 4.25. A good correlation between these two parameters (with $R^2 = 0.71(71\%)$) and a linear relationship between SPT and SR is observed as expressed in the following empirical equation:

$$V_p = 31(N_{60}) + 149.5 \quad (4.5)$$

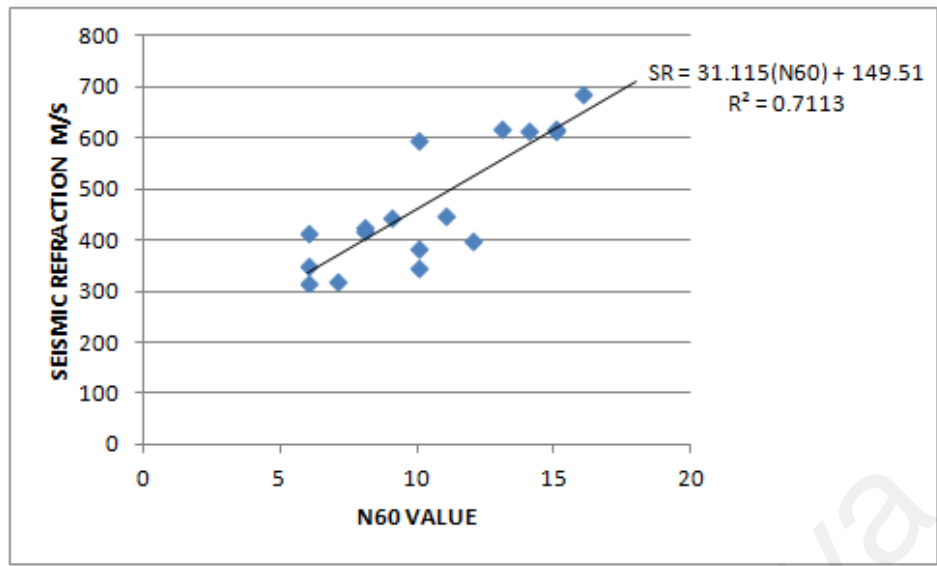


Figure 4.25: The relationship between SR and SPT values.

Moreover, a correlation between SR and ERT values is conducted (Figure 4.26) to introduce an empirical equation that can be used directly to estimate the SPT values and the weathering grade from ERT and SR values with low cost and efforts. Figure 4.26 presents a good correlation between these two parameters with correlation coefficient of $R^2=0.71$ (71 %) by an empirical equation:

$$V_p = 0.86(\text{RES}) + 332 \quad (4.6)$$

After compensation the values of RES in equation 4.4, a new equation made as following:

$$V_p = 0.86(32 \cdot N_{60}) - 166 + 332 \quad (4.7)$$

$$\text{Or } N_{60} = (V_p - 166) / 27.5 \quad (4.8)$$

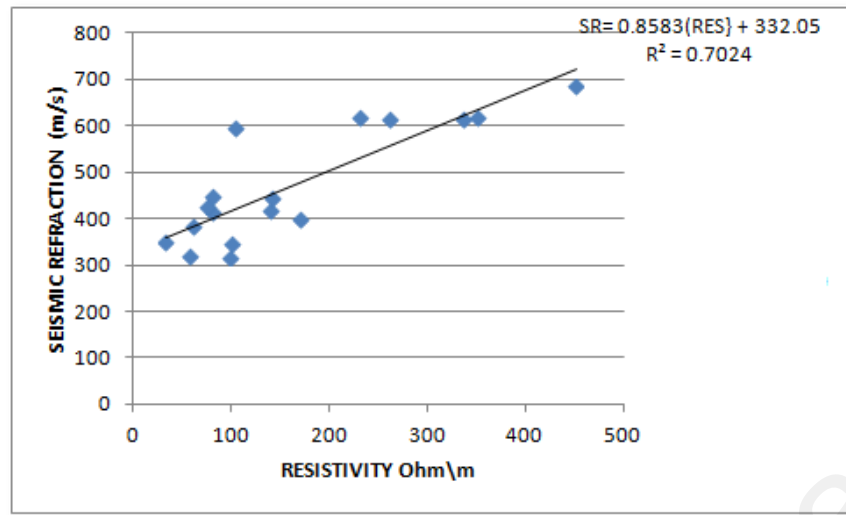


Figure 4.26: The relationship between ERT and SR values.

This study develops an empirical relationship between the p-wave velocity and the corrected SPT values (Figure 4.26). This equation supports the finding of present study, which can provide spatial information for the subsurface condition in landslide-prone areas with low cost and effort. In addition, the grade of weathering can be derived from this equation based on previous findings.

Due to the cost and time required for uniaxial compressive strength (UCS), the values of UCS are estimated from PLI by many authors (Abdul Karim *et al.*, 2018; Lai *et al.*, 2014; Quane & Russel, 2003). In this context, the most common relationship between UCS and PLI in granite rocks has been developed by Ghos (1991), ISRM (1981) and Kahraman (2015). The average values of the present study are derived from three empirical equations as shown in Table 4.12. As shown in this, the UCS values for the present study are in a range between 27 and 34) MPa, which are classified as very in low in strength. This range is within the Malaysian granitic range that found by Lia *et al* (2014) as the authors found that the UCS between 5 and 109 MPa.

Table 4.12: Listing of the UCS and PLI values from previous studies.

DEPTH	VP (m/s)	PLI (present study)	GHOS 1991 MPa	ISRM 1985 MPa	KAHRAMAN 2015	AVERAGE (UCS) MPa
15	750	1.47	23.52	35.28	24.8714	28
17	1100	1.67	26.72	40.08	28.9554	32
18	1700	1.81	28.96	43.44	31.8142	35
19	1500	1.7	27.2	40.8	29.568	33
20	1500	1.66	26.56	39.84	28.7512	32
22	1800	1.85	29.6	44.4	32.631	36
23	2200	1.91	30.56	45.84	33.8562	37
24	2100	1.77	28.32	42.48	30.9974	34
25	2700	1.84	29.44	44.16	32.4268	35

The empirical relationship between P-wave and UCS is presented in Figure 4.27 and the UCS values for the study area in Figure 4.28, and 4.29.

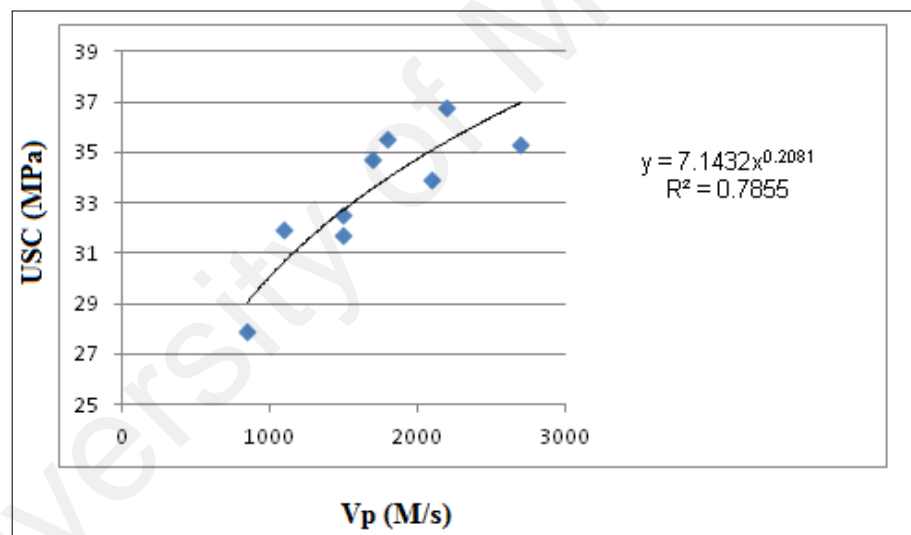


Figure 4.27: The empirical relationship for UCS –P-wave values for SMK Bukkit Tinggi area.

As shown in Figure 4.27 a good correlation between these two parameters with correlation coefficient of $R^2=0.78$ (78%) as per the following empirical equation:

$$UCS = 7.14 (Vp)^{0.21} \quad (4.9)$$

Application of this equation is useful in a tropical environment to identify the strength of granite and grade weathering of with respective to depth. Furthermore,

Classification of the weathering grade in the study area using UCS values is shown in Table 4.13 below.

Table 4.13: The relationship between UCS and weathering grade.

Depth	UCS	GRADE
<15	<27	VI- V
15-23	27-34	IV-III
>23	>34	III

The transfer of equations 4.5 and 4.9 to generate the corrected SPT and UCS values and the corresponding weathering grade is done by using Surfer 13 software. Three examples are considered to verify the validity of these equations as shown in Figure 4.28 and 4.29.

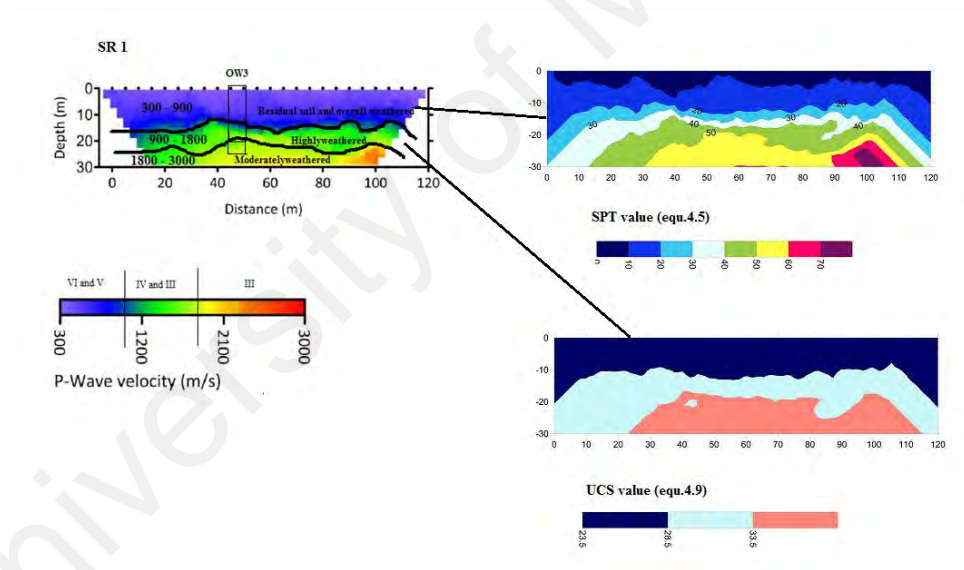


Figure 4.28: The relationship between SR, SPT, UCS and weathering grade for SR1.

Figure 4.28 presents the seismic tomography images of SR1 and the generated SPT, USC results. Based on the seismic tomography images, three zones are observed. The upper zone (≤ 15 m) has P-wave velocity from 300 m/s to 9000 m/s, and its weathering grade is classified as VI-V. The second zone (15-23 m) with P-wave velocity values of 900 m/s to 1800 m/s is classified as highly weathered granitic rocks (grade-IV). The third layer with P-wave velocity values (>1800) is classified as (grade-III). The seismic

tomography images show a sharp boundary interface approximately at a depth of 15 m, which corresponds to contrasting elastic properties of the subsurface materials across the boundary. The generated SPT values support the SR results where a range of SPT values (< 10) appear at depths between 5 m to 15 m, corresponds to low P-wave velocity due to loose/poorly sorted materials. Additionally, the SPT values between 10 and 30 appear at depth 5-15, indicating the presence of dense materials. The SPT result has relatively > 50 values appeared at depth 15 m, showing the beginning of the resistive zone. The UCS values are almost similar to that expected from SR and SPT interpretation, indicating the presence of three zones. The first zone with depth < 15 m and UCS values of 23.5- 28.5 MPa overly the second zone with depth 15-23 m and UCS values of 28.5- 33.5 MPa. The third zone has UCS value > 33.5 MPa, indicating the presence of variable materials in subsurface with depth.

Figure 4.29 presents the seismic tomography images of SR1 and the generated SPT, and USC results indicating the presence of two zones. The first zone carries an average P-wave velocity from 300 to 900 m/s. The first one is a zone of weathering with grade VI to V classification and thickness of 12 to 15.5 meters from the ground surface. The second zone underneath has a P-wave velocities range from 900 to 1800 m/s corresponding to weathered granite.

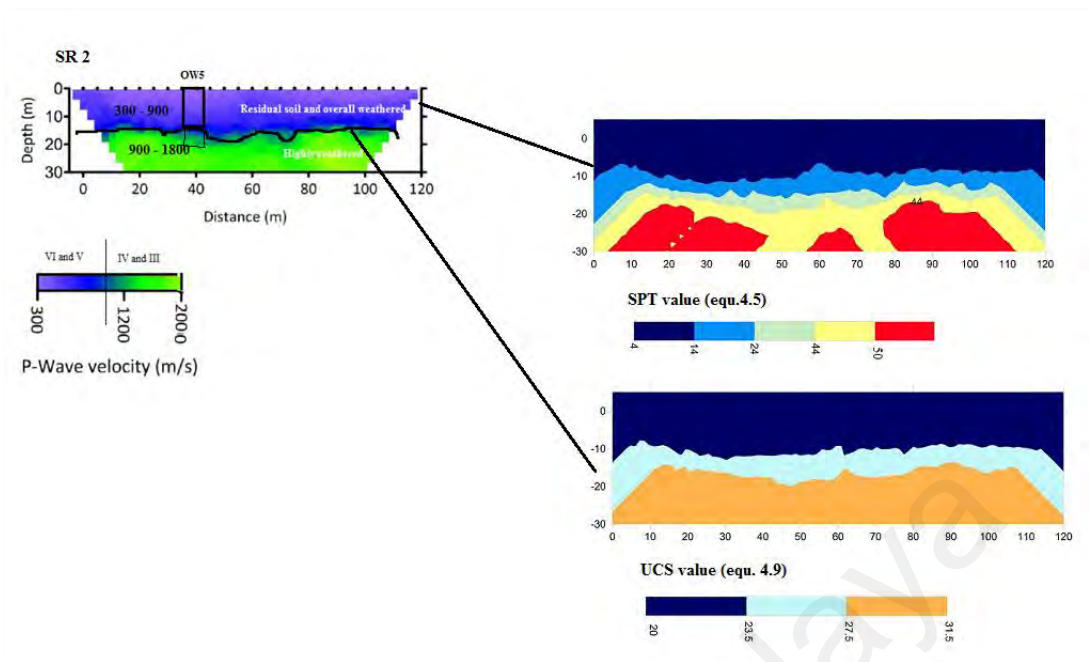


Figure 4.29: The relationship between SR, SPT, UCS and weathering grade for SR2.

This zone is of high weathered granitic rocks (classified as grade IV) begins at a depth of 15.5 meters with a thickness range of 4 to 8 meters. Additionally, the SPT values of 4 -24 are relevant to the first zone, indicating the presence of dense materials, while the SPT values of 24 – 50 are relevant to the second zone. The high values of SPT >50 appear at 15 meters depth, corresponding to the presence of granitic rocks. The UCS values are compatible with the SR and SPT results (as expected), also indicating the presence of two zones. The first zone with <15m depth and UCS value of 23.5 to 27.5 MPa overly the second zone with a depth > 15 m and UCS values of 27.5 to 33.5 MPa. The third zone has values of >33.5 MPa.

As indicated in Figures (4.24 and 4.28) the generated SPT values from RES and SR are similar; showing significant changes at the same depth. This lead to verify the above-mentioned findings that the materials above the slip surface are loose in strength and a sharp boundary interface is located approximately at a depth of 15 m. Therefore, this finding proves the efficiency of using geophysical techniques in landslide area for correlation purpose and for introducing new empirical equations in tropical environmental study.

4.5.3 Weathering Zone Interpretation

P-wave velocity in the field is heavily influenced by many factors such as the existence of cracks and squats (particularly in granitic rocks), porosity and groundwater conditions. Many of the weathered zones layers are recorded for each line using seismic refraction survey where P-wave showed decreasing weathering grade of rock with depth. Thus, based on the results obtained, grade VI residual soil and grades V weathered rock the exposed surface layer. Grade VI residual soil has a P-wave velocity less than 300 m/s, while that for grade V granitic rocks ranged from 300 to 900 m/s.

The relationship between P-wave velocity values and the grade of weathering in each part of the study area are summarized in Table 4.14.

Table 4.14: The relationship between P-wave velocity and Rock weathering grade obtained in the study area.

GEOLOGICAL CLASSIFICATION	P- WAVE VELOCITY ms⁻¹	WEATHER GRADE
Residual soil and overall weathered	300 – 900	VI and V
Highly weathered	900 – 1800	IV and III
Moderately weathered	1800 – 3000	III

4.5.4 Groundwater Dynamics and Flow Behaviour

The origin and source of groundwater in the landslide area were determined by many previous studies (Tullen, 2006; Peng *et al.*, 2007; Syakir *et al.*, 2018). The present study found that the groundwater has contributed to the stream flow in the same direction as that of the mass movement. The results presented here indicated that the isotope data of surface and groundwater are distributed along the LMWL, indicating that stable isotopes of both surface and groundwater have no effects of evaporation and can thus be regarded as conservative. Furthermore, it has been observed that rainfall is the main source of the groundwater recharge in the area through the cracks and weak zones.

These results are in good agreement with the previous researches, which determines the source and origin of the groundwater in the landslide area through recharge from rainfall (Hasin *et al.*, 2009; Sykir *et al.*, 2018). These finding thus enhanced an understanding of the hydrological process in the SMK area and accordingly helped in developing an initial conceptual model.

4.6 Identification of Weakness Plane (Slip surface)

As a result of the integrated geophysical, engineering and isotopes a possible slip surface is located at a depth of 15m from the ground surface (Figure 4.30). The geological properties and classification of soil and rocks in the SMK Bukit Tinggi area are summarized in Table 4.14.

As summarized in Table 4.15, the investigated subsurface consists of three main zones i.e., a zone of loose/unconsolidated materials, a zone of weathered materials and a zone of hard materials/bedrock respectively. The assume landslide surface is detected between zone 1 and 3, where the materials show large differences in physical properties based on primary velocity obtained. The difference between weak zones with depth is occurring due to the assumption that subsurface materials have experienced additional weathering processes.

Moreover, the fill materials in the study area have the same properties with the underlying materials i.e., SPT Values, indicating the presence of loose material thus corresponding to uncompacted material. The contact between fill material and the underlying materials is considered a weakness zone.

The present findings agree with some previous research findings, which it has been concluded that materials above the weakness plane have big variation in physical properties such as a slip mass show lower seismic velocity than the underlying stable strata (Al-Saigh & Al-Dabbagh 2010; Glade *et al.*, 2005; Caris and Van, 1991). The low

P-wave velocity thus corresponds to landslide mass whereas the high P-wave velocity corresponds to underlying surface of bedrock (Göktürkle 2008).

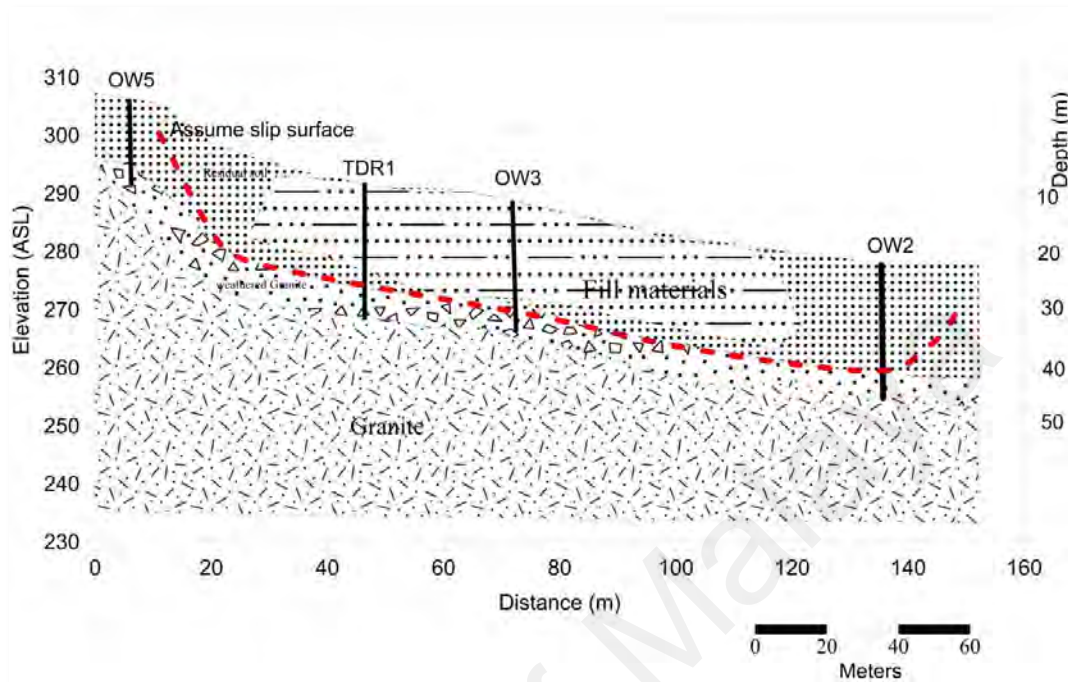


Figure 4.30: The Cross sections for SMK Bukit Tinggi area, showing predicted depths of assume slip surface, and weathered granite.

It is also predicted that the rates of weathering are influenced by climate and rock characteristics in the area. The weathering process greatly increased due to a large amount of rainfall and moisture, thus increasing the rate of change in subsurface material from homogeneous to heterogeneous (Abidin *et al.*, 2012). As noted above, in addition to cut and fill materials on the original ridge topography that contributed to weakening the ground foundation for long term stability, the underground water infiltration rainfall is considered as a vital triggering factor for the expected landslide in SMK area. The underground water infiltration through the surface cracks and a resultant chemical weathering is creating an environment for landslide hazards and an expected structure failure in the area.

Table 4.15: Summary of the physical properties obtained from this study for SMK Bukit Tinggi area.

Depth	P-wave velocity m/s	RQD	N(60)	Weathered granite grade	Zone classification	Geological classification
<15 M	300-900	-	< 29	VI- V	Zone A	Very poor (Residual soil and extremely weathered)
15-23 M	900-1800	< 50	29-60	IV-III	Zone B	Poor (Highly weathered)
> 23	>1800	50- 75	> 60	III	Zone C	Fair (moderately weathered)

The underground chemical weathering takes place when water seeps into the materials through fractures, which rate of deep weathering material increase. The weathered and fractured materials then decomposed into fine-grained materials, and some of them might have filled the existing fractures, which probably paved a way for variable P-wave velocity in the subsurface. Over a period of years, an increase in weathering may erode the low resistant rock layers, undermining the slope stability due to the seepage process between two layers of different permeability. The infiltration process during the heavy rainfall increases the groundwater level in a saturated zone causing an increasing in soil mass and in pore water pressure. Such a condition would reduce the internal strength of subsurface materials, and eventually pave a way slope failure. Any seismic activity during that process could contribute to increase the degree of deformation in the SMK Bukit Tinggi area, especially in area near the active fault segment.

As a result of the integrated investigation by the present study, a conceptual model is developed for landslide potentiality in SMK Bukit Tinggi area (Figure 4.31). This model can be considered as a general landslide model for landslide-prone (tropical

hotspot area) area because it is developed by using both of conventional and advanced methods.

The here presented model can be coupled with other models to improve landslide monitoring and prediction such as identifying local landslides prone area. This model can also be converted into a real-time landslide prediction model by further improvement.

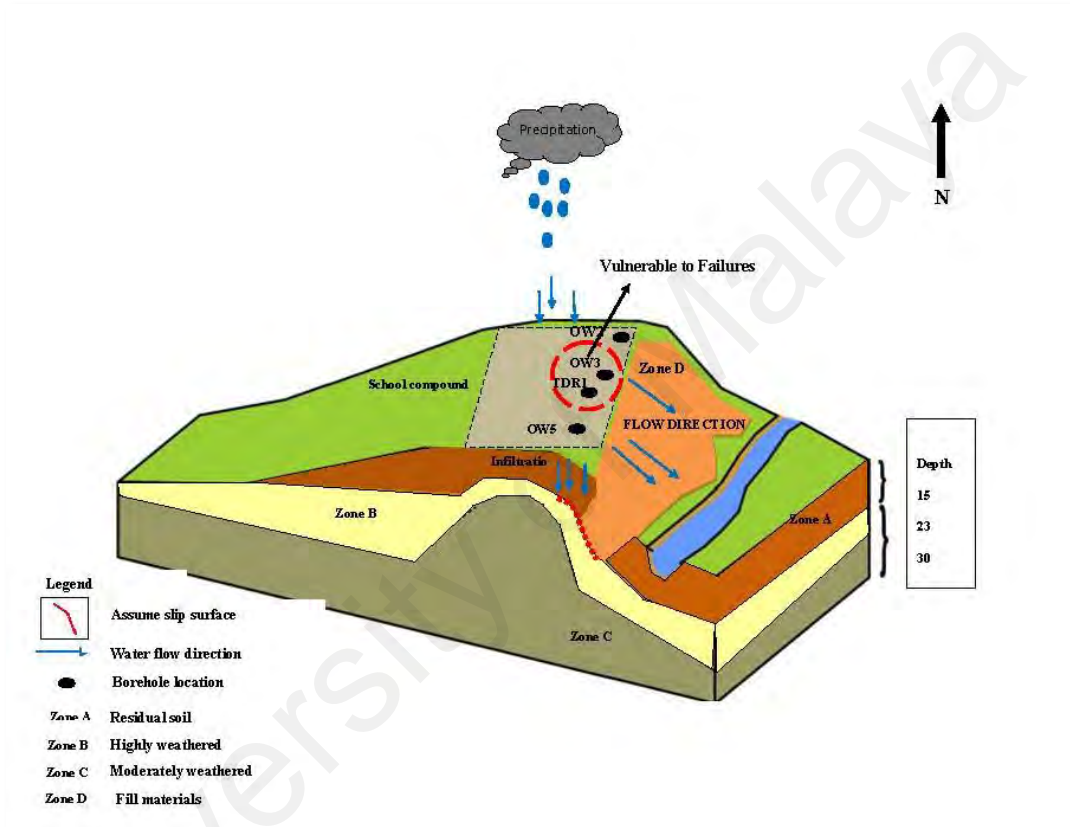


Figure 4.31: The developed conceptual model for landslide prone area.

4.7 Summary

This chapter presents the obtained results from all methods and techniques used in SMK Bukit Tinggi area in order to assess and evaluate the main triggering factor and mechanism of the landslide problem. This chapter also highlights the efficiency of using integrated methods in landslide related investigation. The obtained results were deeply discussed to get a comprehensive understanding of the subsurface conditions.

Furthermore, this chapter determines the physical properties of soil and rocks and identifies the possible slip surface in the SMK Bukit Tinggi area. It also gives comprehensive and clear images of the groundwater origin, flow and the expected hazards of slope instability in the area.

Additionally, this chapter discusses the possible correlation between geophysical and geotechnical parameters. Based on this correlation, the efficiency of geophysical parameters is introduced as new empirical equations that can be applied to landslide-prone area in a tropical environment.

Moreover, this chapter discusses a transfer of all finding from conventional and advanced methods to create a final conceptual model for landslide potential in the SMK Bukit Tinggi.

University of Malaya

CHAPTER 5: CONCLUSIONS

5.1 Introduction

This research project was designed and aimed to study the effectiveness of integrated geophysical, engineering and environmental isotope techniques for improved assessment of the landslide-prone area in SMK Bukit Tinggi. In this chapter, the summary of findings from this project and how it fulfills the proposed objectives is highlighted. The main research contributions are concluded in the following sections.

5.2 Conclusions

This research project examined the use of conventional and advanced techniques (including geophysical, engineering, geological and environmental isotope techniques) to characterize the subsurface condition in the landslide-prone area. Furthermore, the selected methods enhance the understanding of landslide slip surface, triggering factors, mechanism and hazard mitigation.

Based on the review of literature in Chapter 2, a research strategy was developed to assess different mechanisms that trigger landslide occurrences and, identify their contributing factors and reduce their adverse impacts. As mentioned above, the active segments of the NW-SE Bukit Tinggi fault can be considered as potential sources of earthquakes in the SMK area. Any future activity along this fault can thus trigger a landslide in this area.

Accordingly, various methods (as mentioned in chapter 3) were considered in a finest way to scientifically overcome researches the problems. These methods included certain geophysical, environmental and geotechnical techniques. The geophysical techniques applied include resistivity and seismic refraction, while others are geological terrain mapping, soil and rock sampling for laboratory testing, water sampling and other best-suited techniques for achieving the research objectives.

Several findings are discussed in chapter 4; the field geological terrain mapping is conducted for SMK area. The results offer a better perspective for the terrain features by introducing improved and updated information on landslide-related features.

The geophysical techniques have their own research objectives for this study; the most important among them is to identify different hydrogeological units and to determine the subsurface geological features. The function is not just to identify, but also to determine the extent and variability in thicknesses. This will indirectly help in identifying and predicting future potential risk of slope failure/landsliding in the area.

The results from ERT and SR surveys lead to a hypothesized two-layer stratigraphic model. The upper layer is identified at depth up to 15 meters, followed by the second layer.

The results also show an apparent break in the unit, indicative of the presence of weak fractured zone. This leads to the assumption that the electrically conductive upper layer (<500 Ohm-m) is indicative of loose/poorly sorted backfill materials comprising of variable quantities of clay, gravel and sand. This assumption is confirmed by borehole data for soil and rocks as well.

Moreover, this research correlated the SR and ERT results with the geotechnical properties of soil and rocks gathered from borehole data at the study site. Based on the results obtained, the study area is classified into three zones according to weathering grade: The residual soil and extremely weathered granite from top layer are classified as grade-VI and grade-V, respectively. The highly weathered grade-III materials have a P-wave velocity between 1800 and 3000 m/s, while that of grade-IV materials is in a range between 900 and 1800 m/s.

The corrected SPT values of 5 – 50 appear at depth <15, indicating loose to very dense materials, which is in good agreement with Resistivity results, where the low SPT values are related with low RES values. The SPT values of >50 appeared at a depth of

15 meters, indicating the start of a resistive zone (granitic rocks). The ERT data also show a good relationship with the corrected SPT data, as expressed by the empirical equation $RS = 31.733 (N60) - 165.88$. The accuracy of this equation was verified by correlating the corrected SPT values with P-wave velocity and with the results of the conventional test. In addition, this research project introduces several other empirical equations based on physical properties of subsurface materials that can help future researchers to determine the subsurface problems with low cost and effort.

Groundwater direction and origin were determined in this research as well. The result of CBS and stable isotopes show that the groundwater flow is most likely following the same direction as that of mass movement prior to discharging into the nearby stream. Rainfall is considered as the main source for groundwater accumulation, thus increasing the pore water pressure and builds up extra pressure on underground materials. Consequently, it destroys the stability of the slope.

Overall, the use of integrated methods gives a lot of support in defining the capability and efficiency of the geophysical techniques to investigate stability of the slope. Based on these integrated results, an improved conceptual model is created for the study area. This model can be used as an updated alternative landslide model in landslide-prone (tropical hotspot) area due to the fact that it is created based on conventional and advanced methods. However, the presented model can be combined with other models to improve landslide monitoring and prediction in local landslides prone area. With further improvement, this model can be developed into a real-time landslide prediction model.

5.3 Recommendations and Future Work

The obtained integrated results and the presented model of this study on landslide prone areas can be improved by conducting further investigations. Although, the integrated geophysical – geotechnical investigation of soil and rocks and the constructed

empirical equations of this research give promising results, an advanced model has to be developed to properly describe the subsurface lithology and structure in the landslide prone areas. The integrated techniques offer fast and useful data, which can reduce the overall cost of investigations in such area. Moreover, results of stable isotopes (Oxygen and Hydrogen) give power for evaluating the origin and source of groundwater which can develop the hydrogeological process for landslide prone areas.

For future researches on the subject matter, it has to be considered that, 1) what integration of techniques can provide best results in developing a real-time landslide prediction model, 2) how accurate the applied geophysical data are and 3) how are the relationships between the geophysical and geotechnical parameters.

As a remediation suggestion for the SMK site, consolidation foundation grouting in the vulnerable to failure area (refer to Figure 4.31) is a useful method to increase the shear strength for the subsurface materials. This procedure will help minimize water infiltration in the weak zones and thus maintain slope stability in the area.

REFERENCES

- Abd Manap, M., Ramli, M. F., Wan, N., & Surip, N. (2010). Application of remote sensing in the identification of the geological terrain features in Cameron Highlands, Malaysia. *Sains Malaysiana*, 39(1), 1-11.
- Abidin, M. H. Z., Madun, A., Tajudin, S. A. A., & Ishak, M. F. (2017). Forensic assessment on near surface landslide using electrical resistivity imaging (ERI) at Kenyir Lake Area in Terengganu, Malaysia. *Procedia Engineering*, 1(71), 434-444.
- Abidin, M. H. Z., Saad, R., Ahmad, F., Wijeyesekera, D. C., & Baharuddin, M. F. T. (2012). Seismic refraction investigation on near surface landslides at the Kundasang area in Sabah, Malaysia. *Procedia Engineering*, 50, 516-531.
- Aggour, M. S., & Radding, W. R. (2001). *Standard penetration test (SPT) correction* (Report No. MD02-007B48). Retrieved on June 28, 2016, from <https://www.roads.maryland.gov>
- Ahmad, R., & McCalpin, J. P. (1999). *Landslide susceptibility maps for the Kingston Metropolitan Area with notes on their use* (UDS Publication No. 5). Retrieved on April 11, 2016, from <https://www.oas.org/cdmp/document/kma/udspub5.htm>
- Al-Dabbagh, T. H. (1986). A study of residual shear strength of Namurian shale in respect of slopes in north Derbyshire (Doctoral dissertation) University of Sheffield.
- Aleotti, P., & Chowdhury, R. (1999). Landslide hazard assessment: summary review and new perspectives. *Bulletin of Engineering Geology and the Environment*, 58(1), 21-44.
- Aleotti, P., Baldelli, P., Bellardone, G., Quaranta, N., Tresso, F., Troisi, C., & Zani, A. (2002). L'evento meteorico del 13 – 16 ottobre 2000 nel Piemonte Settentrionale: analisi delle precipitazioni e dei processi di versante indotti. *Geologia Technicae Ambientale 1*, 15–25.
- Alexander, J. B. (1956). *Lexique Stratigraphique International, Vol. 3. Asie, fascicules 6b & 7c Malaya*. Paris, France: Centre National de la Recherche Scientifique.
- Alexander, J.B. (1968). *The geology and mineral resources of the Bentong area, Pahang*. Ipoh, Malaysia: Geological Survey Headquarters.
- Ali, S., Biermanns, P., Haider, R., & Reicherter, K. (2019). Landslide susceptibility mapping by using GIS along the China–Pakistan economic corridor (Karakoram Highway), Pakistan. *Natural Hazards and Earth System Sciences*, 19, 999-1022.
- Al-Saigh, N. H., & Al-Dabbagh, T. H. (2010). Identification of landslide slip-surface and its shear strength: A new application for shallow seismic refraction method. *Journal of the Geological Society of India*, 76(2), 175-180.
- Al-Saigh, N. H., & Toffeq, I. N. (1993). Geological and geophysical study of the southern part of Saddam reservoir. *Iraqi Geological Journal*, 27(2), 150-161.
- Alvioli, M., Marchesini, I., Reichenbach, P., Rossi, M., Ardizzone, F., Fiorucci, F., & Guzzetti, F. (2016). Automatic delineation of geomorphological slope units with

- r. slopeunits v1.0 and their optimization for landslide susceptibility modeling. *Geoscientific Model Development*, 9(11), 3975.
- Ayalew, L., Yamagishi, H., & Ugawa, N. (2004). Landslide susceptibility mapping using GIS-based weighted linear combination, the case in Tsugawa area of Agano River, Niigata Prefecture, Japan. *Landslides*, 1(1), 73-81.
- Batayneh, A. T., & Al-Diabat, A. A. (2002). Application of a two-dimensional electrical tomography technique for investigating landslides along the Amman–Dead Sea highway, Jordan. *Environmental Geology*, 42(4), 399-403.
- Bennett, G. L., Miller, S. R., Roering, J. J., & Schmidt, D. A. (2016). Landslides, threshold slopes, and the survival of relict terrain in the wake of the Mendocino Triple Junction, Geology. *The Geological Society of America*, 44(5), 363–366.
- Bery, A. A., & Saad, R. (2012). Clayey Sand Soil's Behaviour Analysis and Imaging Subsurface Structure via Engineering Characterizations and Integrated Geophysical Tomography Modeling Methods. *International Journal of Geosciences*, 3(1), 93.
- Bichler, A., Bobrowsky, P., Best, M., Douma, M., Hunter, J., Calvert, T., & Burns, R. (2004). Three-dimensional mapping of a landslide using a multi-geophysical approach: the Quesnel Forks landslide. *Landslides*, 1(1), 29-40.
- Bogoslovsky, V. A., & Ogilvy, A. (1977). Geophysical methods for the investigation of landslides. *Geophysics*, 42(3), 562-571.
- Bonnard, C., & Noverraz, F. (2001). Influence of climate change on large landslides: Assessment of long-term movements and trends. In M. Kühne (Ed.), *International Conference on Landslides: Causes Impact and Countermeasures* (pp. 121-138). Davos, Switzerland: VEG.
- Brand, E. W., (1985). Predicting the performance of residual soil slopes. In *Proceedings of the 11th International Conference on Soil Mechanics and Foundation Engineering* (Vol. 5, pp. 2541-2578). Rotterdam, The Netherlands: A.A. Balkema.
- Broeckx, J., Vanmaercke, M., Duchateau, R., & Poesen, J. (2017). A landslide susceptibility map of Africa. *EGU General Assembly Conference Abstracts*, 19, 27.
- Bruno, F., & Marilier, F. (2000). Test of high-resolution seismic reflection and other geophysical techniques on the Boup landslide in the Swiss Alps. *Survey Geophysics*, 21(4), 333-350.
- Canli, E., Mergili, M., Thiebes, B., & Glade, T. (2018). Probabilistic landslide ensemble prediction systems: Lessons to be learned from hydrology. *Natural Hazards and Earth System Sciences*, 18(8), 2183-2202.
- Caris, J. P. T., & Van Asch, T. W. (1991). Geophysical, geotechnical and hydrological investigations of a small landslide in the French Alps. *Engineering Geology*, 31(3-4), 249-276.
- Carpentier, S., Konz, M., Fischer, R., Anagnostopoulos, G., Meusburger, K., & Schoeck, K. (2012). Geophysical imaging of shallow subsurface topography and its implication for shallow landslide susceptibility in the Urseren Valley, Switzerland. *Journal of Applied Geophysics*, 83, 46-56.

- Çelik, R. N., Ayan, T., Denli, H., Özlüdemir, T., Erol, S., Groten, E., & Leinen, S. (1999). Landsliding monitoring using GPS and conventional techniques in Gurpınar. *Proceedings of the Third Turkish German Joint Geodetic Days*, 3, 839-848.
- Chen, W., Li, X., Wang, Y., Chen, G., & Liu, S. (2014). Forested landslide detection using LiDAR data and the random forest algorithm: A case study of the Three Gorges, China. *Remote Sensing of Environment*, 152, 291-301.
- Chigira, M., Mohamad, Z., Sian, L. C., & Komoo, I. (2011). Landslides in weathered granitic rocks in Japan and Malaysia. *Bulletin of the Geological Society of Malaysia*, 57, 1–6.
- Corominas, J. & Moya, J. (1999). Reconstructing recent landslide activity in relation to rainfall in the Llobregat river basin, Eastern Pyrenees, Spain. *Geomorphology*, 30(12), 79–93.
- Crosta, G. (1998). Regionalization of rainfall threshold: an aid to landslide hazard evaluation. *Environmental Geology*, 35(2-3), 131–145.
- Cummings, D., & Clark, B. R. (1988). Use of seismic refraction and electrical resistivity surveys in landslide investigations. *Bulletin of the Association of Engineering Geologists*, 25(4), 459-464.
- Dahlin, T. (2001). The development of DC resistivity imaging techniques. *Computers & Geosciences*, 27(9), 1019-1029.
- Dai, F. C., & Lee, C. F. (2002). Landslide characteristics and slope instability modeling using GIS, Lantau Island, Hong Kong. *Geomorphology*, 42(3-4), 213-228.
- De Silva, S., Wightman, N., & Kamruzzaman, M. (2010). Geotechnical ground investigation for Padma Main Bridge. In A. F. M. Saiful Amin (Ed.), *Proceedings of the IABSE–JSCE Conference* (pp. 42-436). Dhaka, Bangladesh: IABSE.
- De Vita, P., Agrello, D., & Ambrosino, F. (2006). Landslide susceptibility assessment in ash-fall pyroclastic deposits surrounding Mount Somma-Vesuvius: Application of geophysical surveys for soil thickness mapping. *Journal of Applied Geophysics*, 59(2), 126-139.
- Denness, B., Conway, B. W., McCann, D. M., & Grainger, P. (1975). Investigation of a coastal landslip at Charmouth, Dorset. *Quarterly Journal of Engineering Geology*, 8(2), 119-140.
- Dostál, I., Putiška, R., & Kušnirák, D. (2014). Determination of shear surface of landslides using electrical resistivity tomography. *Contributions to Geophysics and Geodesy*, 44(2), 133-147.
- ESTFBC. (1996). *Guidelines and Standards to terrain mapping in British Columbia*. Resource inventory committee, Surficial Geological Task Group Earth Science Task Force British Columbia.
- Fathani, T. F., Karnawati, D., & Wilopo, W. (2016). An integrated methodology to develop a standard for landslide early warning systems. *Natural Hazards and Earth System Sciences*, 16(9), 2123-2135.

- Ferrucci, F., Amelio, M., Sorriso-Valvo, M., & Tansi, C. (2000). Seismic prospecting of a slope affected by deep-seated gravitational slope deformation: The Lago Sackung, Calabria, Italy. *Engineering Geology*, 57(1-2), 53-64.
- Flentje, P. N., Chowdhury, R. N. & Tobin, P. (2000). Management of landslides triggered by a major storm event in Wollongong, Australia, *In Second International Congress on Debris Flows Hazard Mitigation* (pp.479-487). Taipei, Taiwan.
- Friedel, S., Thielen, A., & Springman, S. M. (2006). Investigation of a slope endangered by rainfall-induced landslides using 3D resistivity tomography and geotechnical testing. *Journal of Applied Geophysics*, 60(2), 100-114.
- Froude, M. J., & Petley, D. (2018). Global fatal landslide occurrence from 2004 to 2016. *Natural Hazards and Earth System Sciences*, 18, 2161-2181.
- Gallipoli, M., Lapenna, V. I. N. C. E. N. Z. O., Lorenzo, P. I. E. T. R. O., Mucciarelli, M., Perrone, A., Piscitelli, S., & Sdao, F. (2000). Comparison of geological and geophysical prospecting techniques in the study of a landslide in southern Italy. *European Journal of Environmental and Engineering Geophysics*, 4, 117-128.
- Gat, J. R. (1996). Oxygen and hydrogen isotopes in the hydrologic cycle. *Annual Review of Earth and Planetary Sciences*, 24(1), 225-262.
- Gat, J. R., & Gonfiantini, R. (1981). Stable isotope hydrology. Deuterium and oxygen-18 in the water cycle. Retrieved on April 21, 2018, from <https://www.osti.gov/etdeweb/biblio/5130758>.
- Gelisli, K., & Ersoy, H. (2017). Landslide investigation with the use of geophysical methods: A case study in northeastern Turkey. *Advance Biological and Earth Science*, 2, 52-64.
- Gibson, J. J., Edwards, T. W. D., Birks, S. J., St Amour, N. A., Buhay, W. M., McEachern, P., ... & Peters, D. L. (2005). Progress in isotope tracer hydrology in Canada. *Hydrological Processes*, 19(1), 303-327.
- Godt, J. W., Baum, R. L., & Lu, N. (2009). Landsliding in partially saturated materials. *Geophysical Research Letters*, 36(2), 1-5.
- Gritzner, M. L., Marcus, W. A., Aspinall, R., & Custer, S. G. (2001). Assessing landslide potential using GIS, soil wetness modeling and topographic attributes, Payette River, Idaho. *Geomorphology*, 37(1-2), 149-165.
- Guzzetti, F., Cardinali, M., & Reichenbach, P. (1996). The influence of structural setting and lithology on landslide type and pattern. *Environmental & Engineering Geoscience*, 2(4), 531-555.
- Hack, R. (2000). Geophysics for slope stability. *Survey Geophysics*, 21(4), 423-448.
- Haile, N S. (1970). Ores on the geology of the Tambelan, Anambas and Bunguran (Naruna) islands, Sunda Shelf, Indonesia, including radiometric age determinations. U.N. ECAFE C.C.O.P. *Technical Bulletin* 3, 55-90.
- Hartinger, H. Brunner, F. K. (2000). *Development of a monitoring system of landslide motions using GPS*. Paper presented at the Ninth FIG International Symposium

on Deformation Measurements, Olsztyn, Poland. Retrieved on June 5, 2018, from <http://citeseerx.ist.psu.edu/viewdoc/download?>

- Havevith, H. B., Jongmans, D., Abdrakhmatov, K., Trefois, P., Delvaux, D., & Torgoev, I. A. (2000). Geophysical investigations of seismically induced surface effects: case study of a landslide in the Suusamyр valley, Kyrgyzstan. *Surveys in Geophysics*, 21(4), 351-370.
- Huang, C. C., Lo, C. L., Jang, J. S., & Hwu, L. K. (2008). Internal soil moisture response to rainfall-induced slope failures and debris discharge. *Engineering Geology*, 101(3-4), 134-145.
- Huat, L. T., Ali, F., & Ibrahim, A. S. (2012). An Investigation on one of the rainfall-induced landslides in Malaysia. *Electronic Journal of Geotechnical Engineering*, 17, 435-449.
- Humyra, T., Awall, M. R., Mofiz, S. A., & Sobhan, M. A. (2012). Preparation of SPT contour Map of Rajshahi City Area and its application to foundation design. *International Journal of Civil & Environmental Engineering IJCEE-IJENS*, 12(2), 11-16.
- Hutchinson, C. S., & Tan, D. N. K. (Eds.). (2009). *Geology of Peninsular Malaysia*. Kuala Lumpur, Malaysia: University of Malaya.
- Hutchinson, J. N. (1988). General report: Morphological and geotechnical parameters of landslides in relation to geology and hydrogeology. In C. Bonnard (Ed.), *Fifth International Symposium on Landslides* (Vol. 1, pp. 3-35). Rotterdam, The Netherlands: Balkema.
- Islam, R & Zaw, W. (2005). Rofiqul Islam. 2005. Engineering geology and geophysical studies of granite weathering profile at Bukit Fraser, Pahang. (*Graduate Thesis*) National University of Malaysia.
- Ismail, N. I., & Yaacob, W. Z. (2018). Application of electrical resistivity tomography (ERT) for slope failure investigation: A case study from Kuala Lumpur. *Jurnal Teknologi*, 80(5), 79-86.
- Jaapar, A. R. B. (2006). *A framework of a national slope safety system for Malaysia*. (Master's Thesis) University of Hong Kong. Retrieved on 21 March 2016 from <http://hub.hku.hk/handle/10722/50173>
- Jamaludin, S. (2006). *Development of a cut slope stability assessment system for Peninsular Malaysia* (Unpublished doctoral dissertation). University Putra Malaysia, Serdang, Malaysia.
- Jamaluddin, T. A. (2015, March). *Large-scale landslides - some case studies from Malaysia*. Paper presented at the International Symposium on Multi-Hazard and Risk 2015, Kuala Lumpur, Malaysia.
- Jonathan, M. Carey, M. J., Massey, C. I., Lyndsell, B., & Petley, D. N. (2018). Displacement mechanisms of slow-moving landslides in response to changes in pore water pressure and dynamic stress. *Earth Surface Dynamic*, 73, 1-27.
- Jones, C.R. (1973b). Lower Palaeozoic. In: Gobbet, D.J & Malay Peninsula. *Overseas Geology and Mineral Resource* 44, 1-28.

- Jongmans, D., & Garambois, S. (2007). Geophysical investigation of landslides: a review. *Bulletin de la Société Géologique de France*, 178(2), 101-112.
- Kalkan, Y. (2007). Atatürk Barajında Jeodezik Yöntemlerle Deformasyonların İzlenmesi [Monitoring of Deformation in Ataturk Dam by Using Geodetic Method]. *Projesi Teknik Raporu, DSİ Genel Müdürlüğü*, Ankara, Turkey.
- Kalkan, Y., & Alkan, R. M. (2006). Mühendislik yapılarında deformasyon ölçmeleri. *In 2nd Natinoal Engineering Surveying Symposium*, (pp. 23-25), Turkey.
- Kausarian, H., Shamsudin, A. R., & Yuskar, Y. (2014). Geotechnical and rock mass characterization using seismic refraction method at Kajang rock quarry, Semenyih, Selangor Darul Ehsan. *Journal of Ocean, Mechanical and Aerospace*, 14, 12-17.
- Kaya, A., & Karaman, K. (2016). Utilizing the strength conversion factor in the estimation of uniaxial compressive strength from the point load index. *Bulletin of Engineering Geology and the Environment*, 75(1), 341-357.
- Kazmi, D., Qasim, S., Harahap, I., Baharom, S., Imran, M., & Moin, S. (2017). A study on the contributing factors of major landslides in Malaysia. *Civil Engineering Journal*, 2 (12), 669-678.
- Kearey, P., Brooks, M., & Hill, I. (2002). An introduction to geophysical exploration 3rd ed. Hong Kong: Blackwell, Oxford.
- Kearl, P. M. (1997). Observations of particle movement in a monitoring well using the colloidal borescope. *Journal of Hydrology*, 200(1-4), 323-344.
- Keller, G. V., & Frischknecht, F. C. (1966). *Electrical methods in geophysical prospecting*. Oxford, UK: Pergamon Press.
- Kuo, H. L., Lin, G. W., Chen, C. W., Saito, H., Lin, C. W., Chen, H., & Chao, W. A. (2018). Evaluating critical rainfall conditions for large-scale landslides by detecting event times from seismic records. *Natural Hazards & Earth System Sciences*, 18(11), 2877-2891.
- Lacasse, S., Nadim, F. (2009). Landslide risk assessment and mitigation strategy. In K. Sassa & P. Canuti (Eds.), *Landslides – Disaster Risk Reduction* (pp. 31-61). Berlin, Germany: Springer.
- Lai, G. T., Rafek, A. G., Serasa, A. S., Simon, N., Ern, L. K., & Hussain, A. (2014). Empirical correlation of uniaxial compressive strength and primary wave velocity of Malaysian granites. *The Electronic Journal of Geotechnical Engineering E*, 19, 1063-1072.
- Lapenna, V., Lorenzo, P., Perrone, A., Piscitelli, S., Sdao, F., & Rizzo, E. (2003). High-resolution geoelectrical tomographies in the study of Giarrossa landslide (southern Italy). *Bulletin of Engineering Geology and the Environment*, 62(3), 259-268.
- Lee, K. S., & Kim, Y. (2007). Determining the seasonality of groundwater recharge using water isotopes: a case study from the upper North Han River basin, Korea. *Environmental Geology*, 52(5), 853-859.

- Lee, K. S., Wenner, D. B., & Lee, I. (1999). Using H-and O-isotopic data for estimating the relative contributions of rainy and dry season precipitation to groundwater: Example from Cheju Island, Korea. *Journal of Hydrology*, 222(1-4), 65-74.
- Lee, L. M., Kassim, A., & Gofar, N. (2011). Performances of two instrumented laboratory models for the study of rainfall infiltration into unsaturated soils. *Engineering Geology*, 117(1-2), 78-89.
- Lee, S., & Pradhan, B. (2006). Probabilistic landslide hazards and risk mapping on Penang Island, Malaysia. *Journal of Earth System Science*, 115(6), 661-672.
- Lee, S., & Talib, J. A. (2005). Probabilistic landslide susceptibility and factor effect analysis. *Environmental Geology*, 47(7), 982-990.
- Li, F., Pan, G., Tang, C., Zhang, Q., & Yu, J. (2008). Recharge source and hydrogeochemical evolution of shallow groundwater in a complex alluvial fan system, southwest of North China Plain. *Environmental Geology*, 55(5), 1109-1122.
- Loke, M. H. (2004, July 26). *Tutorial: 2-D and 3-D electrical imaging surveys*. Retrieved on June 22, 2017, from https://sites.ualberta.ca/~unsworth/UA-classes/223/loke_course_notes.pdf
- Malehmir, A., Saleem, M. U., & Bastani, M. (2013). High-resolution reflection seismic investigations of quick-clay and associated formations at a landslide scar in southwest Sweden. *Journal of Applied Geophysics*, 92, 84-102.
- Matori, A. N., Basith, A., & Harahap, I. S. H. (2012). Study of regional monsoonal effects on landslide hazard zonation in Cameron Highlands, Malaysia. *Arabian Journal of Geosciences*, 5(5), 1069-1084.
- Mauritsch, H. J., SeiberL, W., Arndt, R., Romer, A., Schneiderbauer, K., & Sendlhofer, G. P. (2000). Geophysical investigations of large landslides in the Carnic region of southern Austria. *Engineering Geology Journal*, 56(3-4), 373-388.
- McCann, D. M., & Forster, A. (1990). Reconnaissance geophysical methods in landslide investigations. *Engineering Geology*, 29(1), 59-78.
- Metcalf, I. (1999). The paleo Tethys in East Asia. *Geological Society of Malaysia Bulletin*, 43, 131-143.
- Mohamad, Z., & Chow, W. S. (2003). Geological terrain mapping in Cameron Highlands district, Pahang. *Geological Society of Malaysia, Bulletin* 46, 69-73.
- Morgan, B. A., Wiczorek, G. F., Campbell, R. H., & Gori, P. L. (1997). Debris-flow hazards in areas affected by the June 27, 1995, storm in Madison County, Virginia, open file report, *United State Geology Survey*, 15, 97-438.
- Mukhlisin, M., Idris, I., Salazar, A. S., Nizam, K., & Taha, M. R. (2010). GIS based landslide hazard mapping prediction in Ulu Klang, *Malaysia. Journal of Mathematical and Fundamental Sciences*, 42(2), 163-178.
- Ng, T. F. (1992). Shore Scleroscope Hardness of the Kuala Lumpur Granite, Peninsular Malaysia. *Warta Geologi*, 18(4), 154-159.

- Ng, T. F. (1994). Microstructures of the deformed granites of eastern Kuala Lumpur—Implications for mechanisms and temperatures of deformation. *Geological Society of Malaysia Bulletin* 35, 47-59.
- Norbury, D. R. (1986). The point load test. Geological Society, London *Engineering Geology Special Publications*, 2(1), 325-329.
- Nordin, M. M., & Mohamed, Z. (2013). Empirical Correlation of P-wave Velocity to the Density of Weathered Granite. In *International Civil and Infrastructure Engineering Conference* (pp. 489-499). Singapore: Springer.
- Nutalaya, P., 1991. Catastrophic landslides and sheet flooding in an intermontane tropical basin, southern Thailand. *Asian Institute of Technology*, Bangkok, Thailand.
- Oh, H. J., & Lee, S. (2011). Landslide susceptibility mapping on Panaon Island, Philippines using a geographic information system. *Environmental Earth Sciences*, 62(5), 935-951.
- Owen, L. A., Sharma, M. C., & Bigwood, R. (1995). Mass movement hazard in the Garhwal Himalaya: The effects of the 20 October 1991 Garhwal earthquake and the July-August 1992 monsoon season. In D. F. M. McGregor & D. A. Thompson (Eds.), *Geomorphology and land management in a changing environment* (pp. 69-88). Chichester, UK: Wiley.
- Oyediran, I.A., & Falae, P.O. (2018). Integrated Geophysical and Geotechnical Methods for Pre-Foundation Investigations. *Journal of Geology and Geophysics*, 8(1), 1-9.
- Pain, C. F. (1985). Mapping of landforms from Landsat imagery: an example from eastern New South Wales, Australia. *Remote Sensing of Environment*, 17(1), 55-65.
- Paronuzzi, P., Del Fabbro, M. & Maddaleni, P. (2002). Frane superficiali tipo slide debris flow causate dal nubifragio del 21/22 giugno 1996 nella Val Chiarso` (Alpi Carniche, Friuli), *Memorie della Societa Geologica Italiana*, 57, 443-452.
- Peng, T. R., Wang, C. H., Hsu, S. M., Wang, G. S., Su, T. W., & Lee, J. F. (2010). Identification of groundwater sources of a local-scale creep slope: Using environmental stable isotopes as tracers. *Journal of Hydrology*, 381(1-2), 151-157.
- Peng, T. R., Wang, C. H., Lai, T. C., & Ho, F. S. K. (2007). Using hydrogen, oxygen, and tritium isotopes to identify the hydrological factors contributing to landslides in a mountainous area, central Taiwan. *Environmental Geology*, 52(8), 1617-1629.
- Polloni, G., Ceriani, M., Lauzi, S., Padovan, N., & Crosta, G. (1992). Rainfall and soil slipping events. In *Valtellina. Proceeding of the VI International Symposium on Landslides, Christchurch, I*, 183-188.
- Pradhan, B. (2010). Remote sensing and GIS-based landslide hazard analysis and cross-validation using multivariate logistic regression model on three test areas in Malaysia. *Advances in Space Research*, 45(10), 1244-1256.

- Pradhan, B., & Lee, S. (2010). Delineation of landslide hazard areas on Penang Island, Malaysia, by using frequency ratio, logistic regression, and artificial neural network models. *Environmental Earth Sciences*, 60(5), 1037-1054.
- Pradhan, B., & Youssef, A. M. (2010). Manifestation of remote sensing data and GIS on landslide hazard analysis using spatial-based statistical models. *Arabian Journal of Geosciences*, 3(3), 319-326.
- Pradhan, B., Chaudhari, A., Adinarayana, J., & Buchroithner, M. F. (2012). Soil erosion assessment and its correlation with landslide events using remote sensing data and GIS: a case study at Penang Island, Malaysia. *Environmental Monitoring and Assessment*, 184(2), 715-727.
- Public Work Department. (2009a). Final Investigation Report Investigation of Slope Failure at Taman Bukit Mewah. Bukit Antarabangsa Hulu Klang Selangor. Cawangan Kejuruteraan Cerun, Jabatan Kerja Raya Malaysia.
- Public Works Department, (2009b). National Slope Master Plan. Sectoral Report Research and Development, Jabatan Kerja Raya Malaysia.
- Qasim, S., Harahap, I. S. H., Osman, S., & Baharom, .S. (2013). Causal factors of Malaysian landslides: A narrative study. *Research Journal of Applied Sciences, Engineering and Technology*, 5(7), 2303-2308.
- Quane, S. L., & Russell, J. K. (2003). Rock strength as a metric of welding intensity in pyroclastic deposits. *European Journal of Mineralogy*, 15(5), 855-864.
- Rahman, H. A., & Mapjabil, J. (2017). Landslides Disaster in Malaysia: an Overview. *Health and the Environment Journal*, 8(1), 58 –71.
- Reynolds, J. (1997). *An introduction to applied and environmental geophysics*. Chichester, UK: Wiley and Sons.
- Richardson, J. A. (1939). *The Geology and Mineral Resources of the Neighbourhood of Raub, Pahang, Federated Malay States, with an account of the Geology of the Raub Australia Gold Mine*. Federated Malay States, Singapore: Geological Survey Department.
- Richardson, J.A. (1950). *The geology and mineral resources of the neighbourhood of Chegar Perah and Merapoh, Pahang*. Federation of Malaya, Batu Gajah: Geological Survey Department.
- Roslee, R., Jamaluddin, T. A., & Talip, M. A. (2010). Aplikasi GIS dalam penaksiran risiko gelinciran tanah (LRA): Kajian kes bagi kawasan Kota Kinabalu, Sabah, Malaysia, Application of GIS in landslide risk assessment (LRA): A case study for Kota Kinabalu, Sabah, Malaysia. *Bulletin of the Geological Society of Malaysia*, 57(57), 69-83.
- Saad, R., Abdel Wahab, H. M., Nawawi, M. N. M., Alfouzan, F., & Maleki, Z. (2008, December). *Monitoring slope failure using 2d electrical resistivity imaging in Pahang, Malaysia*. Paper presented at the International Conference on Environment, Penang, Malaysia. Retrieved on October 11, 206, from <https://scholar.google.com.my/scholar?>
- Sastry, R. G., Mondal, S. K., & Pachauri, A. K. (2006). 2D electrical resistivity tomography of a landslide in Garhwal Himalaya. In *Proceedings of the 6th*

- International Conference and Exposition on Petroleum Geophysics* (Vols. 1-2, pp. 977-1001). Dehradun, India: Society of Petroleum Geophysicists (India).
- Sew, G. S., & Chin, T. Y. (2002, July). *Mitigating the risk of landslide on hill-site development in Malaysia*. Paper presented at the 2nd World Engineering Congress, Kuching, Malaysia. Retrieved on August 25, 2016, from http://www.gnpgeo.com.my/download/publication/SL_01.pdf
- Sew, G., & Tan, Y. C. (2006, August). *Landslides: Abuses of the prescriptive method*. Paper presented at the International Conference on Slope, Kuala Lumpur, Malaysia. Retrieved on January 26, 2017, from http://www.gnpgeo.com.my/download/publication/2006_04.pdf
- Sezer, E. A., Pradhan, B., & Gokceoglu, C. (2011). Manifestation of an adaptive neuro-fuzzy model on landslide susceptibility mapping: Klang valley, Malaysia. *Expert Systems with Applications*, 38(7), 8208-8219.
- Sharma, P. V. (1997). *Environmental and engineering geophysics*. Cambridge, England: Cambridge University Press.
- Sharpe, C. F. S. (1938). *Landslides and related phenomena, a study of mass movement of soil and rock*. New York, United States: Columbia University Press.
- Shu, Y.K. (1969). Some NW trending faults in Kuala Lumpur and other areas. *Newsletter Geol. Soc. Malaysia* 17, 1-5.
- Shuib, M. K. (2009). The recent Bukit Tinggi earthquakes and their relationship to major geological structures. *Bulletin of the Geological Society of Malaysia*, 55, 67-72.
- Shuib, M. K., Manap, M. A., Tongkul, F., Rahim, I. B. A., Jamaludin, T. A., Surip, N., ... & Ahmad, Z. (2017). Active faults in Peninsular Malaysia with emphasis on active geomorphic features of Bukit Tinggi region. *Malaysian Journal of Geoscience*, 1(1), 13-26.
- Siswosoebrotho, B. I., K. Ginting & T. L. Soedirdjo(2005). Workability and Resilient Modulus of Asphalt Concrete Mixtures Containing Flaky Aggregates Shape. *Journal of the Eastern Asia Society for Transportation Studies*, 6, 1302-1312.
- Souza, J. M. S., Danziger, B. R., & Danziger, F. A. B. (2012). The influence of the relative density of sands in SPT and CPT correlations. *Soils and Rocks*, 35, 99-113.
- Stauffer, P.H. (1968). The Kuala Lumpur Fault Zone: A proposed major strike-slip fault across Malaysia. *Newsletter Geological Society of Malaysia* 15, 2-4.
- Syakir, M. I., Jamian, N. S., Jaafar, M. H., Yusuff, M. S., Zuknik, M. H., & Mostapa, R. (2018). A Review of Environmental Isotopes: It's Prospective Applications in Disaster-risk Management of Watershed. *Journal of Physical Science*, 29(3), 121-147.
- Syed Omar, S. N., Jeber, F. K. M., & Mansor, S. (2004). GIS/RS for landslides zonation in Pos Slim-Cameron Highlands district, Peninsula Malaysia. *Disaster Prevention and Manageme: An International Journal*, 13(1), 24-32.

- Tang, Z. (1991). *A study of landslides in weathered granitic slopes in Amphoe Phi Pun, Nakhon Si Thammarat, Thailand* (Unpublished master's thesis). Asian Institute of Technology, Bangkok, Thailand.
- Ting, W. H. (1984). Stability of slopes in Malaysia. In A. Balasubramaniam, D. Bergado, S. Chandra, G. Rantucci, *Geotechnical aspects of mass and material transportation: Proceedings of the international symposium, Bangkok, 3-14 December 1984* (pp. 119-128). Rotterdam, The Netherlands: A.A. Balkema.
- Tingsanchali, T. (1989). Debris flow caused by heavy rainfall and landslides. *Technical Journal of Engineering and Information Technology*, 2, 22-31.
- Tsai, T. L., Chen, H. F. (2010). Effects of degree of saturation on shallow landslides triggered by rainfall, *Environmental Earth Sciences*, 59(6), 1285–1295.
- Tsiambaos, G., & Sabatakakis, N. (2004). Considerations on strength of intact sedimentary rocks. *Engineering Geology*, 72(3-4), 261-273.
- Tullen, P., Turberg, P., & Parriaux, A. (2006). Radiomagnetotelluric mapping, groundwater numerical modelling and 18-Oxygen isotopic data as combined tools to determine the hydrogeological system of a landslide prone area. *Engineering Geology*, 87(3-4), 195-204.
- United States Geological Survey. (2004, July). *Landslide types and processes* (Fact Sheet 2004-3072). Retrieved on December 29, 2015, from <https://pubs.usgs.gov/fs/2004/3072/fs-2004-3072.html>
- Van Asch, T. W., Buma, J., & Van Beek, L. P. H. (1999). A view on some hydrological triggering systems in landslides. *Geomorphology*, 30(1-2), 25-32.
- Vandenschrick, G., Van Wesemael, B., Frot, E., Pulido-Bosch, A., Molina, L., Stievenard, M., & Souchez, R. (2002). Using stable isotope analysis (δD - $\delta^{18}O$) to characterise the regional hydrology of the Sierra de Gador, south east Spain. *Journal of Hydrology*, 265(1-4), 43-55.
- Varnes, D. J. (1987). Slope movement types and processes. In *Special Report – Transportation Research Board, National Research Council: Vol. 176*. M. Clark (Ed.), *Landslides: Analysis and control* (pp. 11-33). Washington, DC: National Academy of Sciences.
- Varnes, D. J. (1978). Slope movement types and processes. *Special Report*, 176, 11-33.
- Varnes, D. J. (1983) Time-deformation relations in creep to failure of earth materials. *Proceedings of the Seventh Southeast Asian Geotechnical Conference*, Hong Kong, 2, 107-130.
- Venkatasubramanian, C., & Dhinakaran, G. (2011). ANN model for predicting CBR from index properties of soils. *International Journal of Civil and Structural Engineering*, 2(2), 605-611.
- Vichas, C., Skourtis, C., & Stiros, S. (2001). *Kinematics of a landslide over the Polyphyton Reservoir (Greece)*. Paper presented at the 10th FIG International Symposium on Deformation Measurements, International Federation of Surveyors, Orange, California. Retrieved on October 23, 2017, from <https://www.academia.edu/26168351/>

- Vow, T. (1981). Terrain analysis for transportation systems in British Columbia TRRL. Retrieved on October 15, 2015, from https://scholar.google.com/scholar?hl=en&as_sdt=0%2C5&q
- Wieczorek, G. F. (1996). Landslides: investigation and mitigation. Chapter 4-Landslide triggering mechanisms. *Transportation Research Board Special Report, 247*, 76-90.
- William Spangle and Associates, F. Beach Leighton and Associates, & Baxter, McDonald and Company. (1976). *Earth-science information in land-use planning: guidelines for earth scientists and planners*. (USGS Cir. No. 721). Washington, DC: Government Printing Office.
- Wu, J. & Li, T. (2001). Behaviour and characteristics of debris flows. In Tianchi, L., Chalise, S. R., & Upreti, B. N. (Eds.), *Landslide Hazard Mitigation in the Hindu Kush-Himalayas* (pp. 203-214). Kathmandu, Nepal: International Center for Integrated Mountain Development.
- Wu, X., Chen, X., Zhan, F. B., & Hong, S. (2015). Global research trends in landslides during 1991–2014: a bibliometric analysis. *Landslides, 12*(6), 1215-1226.
- Yang, C. H., Liu, H. C., & Lee, C. C. (2004, January). Landslide investigation in the Li-Shan area using resistivity image profiling method. In *SEG Technical Program Expanded Abstracts 2004* (pp. 1417-1420). Society of Exportation Geophysicists.
- Yeh, H. F., Lee, C. H., & Hsu, K. C. (2011). Oxygen and hydrogen isotopes for the characteristics of groundwater recharge: a case study from the Chih-Pen Creek basin, Taiwan. *Environmental Earth Sciences, 62*(2), 393-402.
- Yilmaz, S., & Kamaci, Z. (2018). Resistivity and Seismic refraction studies on Kissikli landslide (Antalya, Turkey). *International Journal of computational and experiemental sciencs and Engineering, 4*(3), 9-14.
- Yurtsever, Y., & Gat, J. R. (1981). Atmospheric waters. In *IAEA Technical Reports Series: No. 210*. J. R. Gat & R. Gonfiantini (Eds.), *Stable isotope hydrology: deuterium and oxygen-18 in the water cycle* (pp. 103-142). Vienna, Austria: IAEA.
- Zainal Abidin, M.H., Madun,A., Tajudin,S.A., & Ishak,M.F. (2017). Forensic assessment on near surface landslide using electrical resistivity imaging (ERI) at Kenyir Lake Area in Terengganu, Malaysia. *Procedia Engineering, 171*(2017), 434-444.
- Zaki, A., Chai, H. K., Razak, H. A., & Shiotani, T. (2014). Monitoring and evaluating the stability of soil slopes: A review on various available methods and feasibility of acoustic emission technique. *Comptes Rendus Geoscience, 346*(9-10), 223-232.
- Zein, A. K. M., & Sandal, M. A. (2018). Estimation of the strength of Nubian sandstone formation from point load test index and other simple parameters. *MATEC Web of Conferences, 149*, 2024.
- Zhang, L. (2010). Estimating the strength of jointed rock masses. *Rock Mechanics and Rock Engineering, 43*(4), 391-402.

- Zhang, L. (2016). Determination and applications of rock quality designation (RQD). *Journal of Rock Mechanics and Geotechnical Engineering*, 8(3), 389-397.
- Zhang, L., & Einstein, H. H. (2004). Using RQD to estimate the deformation modulus of rock masses. *International Journal of Rock Mechanics and Mining Sciences*, 41(2), 337-341.
- Zhu, Z. W., Liu, D. Y., Yuan, Q. Y., Liu, B., & Liu, J. C. (2011). A novel distributed optic fiber transducer for landslides monitoring. *Optics and Lasers in Engineering*, 49(7), 1019-1024.

University of Malaya

LIST OF PUBLICATIONS AND PAPERS PRESENTED

PUBLICATIONS

1. **Alkhamaiseh, T.**, Mejus, L., Yusoff, I., & Yaccup, R. (2018). Relationships between geophysical and geotechnical parameters focusing on a site specific results of a landslide risk area. *Amazonia Investiga*, 7(15), 386-398.

PAPER PRESENTED

1. Mejus, L., Hashim, M. M. M., Yaccup, R., Azmi, M. I. N., Daung, J. A. D., Mohamad, K., ... & **Alkhamaiseh, T.** (2018). *Evaluating problematic landslide-risked site using hydrogeophysics, isotope and conventional hydrological techniques*. Paper presented at EAGE-HAGI 1st Asia Pacific Meeting on Near Surface Geoscience and Engineering, 9-13 April 2018. Yogyakarta, Indonesia.

University of Malaysia